New Constraints on the Age of Deposition and Provenance of the Metasedimentary Rocks in the Nashoba Terrane, SE New England

Author: MaryEllen Louise Loan

Boston College Electronic Thesis or Dissertation, 2011

Boston College

The Graduate School of Arts and Sciences

Department of Earth and Environmental Sciences

NEW CONSTRAINTS ON THE AGE OF DEPOSITION AND PROVENANCE OF THE METASEDIMENTARY ROCKS IN THE NASHOBA TERRANE, SE NEW ENGLAND

by

MARYELLEN L. LOAN

Submitted in partial fulfillment of requirements

For the degree of

Master of Science

December 2011

TABLE OF CONTENTS

4.0 Results

New Constraints on the Age and Deposition of the Metasedimentary Rocks in the Nashoba terrane, SE New England

By **MaryEllen Loan**
Advisors: **J. Christopher Hepburn, Yvette D. Kuiper, Rudolph Hon**

The Nashoba terrane of SE New England is one of three peri-Gondwanan tectonic blocks caught between Laurentia and Gondwana during the closure of the Iapetus Ocean in the early to mid- Paleozoic. U-Pb analyses (LA-ICP-MS) were carried out on zircon suites from the meta-sedimentary rocks of the Nashoba terrane. The youngest detrital zircons in the meta-sedimentary rocks of the Nashoba terrane are Ordovician in age. There is no significant difference in age between meta-sedimentary units of the Nashoba terrane across the Assabet River Fault Zone, a major fault zone that bisects the NT in a SE and a NW par. Zircon in meta-sedimentary rocks in the Marlboro Fm., the oldest unit of the Nashoba terrane, is rare, which may reflect the basaltic nature of the source material, and is commonly metamict. The Marlboro Fm. contained the oldest detrital grain of all the analyzed samples, with a core of ~3.3 Ga and rim of ~2.6 Ga indicating that it was sourced from Archaen crustal material. Detrital zircons from the Nashoba terrane show a complete age record between the Paleoproterozoic and Paleozoic that strongly supports a provenance from the Oaxiqua margin of Amazonia. The detrital zircon suite of the Nashoba terrane is distinct from both Avalonia and the Merrimack belt; however, they resemble zircon suites from Ganderia. This study proposes that the Nashoba terrane of Massachusetts correlates with the passive trailing edge of Ganderia. Finally, metamorphic zircon analyses of the terrane show that the Nashoba terrane experienced a peak in hydrothermal fluid infiltration during the Neoacadian orogeny.

Acknowledgements

I would like to thank Chris Hepburn and Yvette Kuiper for their guidance and support through the process of researching and writing my thesis. They have been outstanding teachers and mentors. I have grown so much in my education thanks to their help. I would also thank Mike Tubrett, Mike Schaffer, and Wilfredo Diegor for teaching me how to use the LA-ICP-MS, and SEM. This has been an invaluable experience.

Funding for this project was provided by the Geological Society of America and by the Boston College Research Incentive Grant to Yvette Kuiper

1.0 INTRODUCTION

1.1 Geologic overview of Massachusetts

The evolution of the Appalachian orogeny is essentially a complex Wilson cycle that begins the breakup of the super continent Rodinia into Laurentia and Gondwana at ca. 750 Ma, and ends with the re-amalgamation of these continents to form Pangaea (Hatcher, 2010). The Appalachian mountain chain as a whole has experienced at least three major orogenies: the Taconic, the Acadian and the Alleghanian, with many regional variations in the components. This research focuses on the NE Appalachians in Massachusetts, where five distinct orogenic events in the Paleozoic are thought to have been caused by the accretion of multiple tectonic blocks to the Laurentian margin (van Staal *et al.*, 2004; 2009; Hatcher, 2010).

In Massachusetts, the original Laurentian coast of the Iapetus Ocean is interpreted to be the area west of the Shelburne Falls arc and Whitcomb Summit Thrust fault zone (WST, Fig. 1; Goldsmith, 1991a). The meta-sedimentary rocks of this region are dominated by detrital zircon age-populations that overlap with well-established events in the Grenville Province (assembly of Rodinia), including the Labradorian orogenic cycle, at ca.1670 – 1610 Ma, the Pinwarian orogeny, at ca. 1510 – 1420 Ma, the Elzevirian orogenic cycle, at ca. 1290 – 1190 Ma, the Shawinigan pulse, at ca. 1190 – 1140 Ma, the Ottawan pulse, at ca. 1080 – 1020 Ma, and the Rigolet pulse, at ca. 1000 – 980 Ma (Wintsch *et al.*, 2007; cf. Rivers, 1997). Neoproterozoic age zircons in this area are rare (Cawood *et al.*, 2001). The remainder of Massachusetts is essentially a composite of terranes that accreted to Laurentia during the closure of the Iapetus Ocean.

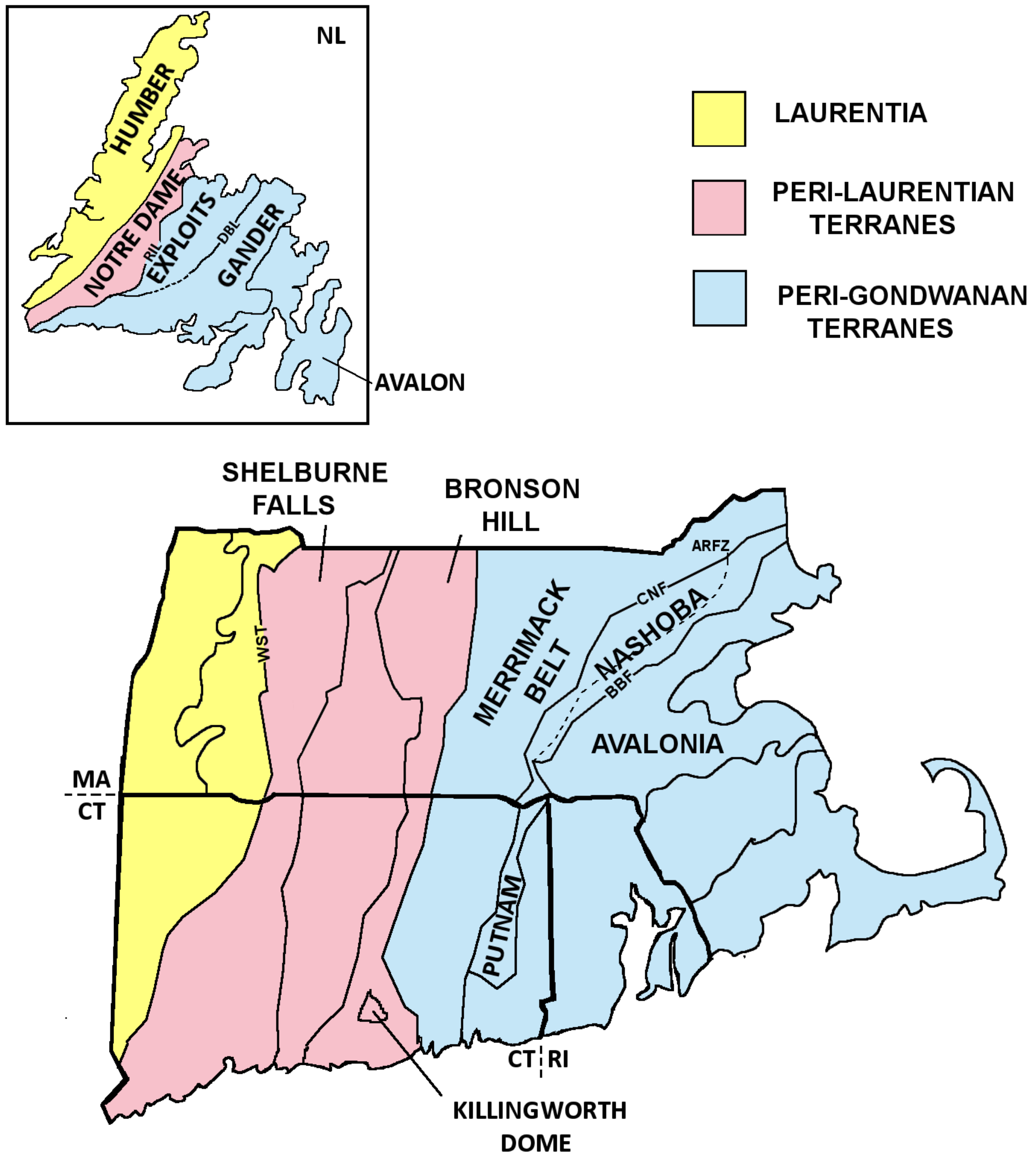

Figure 1: A simplified version of the geology of SE New England (bottom) and Newfoundland (top) modeled after Skehan *et al.*, (1993), Aleinikoff *et al.*, (2007), and Pollock *et al.*, (2007) ARFZ = Assabet River Fault Zone, BBF = Bloody Bluff Fault Zone, CNF = Clinton-Newbury Fault Zone, DBL = Dog Bay Line, RIL = Red Indian Line, WST = Whitcomb Summit Thrust Zone

The first orogenic event in the assembly of Massachusetts is the Taconic orogeny, which is associated with the closure of an ocean basin between the Shelburne Falls arc and the Laurentian margin, and the subsequent accretion of peri-Laurentian terranes (Fig. 1) onto the Laurentian margin (Stanley and Ratcliffe, 1985; Karabinos *et al.*, 1998). In Massachusetts, the peri-Laurentian terranes are interpreted to be the Shelburne Falls arc and the Bronson Hill arc. The Shelburne Falls arc is believed to have formed above an east-dipping (modern orientation) subduction zone in the Early Ordovician, at ca. 470-485 Ma (Karabinos *et al.*, 1998). Continued convergence, and ultimately the collision, of the Shelburne Falls arc with Laurentia led to the uplift of the Taconic mountain chain. After the collision, subduction stepped back to the east and the younger Bronson Hill arc formed above a new west-dipping subduction zone, at ca. 442 to 454 Ma (Karabinos *et al.*, 1998). The Taconic orogeny ended with the accretion of the leading edge of the first of the peri-Gondwanan terranes (van Staal *et al.*, 2009). Aleinikoff *et al.*, (2007) determined that the Killingworth Dome (Fig. 1), which is part of the Bronson Hill Anticlinorium in Connecticut, contains peri-Gondwanan aged zircon populations (Aleinikoff *et al*, 2007). If this is correct, then the Bronson Hill arc represents the suture between the peri-Laurentian and peri-Gondwanan terranes. In Newfoundland, this boundary is called the “Red Indian Line”. It has been suggested to extend through Massachusetts to Connecticut (Aleinikoff *et al.*, 2007).

Following a model of five orogenic events (van Staal *et al.*, 2004; 2009), the Salinic orogeny occurred after the Taconic orogeny, but before the Acadian orogeny. In Newfoundland, it is currently accepted that the Salinic orogeny marks the accretion of the leading edge of Ganderia to the Laurentian margin during the Silurian and the closure of a wide back-arc basin within Ganderia, at ca. 425 to 450 Ma (van Staal *et al.*, 2004; Valverde-Vaqureo *et al.*, 2006; van Staal *et al.*, 2009). The term "Ganderia" has been used to describe a composite of peri-Gondwanan terranes that accreted after the peri-Laurentian terranes but before the arrival of Avalonia (Van Staal *et al.*, 2009). In Massachusetts, it was not certain whether or not the Merrimack and Nashoba terranes (Fig.1.0) should be included in "Ganderia" because the age and geologic history of the terranes are not well constrained. This is one of the questions this study set out to answer.

The Acadian orogeny is regarded as the subsequent collision of Avalonia (a term used to group all of the Avalon-type terranes together despite modern geographic separation) with the composite Laurentian margin in the Devonian, at ca. 400–420 Ma, the timing of which varies along strike (Keppie *et al.*, 1998; Dorais *et al*., 2001; Barr *et al.*, 2003; van Staal *et al.*, 2005; 2009; Hatcher, 2010). This time period was marked by sillimanite-grade metamorphism and abundant plutonism in the Nashoba terrane (Hepburn *et al.*, 1995; Hatcher, 2010). The timing of the Acadian orogeny is also constrained by the upper-Silurian, lower-Devonian arc magmatism on the trailing edge of Ganderia bordering Avalonia (Moench *et al.*, 2003; Hepburn *et al.*, 1995; van Staal *et al.*, 2009).

The Neoacadian orogeny is associated with the docking of the Meguma terrane to the composite Laurentian margin in the Devonian- Carboniferous, at ca. 350–400 Ma (van Staal *et al.*, 2009). The Meguma terrane is not visible in New England but has been traced offshore of Cape Cod by geophysical and well data (Pe-Piper *et al.*, 1999). The Neoacadian orogeny was proposed by Robinson *et al.*, (1998) to differentiate a major orogenic event in SE New England from the Acadian orogeny. Evidence for the

Neoacadian orogeny is not present in Newfoundland (van Staal *et al.*, 2009). The Neoacadian orogeny in Massachusetts may be localized and related to accretion of the Meguma terrane. Alternatively, it is simply an extension of the Acadian orogeny in New England (van Staal *et al.*, 2009; Hatcher, 2010).

Finally, at ca. 300-350 Ma, the assembly of the super-continent Pangaea was completed by the docking of Gondwana with Laurentia during the Alleghanian orogeny. In Massachusetts, the effects of the Alleghanian orogeny were thought to have been restricted to the Avalon terrane where known Alleghanian-aged metamorphism is present in deformed and metamorphosed Pennsylvanian rocks (Wintsch *et al.*, 2003; Hon *et al.*, 2007). This interpretation was based on the lack of known evidence for Alleghanian deformation and metamorphism in the Nashoba terrane. However, terranes west of the Nashoba, such as the Bronson Hill arc, do show an extensive Alleghanian overprint, suggesting that the Alleghanian was a widespread period of regional metamorphism. The Nashoba terrane was thought to have been unique in that it did not experience the Alleghanian thermal event (Wintsch *et al.*, 2003). However, recent U-Pb dating of monazite and $^{40}Ar/^{39}Ar$ cooling ages of biotite in the Nashoba terrane has shown a hydrothermal Alleghanian-aged signature in the Nashoba terrane (Stroud *et al.*, 2009; Reynolds *et al.*, 2010).

The Appalachian orogeny is complex and its evolution is not well constrained in SE New England. The goal of this study is to enhance our understanding of the geologic history of SE New England through a detrital zircon study of the main meta-sedimentary units of the Nashoba terrane, the central of the three peri-Gondwanan terranes of Massachusetts. The following is a brief description of these three peri-Gondwanan terranes, from west to east, and the previous work that has contributed to our understanding of their geologic history.

1.2 The Merrimack belt

The Merrimack belt is thought to extend in Massachusetts from northwest of the Clinton-Newbury fault zone (CNF) to the Bronson Hill Arc (Fig. 1). The Merrimack belt is in fault contact with the Nashoba terrane across the Clinton-Newbury fault zone. It structurally overlies the Nashoba terrane as indicated by a sharp contrast between the greenschist facies rocks of the Merrimack belt and the upper amphibolite facies rocks of the Nashoba terrane (Goldsmith, 1991a; Markwort *et al.*, 2007; Wintsch *et al.*, 2007). The western bounding fault of the Merrimack belt is obscured by Mesozoic-age rocks (Aleinikoff *et al*., 2007). The Merrimack belt is composed mainly of impure quartzites, schists and calc-silicate rocks that likely formed as deep-water turbidite sequences (Goldsmith, 1991a; Hon *et al.*, 2007). Metamorphism in the Merrimack belt of Massachusetts increases from the greenschist facies in the east to the amphibolite facies in the west and is generally thought to be a result of the Acadian orogeny (Zen *et al.*, 1983; Wintsch *et al.*, 2007). Similarities in igneous intrusion histories between the Nashoba and Merrimack terrane have led researchers to suspect that the two terranes are related. However, U-Pb analyses of detrital zircon from meta-sedimentary rocks in the Merrimack belt are as young as Siluro-Devonian in age (Wintsch *et al.*, 2007), which is much younger than the estimated age of metasedimentary rocks of the Nashoba terrane.

1.3 The Nashoba terrane

The Nashoba terrane (Fig. 1) is separated from the structurally overlying Merrimack terrane to the west by the Clinton-Newbury fault zone (CNF, Fig. 1; Zen *et al*, 1983; Goldsmith, 1991a). To the east, it is separated from the structurally underlying Avalon terrane by the Burlington Mylonite zone, which was later overprinted by the brittle Bloody Bluff fault zone (BBF, Fig. 1; Goldstein, 1989; Goldsmith, 1991a; Hepburn *et al.*, 1995). The Assabet River fault zone (ARFZ, Fig. 1) is a large mylonitic fault zone that bisects the Nashoba terrane (Goldsmith, 1991a; Hepburn et al., 1995). The units to the southeast of the ARFZ are interpreted to have resulted from deposition in a marine basin near a volcanic source based on the abundance of amphibolite of volcanic origin (Goldsmith, 1991a). The units to the northwest of the ARFZ represent a more distal part of a basin, as evidenced by the greater volume of pelitic schist and calc-silicate rocks (Goldsmith, 1991a).

Interpretation of the terrane is complicated by multiple episodes of deformation and high grade metamorphism, which has destroyed any fossil age indicators (Hepburn and Munn, 1984). In addition, major faults, folds, and ductile shear zones are present throughout the terrane (Zen *et al.*, 1983; Goldsmith, 1991a) that result in complex relationships and make relative dating methods based on stratigraphy extremely difficult. Previous studies the Nashoba terrane have constrained three major metamorphic events (Hepburn *et al.*, 1995; Jerden *et al.*, 1997; Stroud *et al.*, 2009). The first event (M1) occurred from 435 to 400 Ma and is associated with sillimanite zone metamorphism. The second event (M2) occurred at ca. 390 Ma and is associated with metamorphism and migmitization up to the second sillimanite zone. The third metamorphic event (M3) occurred at ca. 385-360 Ma and is interpreted as a retrograde greenschist facies metamorphism associated with uplift of the terrane. In addition, hydrothermal growth of monazites occurred at ca. 360-305 Ma (Jerden *et al.*, 1997; Stroud *et al.*, 2009).

1.4 The Avalon terrane

The Avalon terrane lies southeast of the Bloody Bluff fault zone. It is composed of Neoproterozoic aged granitoid rocks that were intruded by Ordovician to Devonian age plutons (Hon *et al.*, 2007*).* The Avalon terrane of Massachusetts is correlative with the type Avalon terrane of Newfoundland based on fossil evidence (Rast and Skehan, 1993) and on critical 630-590 Ma calc-alkaline plutonic-volcanic events (Zartman and Naylor, 1984; Thompson *et al.*, 2007). Igneous activity in the Boston area is dominated by the widespread ca. 610 Ma Dedham Granite(Hepburn *et al.*, 1993) and by the ca. 599 Ma Westwood Granite (Thompson *et al.*, 1996; 2007). The igneous rocks of the Boston area are overlain by Ediacaran-aged conglomerate (Thompson and Bowring, 2000), mudstone (Billings, 1976), and Cambrian-Ordovician aged fossiliferous platform deposits (Thompson *et al.*, 2003; 2007). The Avalon terrane is essentially un-metamorphosed (Cameron and Naylor, 1976) and in the Boston area experienced metamorphism no higher than the greenschist facies (Hepburn *et al.*, 1993).

1.5 Purpose

This study focused on the depositional age and provenance of the meta-sedimentary rocks of the Nashoba terrane, the central of the three SE New England peri-Gondwanan tectonic blocks. Because of its uranium content, widespread occurrence, and resistance to erosional and metamorphic processes, (Cherniak and Watson, 2000; Faure and Mensing, 2005; Wintsch *et al.*, 2007), zircon is an extremely valuable mineral in age and provenance studies (Mezger *et al*., 1997). Detrital zircons in meta-sedimentary rocks may record complex histories. The timing of the initial magmatism or metamorphism that formed the original zircon may be preserved in the cores of zircon grains and, if applicable, the age of subsequent igneous/metamorphic events may be preserved in their overgrowths. Detrital zircons of the meta-sedimentary rocks were dated in order to investigate the 1) age of deposition of the individual units, 2) relationship of units within the terrane, specifically with respect to the Assabet River fault zone 3) proximity to adjacent micro-continents or terranes during the formation of the terrane, 4) correlation with other regions of the Northern Appalachians, and 5) the provenance of the Nashoba terrane with respect to the Amazonian or West African shield of Gondwana (Thompson *et al.,* 2007, Nance *et al.,* 2008).

2.0 STRATIFIED UNITS OF THE NASHOBA TERRANE

In general, the Nashoba terrane consists of mafic meta-volcanic and meta-sedimentary rocks (Marlboro Formation), volcanogenic sedimentary rocks (Nashoba Formation), a schistose unit (Tadmuck Brook Schist) and two gneissose units: the Fish Brook Gneiss (499 +6/-3 Ma) - an orthogneiss (Hepburn *et al.*, 1995) and the Shawsheen Gneiss - a paragneiss (Fig. 2.0; Bell and Alvord, 1976; Hepburn *et al.*, 1995). The northern portion of the terrane is dominated by abundant granitic and intermediate composition plutons, including two phases of the Andover Granite, at ca. 408±22 Ma and 450±22 Ma, the Indian Head Hill Granite at ca. 402±5 Ma and 349±4Ma, the Sharpner's Pond Diorite, at ca. 430±5 Ma (Zartman and Naylor, 1984), and the Straw Hollow Diorite at ca. 385±10 Ma (Acaster and Bickford, 1999). The Nashoba terrane was interpreted by Bell and Alvord (1976) to be a steeply NW dipping homoclinal stratigraphic sequence (Bell and Alvord, 1976), but deformation and faulting have obscured stratigraphic relations. The Nashoba terrane is divided by several major fault zones that parallel the strike of the stratigraphic units (Goldsmith *et al.*, 1991a). One major fault zone, the Assabet River fault zone (ARFZ; Fig. 2.0), bisects the Nashoba terrane. This study will test if the ARFZ represents a terrane boundary, similar to the Clinton-Newbury or Bloody Bluff fault zones. For this study, the meta-sedimentary rocks of the Nashoba terrane are divided into those that are located northwest of the ARFZ and those that are located southeast of the ARFZ.

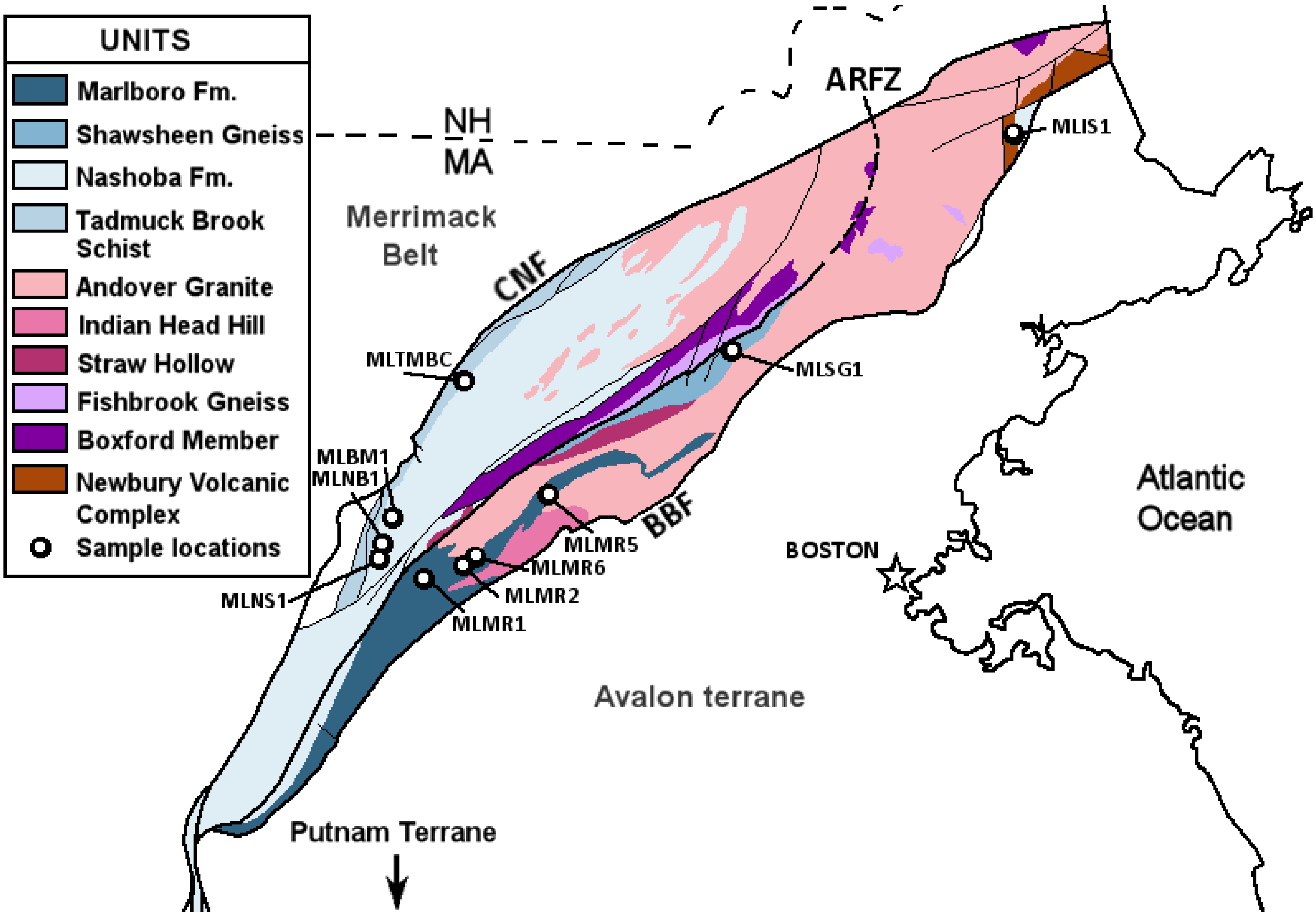

Figure 2.0: Geological map of the Nashoba terrane based on Massachusetts Office of the State Geologist Bedrock Map of Massachusetts overlay for Google Earth. Map shows major formations of the Nashoba terrane and the locations of samples collected for this study. Exact samples locations found in appendix A. ARFZ = Assabet River Fault Zone.

2.1 Southeastern Nashoba Terrane

Currently, the easternmost metasedimentary unit of the Nashoba terrane is thought to be the Marlboro Formation (Fig. 2.0), which lies just west of the Bloody Bluff fault zone. The Marlboro Formation is composed largely of hornblende-plagioclase amphibolites, but it also contains felsic granulites, gneisses and meta-sedimentary rocks that are generally rusty weathering sillimanite schists (Bell and Alvord, 1976; DiNitto *et al.*, 1984; Goldsmith, 1991a). Geochemical studies on the amphibolites from the Marlboro Formation indicate that they were originally mantle derived (Kay *et al.*, 2009), mildly alkaline to high alumina tholeitic basalts that likely formed in a volcanic arc/back arc setting (DiNitto *et al.*, 1984). The Marlboro Formation has traditionally been interpreted to be the source of the meta-sedimentary rocks of the Nashoba Formation (Hepburn and Munn, 1984, Goldsmith, 1991a).

Several attempts have been made to directly date the Marlboro Formation. Acaster and Bickford (1999) reported the age of the Marlboro Formation to range between 425 ± 2 Ma to 584± 8 Ma, based on U-Pb analyses of zircon in the Grafton Gneiss, the Sandy Pond Amphibolite Member, and the Milham Reservoir "Granulite" Member of the Marlboro Formation. More recent ages include an approximately 540 Ma mafic boudin in the Quinnebog Formation (a unit in Connecticut that is correlated with the Marlboro Formation), the cross-cutting Grafton Gneiss at ca.515 ± 6 Ma, and structurally overlying volcaniclastic rocks that were determined to be ca.501 ± 3 Ma (Walsh *et al.*, 2011). Thus, the reported ages of the Marlboro Formation volcanics range between ca. 501 Ma and 540 Ma

(Walsh *et al.*, 2011) and, despite numerous attempts, the age of the unit is not well constrained.

The Shawsheen Gneiss is a muscovite-biotite-plagioclase-quartz paragneiss, which is believed to have been derived from the detritus of volcanic rocks of intermediate to mafic composition (Olzewski, 1980). The unit was originally considered lithologically similar to the Nashoba Formation but was later established as a separate formation because it is separated from the Nashoba Formation by the Fishbrook Gneiss and Assabet River fault zone (Goldsmith, 1991a; Fig. 2.0). The Shawsheen Gneiss was previously dated by Olzewski (1980) using U-Pb analyses of zircon on multiple zircon fractions. The resulting discordia was based on only three zircon fractions and led to unreliable upper and lower intercept ages. The upper intercept was reported as 2042± 52 Ma and the lower intercept at 517± 16 Ma (Olzewski, 1980). Olzweski (1980) hypothesized that the Shawsheen Gneiss had a very old source and that it was similar to the Westboro Formation in the Avalon terrane based on color and morphology of the zircon grains, but was unable to determine the age of the unit.

2.2 Northwestern Nashoba Terrane

The Nashoba Formation (Fig. 2.0) occupies about one third of the Nashoba terrane and is composed largely of biotite-feldspar gneiss and biotite schists with subordinate calc-silicate rocks, impure quartzites, and pelitic schists (Hepburn and Munn, 1984; Goldsmith, 1991a). The degree of migmatization generally increases toward the northeast. The metamorphic grade of the Nashoba Formation is generally high-grade in the sillimanite or sillimanite K-Feldspar zones. Previous mapping of the Nashoba terrane separated the various rock types of the Nashoba Formation into separate members (Bell and Alvord, 1976). Currently, the only differentiated member of the Nashoba Formation is the Boxford member (Fig. 2.0), which consists mainly of amphibolites, and is the only member of the Nashoba Formation that is clearly recognized to occur in several areas along strike (Goldsmith *et al.*, 1991a). The Nashoba Formation is correlated with the Tatnic Hill Formation of the Putnam terrane of Connecticut (Wintsch *et al.*, 2007) and may correlate with the Rye Formation in New Hampshire and Maine (Goldsmith, 1991a).

The Tadmuck Brook Schist (Fig. 2.0) is interpreted to be the youngest stratigraphic unit of the Nashoba terrane (Bell and Alvord, 1976; Fig. 2.1). The formation increases in metamorphic grade from the NW to the SE from the greenschist through the upper amphibolite facies (Jerden *et al.*, 1997). Because of the considerable variation in metamorphic grade and mineral assemblage along strike, there is some uncertainty whether the Tadmuck Brook Schist is a single formation, and whether it should be considered part of the Nashoba and/or

Merrimack terranes (Goldsmith, 1991a). The westernmost border of the Nashoba terrane is considered to be the Clinton-Newbury fault zone (Fig. 2.0); however, some argue that the Tadmuck Brook Schist extends further into the Merrimack terrane and is correlated with the Tower Hill and Vaughn Hill quartzites, although stratigraphic relationships are obscured across the fault zone (Goldsmith, 1991a).

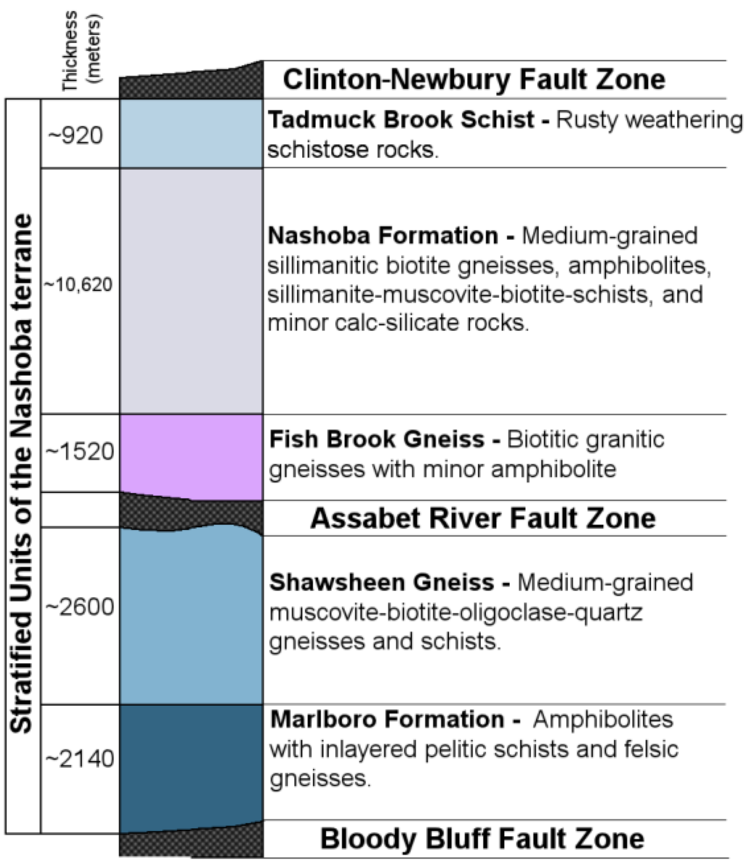

Figure 2.1: Stratified units of the Nashoba terrane, modified from Bell and Alvord (1976).

2.3 Newbury Volcanic Complex

The Newbury Volcanic Complex was described in detail by Shride (1976) as a combination of andesite, rhyolitic tuff, basalt flows and some marine "mudrocks," all of which are metamorphosed to no higher than the lower greenschist facies. The unit is interpreted to be fault bounded between the Nashoba and Avalon terrane with no exposed contacts and no known correlation with adjacent units. It is unclear whether the Newbury Volcanic Complex belongs to the Nashoba terrane or to the Avalon terrane, or some other unknown terrane. Trace element geochemistry shows that the Newbury Volcanic complex most likely formed in a continental arc-environment and it is thought to correlate with the coastal volcanic belt in Maine (Gates and Moench, 1981; Hepburn *et al.*, 1995; 2004).

3.0 ANALYTICAL METHODS

Zircons were isolated in the Mineral Separation Lab at Boston College using standard crushing and grinding methods and separation techniques. Throughout the process, all of the equipment was thoroughly cleaned before and after each use with wire brushes, ethyl alcohol and compressed air in order to prevent contamination. The following is a summary of the separation procedures.

At least fifty pounds of each sample that was collected in the field was scrubbed individually with wire brushes under running water to remove loose detritus. Larger pieces were taken to a rock preparation area and manually broken into pieces suitable for the crusher, using a sledge hammer in a cleaned area. Once the rock was reduced in size these pieces were washed and scrubbed again in order to eliminate the possibility of contamination from the sample preparation area. The rock fragments were then allowed to dry before being placed in clean, labeled, plastic sample bags. A small portion of each sample was set aside for thin sections.

The mineral separation lab at Boston College is equipped with a Bico International Inc. "Chipmunk" Jaw Crusher. The jaw crusher is assembled to accommodate a thick sheet of plastic tubing that is sealed on one end to form a bag and allows for the sample break-up to be contained within the plastic bag. The gravel sized pieces fall directly into the plastic bag, greatly reducing the risk of contamination from the machine and surrounding area. The bag is then sealed and labeled until the sample is ready to be ground.

Samples were ground using the Bico International Inc. Disc Mill Pulverizer. The grinder functions by dropping gravel sized pieces between two steel plates, one stationary and one rotating. The plates are set to <500μm to produce a fine-grained sand. As with the crusher, the lab has adapted the design of the grinder to accommodate a thick plastic bag.

The ground samples were then transferred to the "ro-tap" sieve shaker. A small portion of the sample was placed in stacked 500μm and 255μm sieves and run in the "ro"-tap for 5-10 minutes, until the sample was fully separated. Based on the fine-grained nature of the samples and the fact that typical igneous zircon grain populations do not exceed 250μm (Hoskin & Schaltegger, 2003), 255μm was considered sufficient for isolating the full range of zircon sizes. Sample grains that were less than or equal to 255μm were combined and stored in labeled plastic containers. Grains that were larger than 500μm were placed back in the grinder and the plate width was decreased in order to promote the break-up of these fragments. Platy minerals, such as mica, are difficult to grind because they commonly align with the plates and fall through the grinder without reducing in size. Therefore, approximately 10-25% of the overall material could not be processed.

The Outotec Wilfley® concentrating table is a method of wet-gravity separation by mineral weight. Running water moves over the surface of the shaker table and drains into plastic containers positioned in a trough (Fig. 3.0). The ground sample is added slowly while maintaining a constant input of grains. In order to preserve the smallest grain-size fraction the water was run slowly and the forward tilt of the table was set shallow. The lightest minerals (tailings) wash off of the table into cups H3-H6 (Fig. 3.0). The heaviest minerals, such as zircon, (concentrates) continue across the table and down the grooved surface into the H-1 cup, the rest collect in H2 (Fig. 3.0). Once the H-1 and H-2 concentrates were obtained they were filtered to remove the water, sprayed with ethyl alcohol, and then immediately dried under a heat lamp to prevent the minerals from oxidizing. The contents of the H-2 container were examined in case an error in separation allowed zircons to end up in this container. The remaining grains from containers H3-H6 were emptied into a clean Pyrex dish, dried in the oven, and stored in plastic containers. The dried H-1 concentrates were then transferred to the Frantz™ Isodynamic separation area.

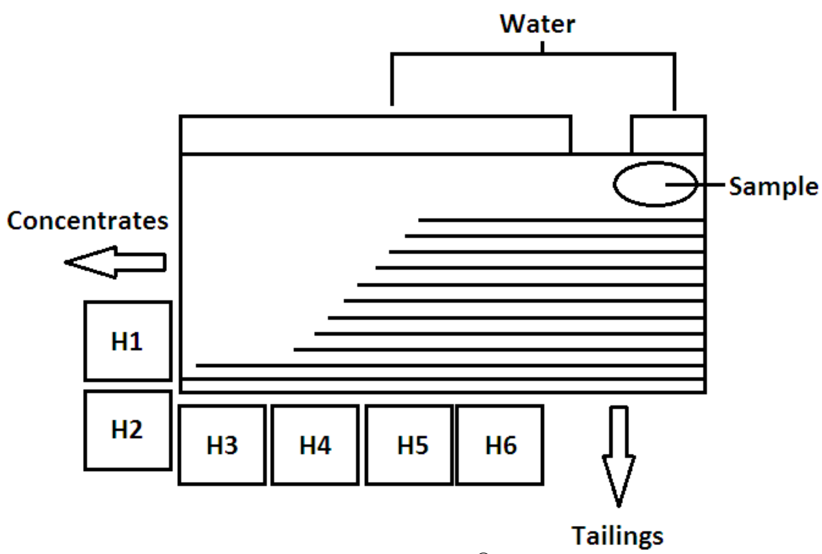

Figure 3.0: A diagram of the Outotec Wilfley® concentrating table and the location of the plastic containers.

Before the samples were placed on the isodynamic separator, a hand-held magnet was used to remove metal filings that result from normal wear and tear of the crusher and grinder. The Frantz® Isodynamic separator was run at a standardized forward and sideways slope to maintain consistency in each sample. The separation was run four times at increasing amperage (Table 3.1) to slowly separate magnetic and paramagnetic minerals. High clarity zircons are non-magnetic at 1.8Amps; however, the paramagnetic separations were collected at 1.5Amps to avoid artificial biasing induced by the Isodynamic Separator (Sircombe, 2002). The Frantz isodynamic separations were carried out before heavy liquid separations in order to reduce the amount of material.

Separation	Amps	Forward Slope	Side Slope
1	0.4	20°	10°
2	0.8	20°	10°
3	1.2	20°	10°
4	1.5	20°	10°

Table 3.1: Magnetic separation settings

Methylene iodide (MEI) is a heavy liquid that has a known density of 3.3g/cm^3. Based on the size of the sample an appropriate amount of methylene iodide was weighed and poured into a separation funnel. The sorted grains were then poured directly into the methylene iodide and carefully swirled to ensure that all of the grains were in suspension. The sample was then allowed to separate. The specific gravity of a zircon grain is 4.6-4.7g/cm^3 and, along with the remaining non-magnetic heavy minerals, sinks to the bottom of the separation funnel. Once all of the grains settled, the heavy minerals were drained out of the separation funnel into a filter and set aside. The lightest minerals, which floated in MEI, were collected into a separate filter. These filters were then rinsed with acetone to remove the methylene iodide, dried under a heat lamp, and then stored in separate glass vials until they could be examined under the microscope.

Approximately 150 zircon grains from each sample were handpicked from the heavy mineral concentrates in alcohol under a binocular microscope using standard optical criteria including color, relief, and morphology (Corfu *et al.*, 2003). The grains obtained from each sample included sizes that were at the limit of our ability to identify morphological properties under the binocular microscope. When possible, these small zircons were collected in addition to the 150 zircon grains in order to prevent biasing the sample. If the LA-ICP-MS spot could fit on the zircon grain then the zircon grain was dated. If the zircons were smaller than the size of the spot, the zircons were imaged using backscattered electron imaging (BSE), but were not dated. It is possible that the smaller zircons could be dated in the future using other methods, such as SHRIMP. However, these zircons were not included in this analysis.

Once the zircon grains were isolated they were visually subdivided into large (150-200µm), medium (100-150µm), and small (50-100µm) populations, which were verified using the camera's calibrated micrometer scale. The sub-populations were mounted in a 25mm diameter epoxy resin grain mounts and polished on the Struers Labo-Pol 5 until the cores were well exposed. The progress of the polishing was checked on a Zeiss Axiosop 40 microscope with transmitted and reflected light facilities. Zircon grains were polished until about one third of the grain was removed and the area of the individual grains appeared equal under transmitted light and reflected light.

The grain mounts were carbon coated and imaged on a FEI Quanta 400 Scanning Electron Microscope by backscattered electron imaging (BSE) and cathodoluminescence (CL) at Memorial University in Newfoundland's (MUN) Inco Innovation Center. BSE images allowed the core and (when applicable) overgrowths in each grain to be differentiated. Precise placement of the laser beam is essential for obtaining distinct ages. Analysis of two or more age domains leads to discordant ages (e.g. Bennett *et al.*, 2009). Due to time constraints, CL images were reserved for zircons that were not well resolved in BSE imaging. In addition, Energy-dispersive X-ray Spectroscopy (EDX) was used to determine the composition of inclusions within the zircon grains. Zircons with inclusions, such as uraninite, were not analyzed.

U-Pb analyses were carried out using Laser Ablation Inductively Coupled Plasma Mass Spectrometry (LA-ICP-MS) at Memorial University. Memorial University is equipped with a Finnigan ELEMENT XR double focusing magnetic sector field ICP-MS coupled to Geolas 193 nm Excimer laser. Once the carbon coating was removed by polishing, the surfaces of the grain mounts were then cleaned with dilute nitric acid to remove any contamination before placing them in the LA-ICP-MS. The ICP-MS was set to perform automated runs over the cores (and when applicable the rims) of each grain that had previously been identified with BSE imaging. A 10μm laser beam rastered over each selection and sampled a 40×40μm square spot. For grains less than ~50μm, or for finer analyses of the zircon growth rings, the raster was set to a 30×30μm raster, but with some compromise to the precision of the analysis. Laser energy was set at 5 J/cm^2.

A nebulized internal standard tracer solution was introduced to the system simultaneously with the ablated solid material. The tracer solution consisted of natural Tl ($^{205}Tl/^{203}Tl$ = 2.3871), ^{209}Bi, enriched ^{233}U, and ^{237}Np (ca. 1 ppb), in a He-Ar carrier gas (Bennett *et al.*, 2009). The isotopic composition of the tracer solution allowed for instrumental mass bias correction. The accuracy and precision of the analyses were assessed through the use of zircon standards 02123 (at ca. 295 Ma), PL (at ca. 337 Ma), and 91500 (at ca. 1066 Ma) whose ages were previously established by Isotope Dilution Thermal Ionization Mass Spectrometry (ID TIMS). Each of the three zircon standards were sampled for every six unknowns. Data correction and reduction was carried out by Mike Tubrett and Wilfredo Diegor at MUN. Raw data were corrected for dead time (20ns) of the electron multiplier using the Excel spreadsheet based program LAMdate (Košler and Sylvester, 2002). Data reduction included correction for gas blank, laser-induced elemental fractionation (c.f. Sylvester and Ghaderi, 1997), and instrument mass bias (c.f. Horn *et al.,* 2000; Košler *et al.,* 2002). There was no common Pb correction. Ages of the unknowns were calculated using LAMdate (Košler et. al 2002) with Isoplot v. 2.06 of Ludwig (1999).

4.0 RESULTS

4.0.1 Data Analysis

A Wetherill's concordia diagram is a standard graphical method for U-Pb studies (Faure and Mensing, 2005). In a concordia diagram the $^{207}Pb/^{235}U$ ratio (Fig. 4.0, orange) defines the x-axis and the $^{206}Pb/^{238}U$ (Fig. 4.0, green) defines the y-axis. The curved line is called the concordia and represents the values of the $^{207}Pb/^{235}U$ and the $^{206}Pb/^{238}U$ at a given time *t*. Data that plot directly on the concordia are called concordant, data that plot below the line are called discordant, and data that plot above concordia are reversely discordant (Faure and Mensing, 2005). Due to the abundance of ^{238}U, the $^{206}Pb/^{238}U$ ratio is especially useful for reporting young <1 Ga ages (Ludwig, 2008; Pollock *et al.*, 2009). The $^{207}Pb/^{206}Pb$ age is useful for grains that are >1 Ga because it directly compares the radiogenic daughter Pb ratios and does not rely on the uranium content, which after billions of years of decay, may be very small (Ludwig, 2008). Also, the $^{207}Pb/^{206}Pb$ age is useful for grains that are slightly discordant because it is more reasonable to assume that if lead loss occurred then the error ellipse has moved toward the origin from its original position on concordia rather than to selectively lose one Pb isotope over the other and move towards the x or y-axis (cf. Faure and Mensing, 2005). The concordia age (Fig. 4.0, light blue) is based on the ratio of $^{238}U/^{206}Pb$ to $^{207}Pb/^{206}Pb$, or the $^{235}U/^{207}Pb$ to $^{207}Pb/^{206}Pb$, and is usually more precise than any of the individual ages since the age is a mathematical combination of all three isotopic ratios (Ludwig, 1998).

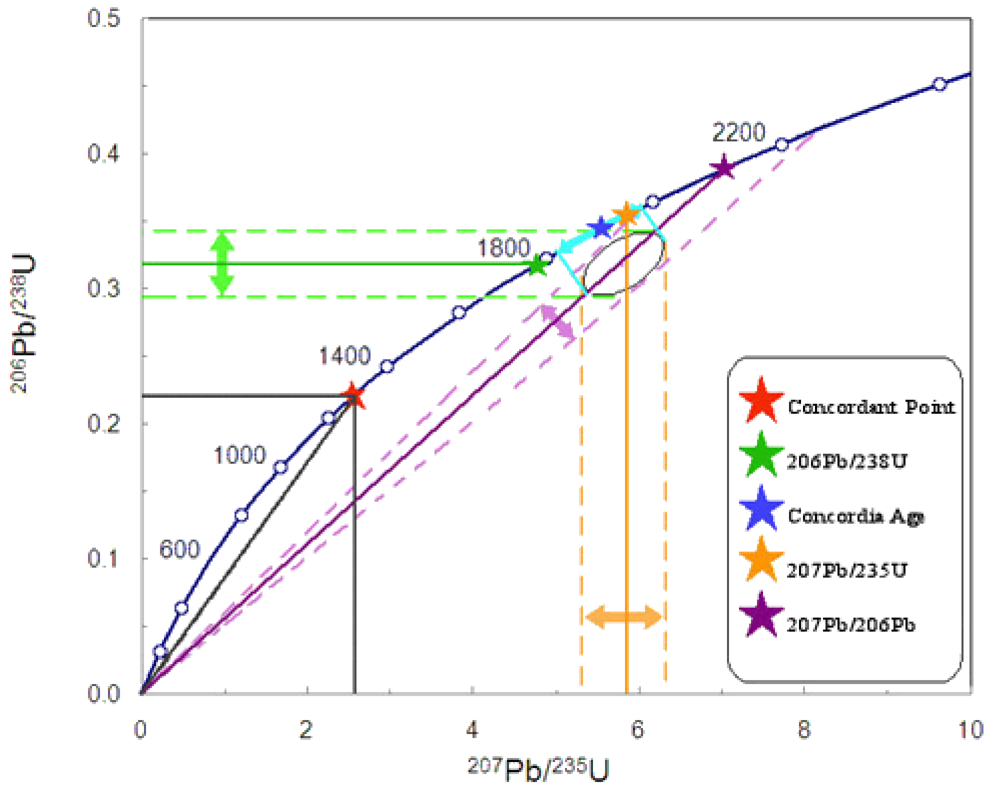

Figure 4.0: An idealized concordia diagram demonstrating the age of a concordant point (Red) and a discordant zircon error ellipse. The age of each ratio is projected on the concordia curve as a star. Individual age errors are given by dashed lines.

Recently, the concordia age has become prevalent for reporting U-Pb data amongst researchers (Košler and Sylvester, 2003; Pollock *et al.*, 2007; 2009); however, much of the Appalachian literature has been, and is currently being, reported using the $^{206}Pb/^{238}U$, $^{207}Pb/^{206}Pb$ ages with their 1σ or 2σ errors (e.g. Wintsch *et al.*, 2007; Fyffe *et al.*, 2009). In order to directly compare the data obtained in this research to previously reported ages in the literature, $^{206}Pb/^{238}U$ ages will be used for zircons younger than 800 Ma, and $^{207}Pb/^{206}Pb$ ages will be used for zircons older than 800 Ma. In this study, errors are reported at the 1σ confidence level. Zircon grains with a probability of concordance less than 0.05, based on 2σ error, were considered discordant and removed from the data interpretation (cf. Košler & Sylvester, 2003).

In addition to the concordia diagram, data from this research will be presented in the form of a probability density plot. A concordia diagram is an excellent tool that allows for the visual evaluation of concordance and analytical error (Sircombe, 2000). However, the disadvantage of a concordia diagram is that, as the number of analyses increases, they can become congested and difficult to read. The probability density plot uses both a frequency curve and histogram to display the same data and is easily readable. The disadvantage of a histogram is that that binning for the histogram disregards analytical error and emphasizes the calculated age (Sircombe, 2000). Unless otherwise noted, in this study, histograms were auto-binned using Isoplot (Ludwig, 2008). The unitless frequency curve may lead to the misinterpretation of the number of zircons in a particular age population based on the height of the line alone, especially when various samples with different numbers of analyses are compared. To prevent this misinterpretation all frequency curves were scaled based on the number of analyses.

4.0.2 Zircon Properties and Morphologies

Th/U ratios can be used to aid in the differentiation between detrital populations and zircon from metamorphic populations. Metamorphic zircons may be produced by high grade metamorphism in the upper amphibolite and granulite facies; therefore, some grains may have grown during metamorphism and not be detritus from eroded source material (Parrish and Noble, 2003). Metamorphic zircons typically have a very low Th/U ratio of < 0.1; however, this is not always the case. For example, some metamorphic zircons can retain igneous-like Th/U ratios due to the absence of coexisting Th-bearing phases, such as monazite (Hoskin and Schaltegger, 2003; Aleinikoff, 2006). Also, the Th/U ratio is not effective in differentiating metamorphically grown zircons from those that are detritus with a metamorphic protolith. Therefore, in this study the Th/U ratio was always be used in conjunction with textural evidence from transmitted light (Fig. 4.1 and Table 4.1) and BSE images (see Chapter 4) for metamorphic growth that are well established in the "Atlas of Zircon Textures" (Corfu, 2003).

There is some discussion about how many grains constitute a statistically representative population of a particular formation. Fedo *et al.*, (2003) expressed that, at least 59 randomly selected grains are necessary to reduce the probability of missing any fraction of a population to 5% through the use of the equation given in Dodson *et al.*, (1988) $p = (1-f)^{k}$, where p is probability, f is the fraction of interest of the whole population, and k is the total number of grains selected. Vermeesch (2004) argued that to achieve 95% confidence that no fraction of the population was missed at least 117 grains need to be analyzed per sample, effectively doubling the required number of grains from what Fedo *et al*. (2003) proposed. Finally, Andersen (2005) stated that hundreds of grains would be necessary to state that a certain population was statistically representative, but admitted that such numbers were commonly unrealistic. Instead, Andersen (2005) proposed that 35 grains chosen at random from a given formation and 15 additional grains specifically selected for differences in morphologies was sufficient to represent all age populations in any given sample. In this study, both Andersen and Vermeesch's recommendations were taken into account by selecting 150 grains for analysis with over 100 at random and the remainder targeted for textural differences under the binocular microscope. Samples that did not yield at least 60 grains are not considered statistically representative but were still analyzed. Zircon morphologies of the Nashoba terrane are shown in Figure 4.1 and described in Table 4.1.

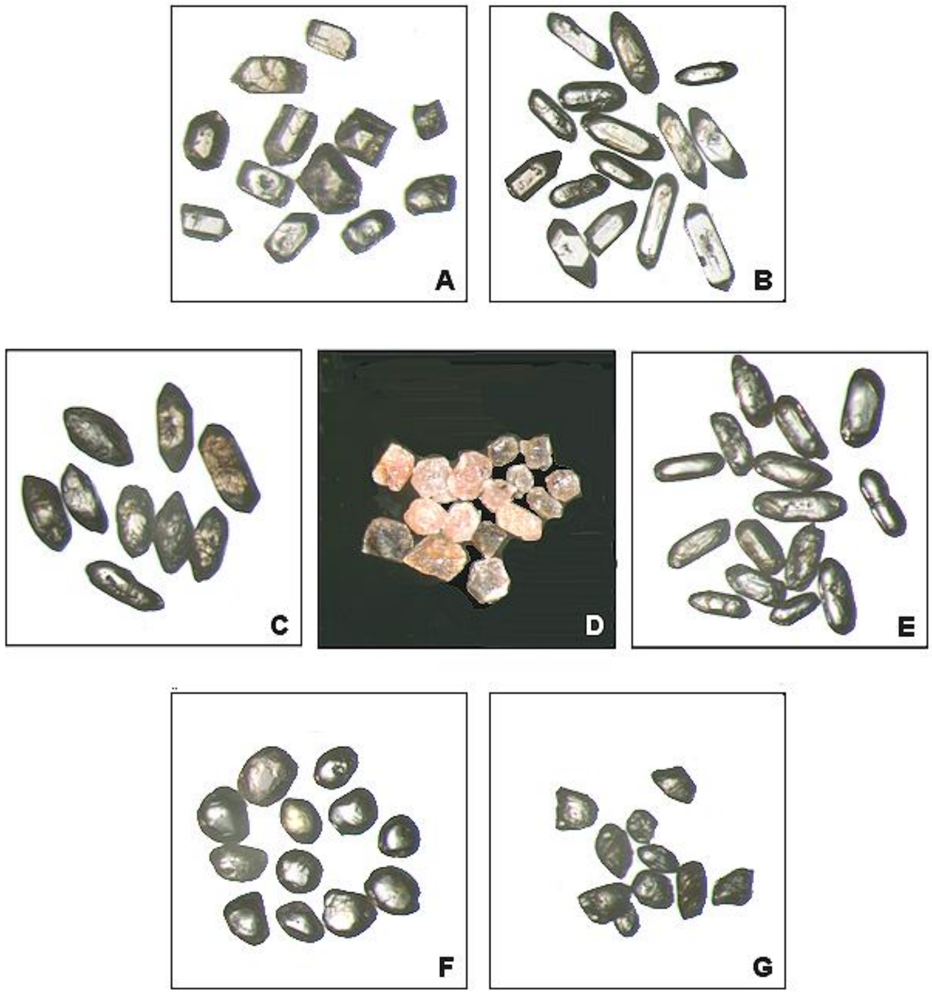

Figure 4.1: A representation of the various zircon morphologies found in the Nashoba terrane meta-sedimentary rock samples. Images were captured using transmitted light under a binocular microscope. Image D appears dark to enhance contrast. See Table 4.1 for descriptions.

POPULATION		SAMPLE NUMBER																				
		Marlboro Formation			**Shawsheen Gneiss**			**Nashoba Formation Gneiss**			**Nashoba Formation schist**			**Nashoba Formation Calc-Silicate**			**Tadmuck Brook Schist**			**Newbury Volcanic Complex**		
		L	**M**	**S**	**L**	**M**	**S**	**L**	**M**	**S**	**L**	**M**	**S**	**L**	**M**	**S**	**L**	**M**	**S**	**L**	**M**	**S**
A	**Faceted, small aspect ratio (2.5:1) colorless to cloudy**				X			X	X		X			X					X		X	X
B	**Faceted, large aspect ratio (4:1) colorless to cloudy**				X	X	X		X		X				X						X	
C	**Abraded, large aspect ratio (4:1), cloudy to rusty**			X	X	X	X	X	X													
D	**Metamict, various shape**			X																		
E	**Rounded edges, long or short aspect ratio, smooth surface clear to cloudy**	X	X	X	X	X	X	X	X	X	X	X		X	X	X			X			
F	**Round, smooth to abraded surface, clear to cloudy**			X	X	X	X	X	X	X	X	X	X		X	X			X		X	X
G	**Broken, large visible cracks, cloudy to rusty**				X	X	X	X	X	X												

Table 4.1: A description the various zircon morphologies found in the Nashoba terrane meta-sedimentary rocks including the formation names and grain size fraction that were included in the analyses. L= Large (150-200µm), M= Medium (100-150µm), S= Small (50-100µm).

In summary, in this study only zircon grains with a probability of concordance >0.05 and a Th/U ratio >0.1 were used for detrital zircon analysis, unless there was strong enough evidence to suggest that the zircon was likely derived from a metamorphic protolith. A sample is considered statistically representative if it contains at least 60 usable grains (Fedo *et al.*, 2003). To prevent bias, zircons were picked randomly, regardless of shape, colour, cloudyness, or presence of inclusions and fractures. Finally, all data in this study are reported using $^{206}Pb/^{238}U$ ages for zircons with ages <800 Ma and $^{207}Pb/^{206}Pb$ for zircons with ages >800 Ma.

4.1 SE NASHOBA TERRANE: MARLBORO FORMATION (MLMRC)

4.1.1 *Sample Locations and Description*

Zircon from meta-sedimentary rocks of the Marlboro Formation is rare, and commonly metamict. In order to try to obtain enough grains for a statistical representation, the Marlboro Formation was sampled in four different locations from areas that are mapped as the Marlboro Formation (Hepburn and DiNitto, 1978; Goldsmith, 1991a: Fig. 4.2). Of the approximately 300 lbs of rock processed, a total of 9 zircon grains yielded concordant data. The data were combined (see below).

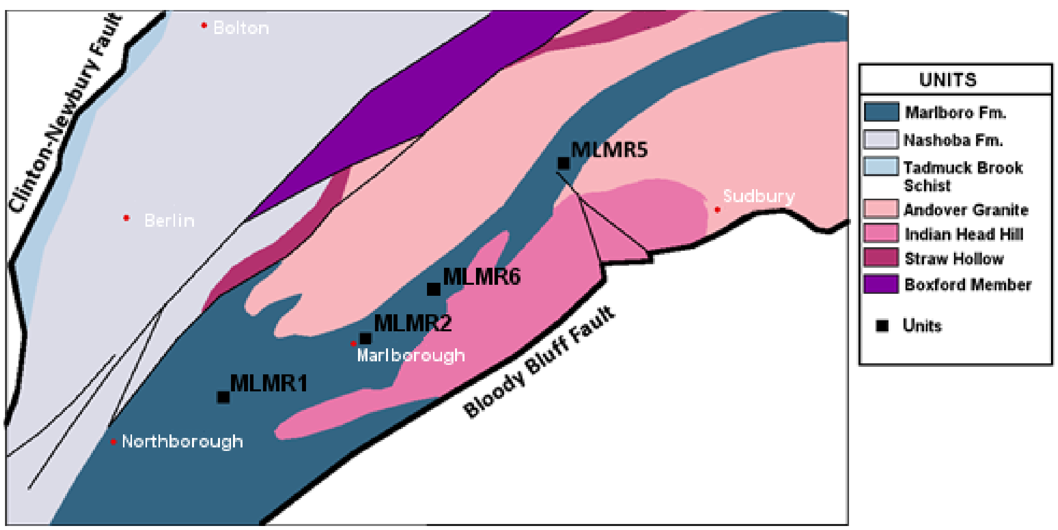

Figure 4.2: Map of Marlboro Formation sample locations, based on Massachusetts Office of the State Geologist Bedrock Map of Massachusetts overlay for Google Earth

Sample MLMR1 (Fig. 4.2) was collected from Hayes Memorial Drive, Marlborough, MA (Appendix A). The outcrop consisted of a rusty-weathering, black to dark-gray garnet-muscovite-biotite-quartz (±sillimanite) schist (Appendix B) interlayered with a dark-gray hornblende-plagioclase-biotite-quartz amphibolite. Garnet and sillimanite are present as thin layers within the schist and the unit is locally mylonitic. The sample was collected from the pelitic layers only. At this location, the Marlboro Formation has previously been sampled for detrital zircons by the United States Geological Survey (USGS) (Walsh *et al.*, 2009); however the USGS was not able to obtain any grains for dating. Of the 9 concordant detrital grains for the Marlboro Formation analysis, 4 were from this location.

Sample MLMR2 (Fig. 4.2) is a silvery to dark-gray, rusty weathering, fine grained garnet-biotite-muscovite-quartz schist (Appendix B). The sample was collected from Main St. in Marlborough, MA (Appendix A). This is the type-locality of Marlboro Formation schist (Emerson, 1917). Of the 9 concordant detrital grains for this analysis, only 1 was obtained from this location.

Sample MLMR5 (Fig. 4.2) was collected from the grounds of the Massachusetts Fire Fighting Academy in Stowe, MA (Appendix A). The hand sample of the MLMR5 unit showed two distinct layers: (1) a muscovite-rich schistose layer and (2) a coarser-grained quartz-rich layer (Appendix B). Large, black, marble-sized quartz crystals were visible within the meta-sedimentary unit. Black quartz forms due to radiation damage of crystal lattice. The radiation damage extended to the zircons, resulting in rusty, amorphous, highly metamict grains.

Sample MLMR6 (Fig. 4.2) was collected from a small outcrop in a housing development in Marlborough, MA (Appendix A). The unit was located along strike with the Main St. exposures. The unit is a rusty, heavily weathered garnet schist (Appendix B). The size of zircon grains in this unit was, in general, very small (≤50µm), which made it difficult to determine the morphology of the grains. The sample was also dominated by titante. Of the 9 concordant zircons, 4 were from this sample.

4.1.2 *Zircon Morphology*

Zircon grains from the combined Marlboro Formation samples were small, typically <100µm. All of the usable grains (from MLMR1, MLMR2, and MLMR6) were clear and rounded to well-rounded (Populations E and F: Fig. 4.1 and Table 4.1). Zircon grains from sample MLMR5 suffered significant metamictization (Population D: Fig. 4.1 and Table 4.1). Energy-dispersive X-ray spectroscopy (EDX) of the MLMR5 zircons confirmed the presence of uraninite inclusions. Uraninite is a mineral that contains uranium and could have formed if the rock was exposed to hydrothermal fluids, which may have leached uranium from the zircons and/or carried uranium into the system (Hoskin and Schaltegger, 2003). Several of the metamict grains did not show uraninite inclusions but appeared to be a bright white color under BSE coupled with the EDX spot, which suggested they were Hf-rich. Because of the uncertainties associated with uraninite inclusions and metamictization, these grains were not analyzed.

4.1.3 *U-Pb Geochronology*

Due to the scarcity of grains in the Marlboro Formation a statistical representation of zircon populations in the formation was not achieved; however, the data obtained from the Marlboro Formation (that has a probability of concordance >0.05 and a Th/U ratio >0.1) is still valid and informative (Table 4.5). The youngest detrital grain from the combined Marlboro samples, mr04a06 (Fig. 4.3), was concordant and yielded a $^{206}Pb/^{238}U$ age of 470 ± 46 Ma (Table 4.5). Zircon mr04a31 (Fig. 4.3) had a Th/U ratio much greater than 0.1 and a probability of concordance >0.05. However, it was removed from the analysis due to the fact that it only had a 61% probability of concordance, it had a substantially older $^{207}Pb/^{206}Pb$ age than mr04a06, and it had abundant cracks and an amorphous shaped core. However, the large uncertainty associated with zircon mr04a06 overlaps the age of zircon mr04a31 and allows for the possibility that the Marlboro Formation might be somewhat younger than 470 Ma. The Marlboro Formation (from outcrop MLMR6) contained the oldest grain found in the Nashoba terrane with a core of 3.36 Ga and a rim of 2.6 Ga. The probability density curve of the Marlboro Formation shows a peak in age at ca. 525 (Fig. 4.4A and B).

mr04a31	mr04a06
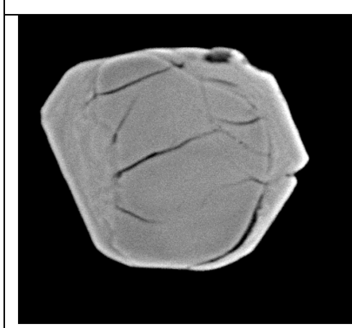	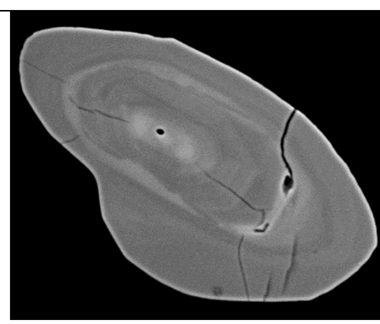
434 ±26	470±46

Figure 4.3: BSE images of zircons mr04a31 and mr04a06. Zircon mr04a31 was not included in the detrital zircon interpretation. Zircon mr04a06 shows zoned core typical of igneous zircons and a metamorphic rim.

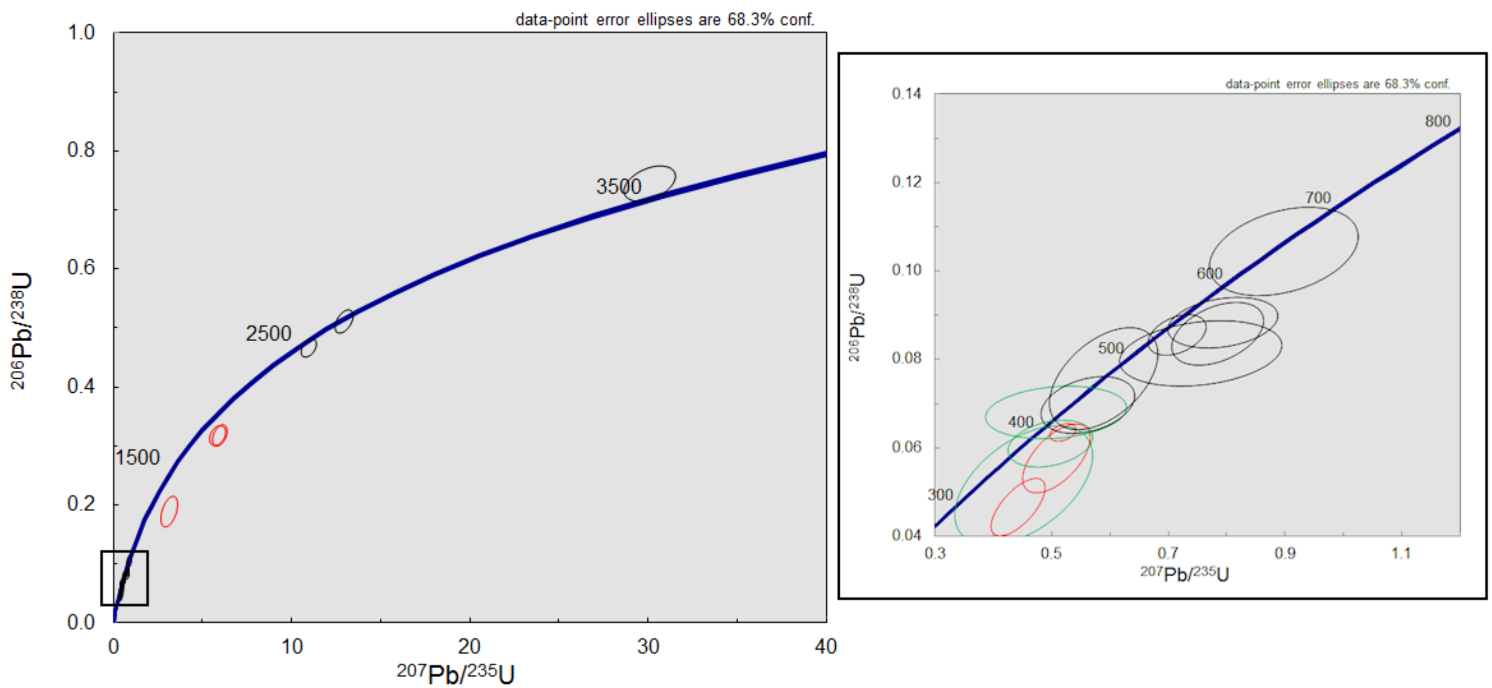

Figure 4.4 A: Concordia diagram of all data from the combined Marlboro Formation (left). Enlarged image of Concordia diagram for youngest zircon ages (right). Black ellipses represent the data that had a probability of concordance > 0.05 and a Th/U >0.1 and were included in the analysis. Red ellipses represent discordant data (< 0.05 probability of concordance) that were not included in this study. Green ellipses represent zircons with a low Th/U ratio (< 0.1) and a texture indicative of being metamorphically grown. The ages of the green ellipses were not included in the detrital zircon analysis but are interpreted in the section on metamorphism (See section 5.8).

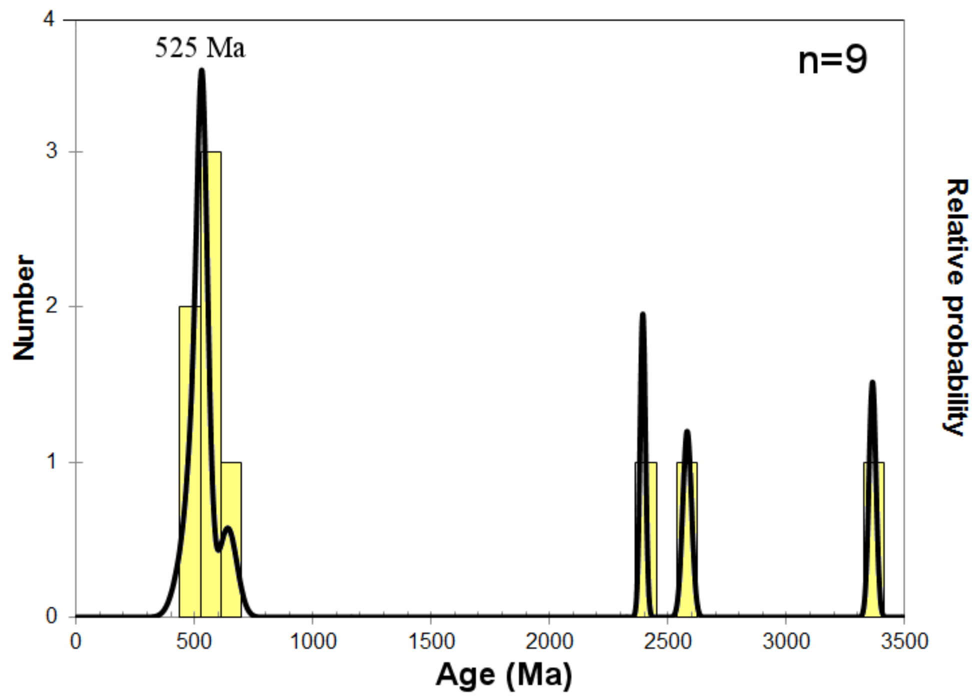

Figure 4.4 B: Probability density diagram of the concordant zircons (>0.05 probability of concordance) from the combined Marlboro Formation. The probability density diagram shows $^{206}Pb/^{238}U$ for zircons < 800 Ma and $^{207}Pb/^{206}Pb$ for zircons >800Ma. The diagram does not include discordant or young, metamorphically grown, zircons.

	Calculated Ages									1/1
MLMRC	**207Pb/ 235U**	**1s error**	**206Pb/ 238U**	**1s error**	**207Pb/ 206Pb**	**1s error**	**Concordia Age**	**2s error**	**Probability of concordance**	**Th/ U**
mr04a06	470	39.2	470	45.7	515	92.8	470	72.1	1.00	0.182
se14a99	571	53.2	504	29.1	715	86.9	514	56.1	0.22	2.968
mr04a05	548	19.5	529	18.0	551	40.8	537	31.3	0.37	0.889
mr04a27	588	29.6	531	27.9	586	28.8	555	48.8	0.07	0.922
mr04a07	593	35.3	545	22.4	879	37.3	555	42.3	0.20	0.871
se14a98	651	45	640	39	679	23	644	68	0.83	0.240
mr04a32	2520	24.0	2467	44.8	2393	11.3	2516	47.8	0.19	0.364
se14a95	2676	24.5	2661	56.0	2581	18.5	2676	48.9	0.77	0.595
se14a94	3490	31.2	3588	73.1	3364	14.6	3490	62.4	0.14	0.356

Table 4.5: U-Pb data from detrital zircon grains of the combined Marlboro Formation with probability of concordance >0.05, a Th/U ratio >0.1, and that were interpreted to be usable for this study (see above). For a complete table of zircon analyses including discordant and metamorphic grains see Appendix C. The ages and associated error used in this study are highlighted in blue.

4.2 SE NASHOBA TERRANE: SHAWSHEEN GNEISS (MLSG1)

4.2.1 *Sample Location and description*

The Shawsheen Gneiss is a paragneiss that is likely derived from volcanic or volcanoclastic material interlayered with sediments (Olzewski, 1980). Samples of the Shawsheen Gneiss were collected from fresh exposures adjacent to the parking lot of an industrial park at 900 Middlesex Turnpike in Billerica, MA (Appendix A). The unit is composed of medium-grained garnet-muscovite-biotite-plagioclase-quartz (± sillimanite) schist to gneiss (Appendix B). The samples were collected at multiple locations around the industrial park to ensure that a statistical representation of detrital zircon populations across layers was analyzed.

4.2.2 *Zircon Morphology*

Approximately 40% of the zircons in the sample consisted of rounded, clear to cloudy grains that retain the typical zircon 4:1 aspect ratio but without any clear faces (population E: Fig. 4.1 and Table 4.1). The second most abundant population consisted of the well rounded, clear to cloudy grains (population F: Fig. 4.1 and Table 4.1), which account for ~30% of the entire zircon population. Many of the remaining grains were cloudy to rusty with various shapes (populations B, C, and G: Fig. 4.1 and Table 4.1); very few grains were faceted with small aspect ratios (population A: Fig. 4.1 and Table 4.1). There is no clear correlation between morphology and the age of the grain, or the Th/U ratio.

4.2.3 *U-Pb Geochronology*

In this sample, 137 grains were analyzed and 100 met the criteria (see section 4.0.1) to be included in this study (Table 4.8). The youngest detrital zircon age of the Shawsheen Gneiss had a ^{206}Pb/^{238}U age of 470±21 Ma based on the weighted average of three detrital grains, mr05a29, mr04a87 and se13a56 (MSWD = 0.25, probability of fit = 0.78; Fig. 4.6). These three grains were selected based on a reasonably high probability of concordance, especially zircon se13a56 (474 ± 13) at 0.96. Zircons with ^{206}Pb/^{238}U ages older than se13a56 (Fig. 4.6) have generally high Th/U ratios and probability of concordance. Zircons se13a69 (446 ± 22 Ma; Appendix C) and mr06a130 (441 ± 21 Ma; Appendix C) had a Th/U ratio greater than 0.1, however, the grains were not included in the weighted average of the youngest detrital ages because of the very low probability of concordance (0.06 and 0.17 respectively). Zircons mr06a157 (672 ± 20 Ma), and se13a61 (1933 ± 24 Ma; Appendix C) had low Th/U but were sufficiently old that they were probably detrital grains from a metamorphic protolith, and therefore included in the detrital zircon analysis.

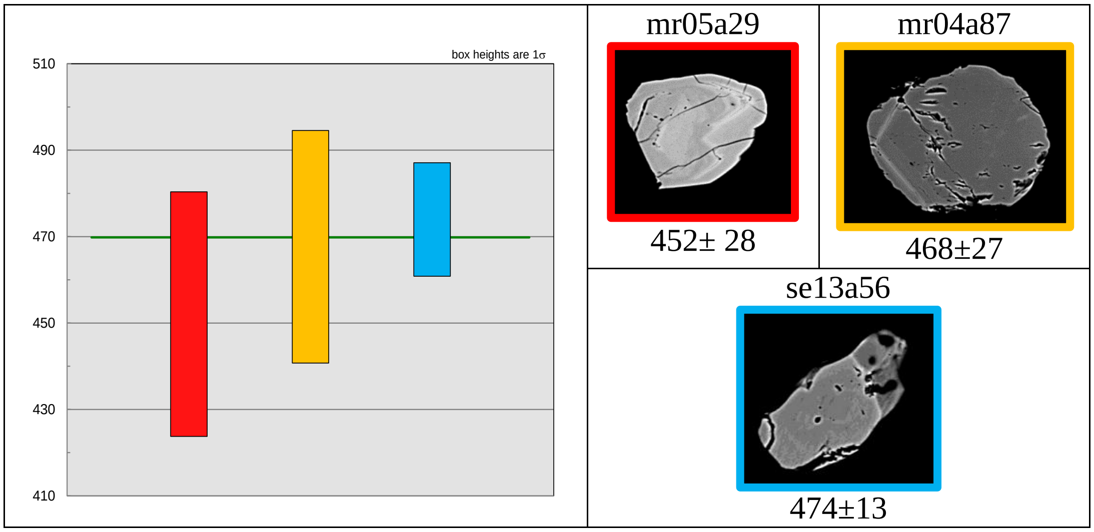

Fig. 4.6: Weighted average of the youngest detrital zircons in the Shawsheen Gneiss, mr05a29, mr04a87 and se13a56. Mean = 468± 20 Ma (MSWD = 0.21, probability of fit = 0.89).

Of the 35 remaining grains that were not included in this analysis, 30 were discordant and 5 were concordant and metamorphic. The discordant grains did not plot on discordia chords and from morphological evidence it was determined that the discordancy was most likely due to cracks, inclusions, or sampling of multiple age domains during the ablation process. No significant information could be gained from these grains. The remaining five grains had a Th/U ratio of < 0.1 and displayed textural evidence indicating metamorphic growth. The weighted average of their ages was at ca. 430 Ma (MSWD = 0.41, probability = 0.87).

The dominant statistical age population in the sample (~40% of the analyses) has a Neoproterozoic age (Ediacaran) of ca. 550 Ma. In addition, there are age clusters in the Mesoproterozoic at ca. 1118 Ma, and in the Paleoproterozoic at ca. 1480 Ma, 1680Ma, and 2065 Ma and a single grain at ca. 2300 Ma.

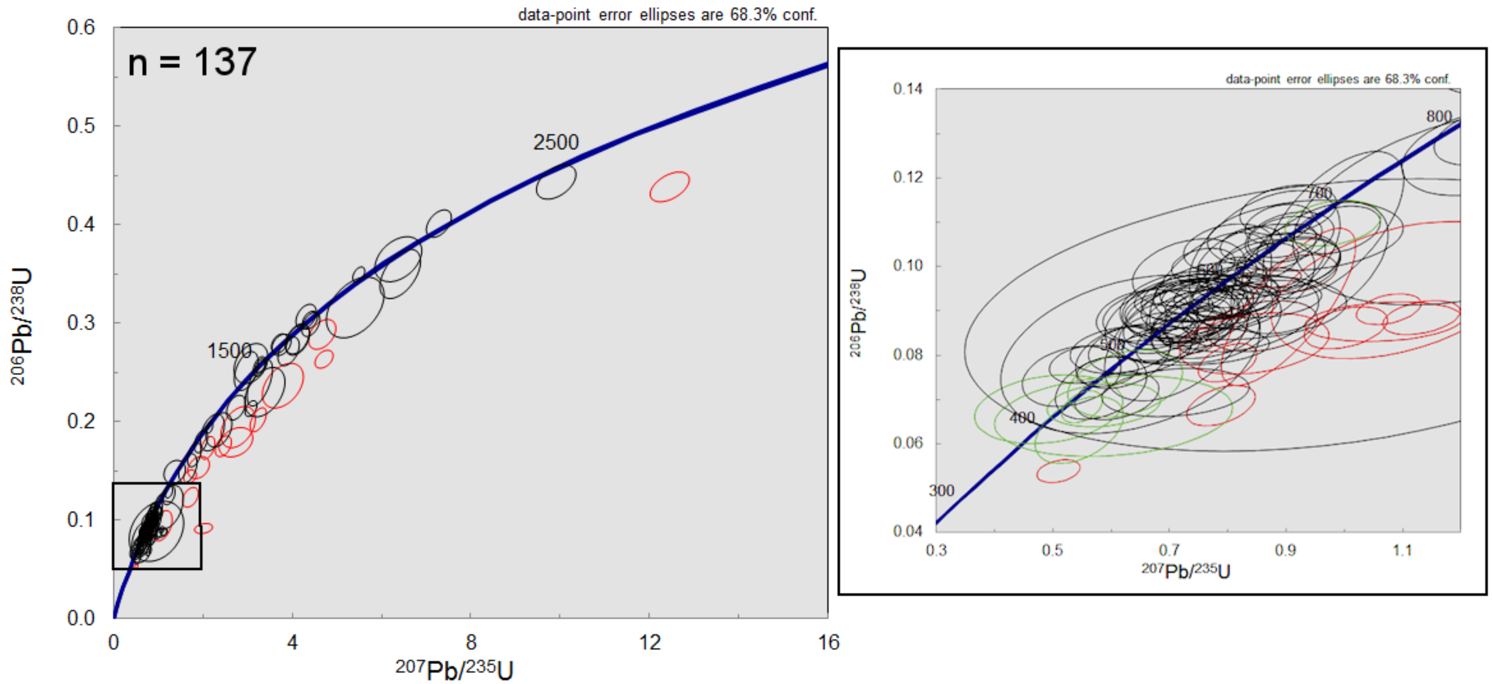

Figure 4.7 A: Concordia diagram of all data from the Shawsheen Gneiss (left). Enlarged image of Concordia diagram for youngest zircon ages between 300 Ma to 800 Ma (right). Black ellipses represent the data that met the criteria of this study and were included in the analysis. Red ellipses represent discordant data (< 0.05 probability of concordance) that was not included in this study. Green ellipses represent zircons with a low Th/U ratio (< 0.1) and a texture indicative of metamorphic growth. The ages of the green ellipses were not included in the detrital zircon analysis but are interpreted in the section on metamorphism (See section 5.8).

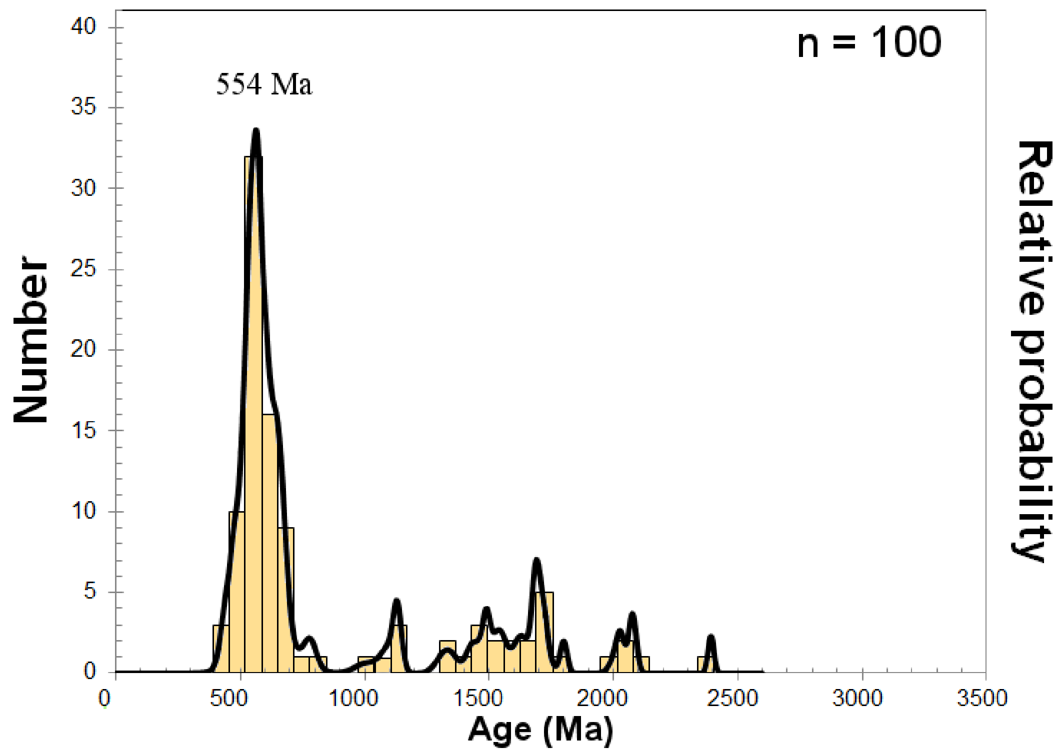

Figure 4.7.B: Probability density diagram of the concordant zircons (>0.05 probability of concordance) from the Shawsheen Gneiss. The probability density diagram shows $^{206}Pb/^{238}U$ for zircons < 800 Ma and $^{207}Pb/^{206}Pb$ for zircons >800Ma. The diagram does not include discordant or young, metamorphically grown, zircons.

Table 4.8 **Calculated Ages** 1/4

MLSG1	207Pb/ 235U	1s error	206Pb/ 238U	1s error	207Pb/ 206Pb	1s error	Concordia Age	2s error	Probability of concordance	Th/U
mr05a29	466	33	452	28	613	28	457	50	0.69	0.342
mr06a41	492	41	458	30	631	42	467	55	0.42	0.062
mr04a87	433	37	468	27	524	47	457	49	0.37	0.624
se13a56	473	22	474	13	566	43	474	25	0.96	0.113
se13a57	448	26	484	17	523	46	475	31	0.18	0.537
mr06a47	490	34	494	28	384	48	492	50	0.91	0.362
se13a60	498	91	497	70	549	43	498	127	1.00	0.582
mr05a48	487	36	503	21	616	52	500	39	0.67	0.306
se13a71	508	36	505	23	555	51	505	43	0.92	1.096
mr06a119	563	50	508	17	1117	52	511	33	0.29	0.108
mr06a140	530	27	510	16	612	50	514	30	0.47	0.731
mr06a137	536	21	516	20	449	35	525	34	0.37	0.528
mr06a85	546	49	517	55	563	46	535	88	0.59	0.406
mr05a51	528	27	526	18	633	42	527	34	0.96	0.580
mr05a18	575	35	526	23	553	49	536	42	0.18	0.929
mr06a111	566	24	530	17	825	43	539	31	0.15	0.585
mr06a117	541	14	535	11	531	26	537	20	0.70	0.597
mr06a100	529	25	536	21	525	34	534	37	0.79	0.789
mr06a75	585	42	538	34	716	54	553	62	0.29	0.744
mr06a139	557	24	540	18	606	41	545	32	0.49	0.655
mr06a126	542	45	542	35	671	45	542	63	1.00	0.656
mr06a131	567	22	543	20	632	36	552	35	0.32	0.599
mr06a65	574	14	544	12	600	26	555	22	0.05	0.886
mr06a97	568	35	548	24	654	54	553	44	0.58	0.772
mr05a30	511	32	550	23	537	47	538	41	0.25	0.560
mr06a149	540	46	550	26	754	50	548	50	0.83	1.559
mr06a118	554	39	551	24	670	51	552	45	0.94	0.337

Table 4.8 **Calculated Ages**

MLSG1	207Pb/ 235U	1s error	206Pb/ 238U	1s error	207Pb/ 206Pb	1s error	Concordia Age	2s error	Probability of concordance	Th/U
mr06a56	610	49	552	34	916	43	566	63	0.26	0.633
mr06a96	538	30	556	18	591	50	553	33	0.57	0.651
mr04a90	612	65	559	28	1196	65	564	54	0.43	0.839
mr06a125	558	44	561	28	693	67	560	52	0.94	0.608
mr05a32	569	23	562	14	695	44	564	26	0.76	0.383
se13a80	599	27	563	17	685	39	570	32	0.20	0.688
mr06a99	607	26	563	19	784	29	575	36	0.11	0.551
mr06a50	594	18	564	13	675	32	573	24	0.12	0.631
mr04a89	553	43	564	29	623	57	561	54	0.81	0.618
mr06a51	566	41	571	19	604	66	570	36	0.92	0.724
mr05a53	632	35	572	16	958	55	578	32	0.10	1.059
mr06a48	562	34	573	21	660	64	570	40	0.77	0.818
mr05a43	564	22	574	15	561	40	572	27	0.65	0.487
mr06a135	596	34	576	18	824	55	579	35	0.57	0.610
mr06a156	603	28	576	20	628	42	583	37	0.37	0.565
mr05a21	563	22	579	13	608	41	576	24	0.49	0.461
mr06a59	582	38	581	26	602	60	581	47	0.98	1.541
mr06a60	580	40	584	50	318	71	581	75	0.92	0.444
mr06a46	621	38	591	39	698	42	606	66	0.46	0.722
mr05a08	598	14	597	11	626	18	597	20	0.96	1.087
mr05a42	610	15	599	15	650	18	604	26	0.51	0.644
mr06a15	600	16	606	14	534	32	604	24	0.72	0.300
mr06a148	559	38	607	29	366	66	590	52	0.23	0.509
mr06a88	673	47	613	57	788	44	654	89	0.25	0.769
mr05a49	653	32	615	26	901	44	627	46	0.27	0.343
mr05a37	573	21	616	15	551	34	603	27	0.05	0.391
mr05a50	657	29	619	21	841	47	629	39	0.21	0.682

Table 4.8 **Calculated Ages** 3/4

MLSG1	207Pb/ 235U	1s error	206Pb/ 238U	1s error	207Pb/ 206Pb	1s error	Concordia Age	2s error	Probability of concordance	Th/U
mr06a151	645	37	620	26	787	39	626	48	0.52	0.894
mr06a136	628	40	621	33	640	66	624	58	0.86	0.880
mr06a95	635	19	622	16	637	30	626	28	0.53	0.851
mr05a38	632	47	633	54	600	48	632	85	0.99	0.472
mr06a57	597	29	639	21	538	41	626	37	0.16	0.560
mr06a147	652	18	641	19	596	23	647	32	0.59	0.470
mr05a58	619	19	645	15	604	26	636	26	0.20	0.789
mr06a145	655	27	653	22	647	41	654	39	0.96	0.797
mr06a127	651	23	654	18	664	34	653	32	0.90	0.134
mr06a146	669	58	656	31	892	52	658	58	0.82	0.162
mr06a86	698	25	663	21	650	45	675	37	0.19	0.710
mr06a110	694	41	669	64	630	28	693	82	0.62	0.278
mr05a07	645	21	670	17	623	31	661	30	0.26	0.847
mr06a157	694	28	672	20	732	38	678	36	0.46	0.074
mr05a52	654	29	689	22	737	48	678	39	0.26	0.636
mr05a47	817	97	693	85	1311	26	735	153	0.24	0.203
mr06a79	818	42	764	37	985	54	785	65	0.24	0.205
mr06a129	818	25	782	23	800	31	797	40	0.20	0.215
mr05a40	876	68	897	44	1005	45	892	80	0.77	0.601
mr06a68	995	52	918	55	1084	32	958	91	0.19	0.144
mr06a106	1048	37	994	45	1111	27	1029	68	0.21	0.160
mr06a116	1164	16	1145	21	1126	14	1158	30	0.36	0.331
mr06a49	1101	34	1067	41	1138	16	1089	62	0.42	0.307
mr06a80	1185	56	1118	67	1315	34	1160	103	0.33	0.542
mr06a45	1231	58	1132	62	1347	33	1183	102	0.15	0.260
mr05a28	1474	22	1471	34	1426	22	1473	43	0.94	1.670
mr05a59	1427	62	1487	69	1464	27	1452	105	0.44	0.217

Table 4.8 **Calculated Ages** 4/4

MLSG1	207Pb/ 235U	1s error	206Pb/ 238U	1s error	207Pb/ 206Pb	1s error	Concordia age	2s error	Probability of concordance	Th/U
mr05a33	1475	45	1387	82	1486	28	1476	89	0.18	0.495
mr05a17	1478	17	1476	23	1490	14	1477	32	0.92	0.295
mr05a41	1340	38	1253	44	1536	25	1305	69	0.06	0.204
mr06a78	1575	26	1590	33	1544	26	1580	47	0.66	0.639
se13a59	1401	46	1448	67	1581	40	1409	88	0.45	0.198
mr05a57	1584	30	1584	36	1618	22	1584	54	0.99	0.539
mr06a61	1618	33	1550	49	1648	22	1605	64	0.14	0.480
mr06a87	1658	35	1608	52	1681	13	1648	68	0.31	0.416
mr06a98	1658	35	1614	51	1693	17	1649	68	0.37	0.950
mr06a101	1716	25	1687	40	1694	14	1712	50	0.44	0.920
mr06a70	1502	69	1336	87	1702	25	1442	131	0.05	0.298
mr05a22	1696	29	1726	41	1720	31	1702	54	0.45	0.317
mr05a23	1712	21	1708	30	1721	15	1711	40	0.89	0.341
se13a61	1899	14	1934	24	1800	14	1902	28	0.12	0.053
mr06a138	2035	41	1937	79	2013	25	2033	82	0.15	1.131
mr06a115	1886	68	1772	100	2029	16	1861	132	0.23	0.112
mr04a88	2029	48	2007	71	2073	14	2025	92	0.75	1.028
mr05a09	2147	23	2176	43	2082	15	2148	45	0.44	0.836
mr06a107	2427	27	2367	51	2392	12	2423	54	0.20	0.289

Table 4.8: U-Pb data from detrital zircon grains of the Shawsheen Gneiss with probability of concordance >0.05 and a Th/U ratio >0.1. For a complete table of zircon analyses including discordant and metamorphic grains see Appendix C. The ages and associated error used in this study are highlighted in blue.

4.3 NW NASHOBA TERRANE: NASHOBA FORMATION GNEISS (MLNB1)

4.3.1 *Sample Location and description*

The Nashoba Formation gneissose unit was freshly exposed due to blasting for a new housing development. The sample was collected from Church St. Village, Northboro, MA (Appendix A). The sample is a garnet-biotite-muscovite-quartz-(±sillimanite) gneiss (Appendix B). The unit contained inter-bedded layers of mylonitic gneiss with a few ~4cm thick strongly sheared quartz veins. Areas with large quartz inclusions were not used in this study.

4.3.2 *Zircon Morphology*

The most abundant zircon morphology in the Nashoba Formation gneiss consisted of slightly rounded, clear to cloudy grains (population E: Fig. 4.1 and Table 4.1) and constituted ~55% of this sample. The second most abundant population consisted of well rounded, clear to cloudy grains (population F: Fig. 4.1 and Table 4.1) which account for ~30% of the total zircon population. The remaining grains were faceted with large aspect ratios (population B: Fig. 4.1 and Table 4.1) or broken with large visible cracks (population G: Fig. 4.1 and Table 4.1). The majority of the grains that retained their typical euhedral shape (population B: Fig. 4.1 and Table 4.1) gave ages within the 500- 600 Ma age range.

4.3.3 *U-Pb Geochronology*

Of the 136 grains that were analyzed in this sample, 79 met the criteria to be included in this study (Table 4.12). The 461±19 Ma youngest detrital zircon age of the Nashoba Formation gneiss was determined by taking the weighted average (Fig. 4.9) of the youngest three grains (MSWD = 0.06, probability of fit = 0.94). The weighted average was taken due uncertainties regarding their moderate probability of concordance but high Th/U ratio. All of the zircons older than these three grains generally had a high probability of concordance and a Th/U ratio >0.1. The dominant statistical age population in the sample (~86% of the analyses) is ca. 532 Ma (Fig. 4.10.B). In addition there are a few Mesoproterozoic, Paleoproterozoic and Achean age clusters.

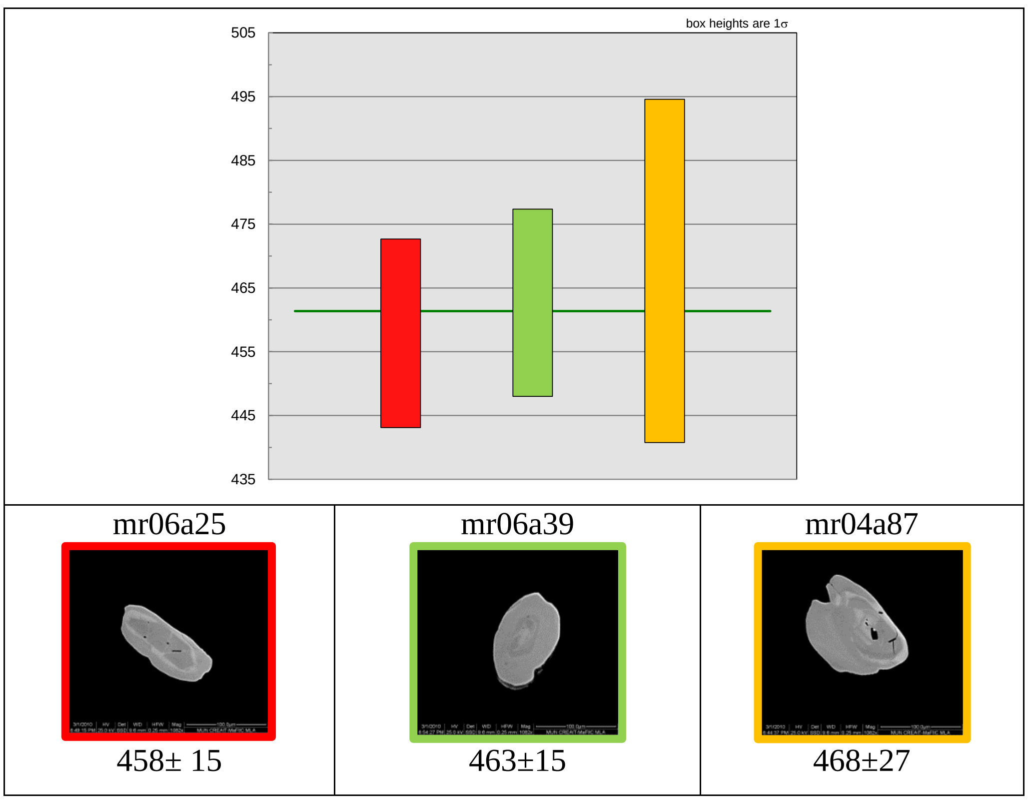

Fig. 4.9: Weighted average of the youngest three detrital zircon grains in sample Nashoba Formation gneiss, mr06a25, mr06a39, and mr04a87. Mean = 461±19 (MSWD = 0.06, probability of fit = 0.94)

Of the 57 remaining grains, 35 were discordant. As in sample MLSG1, the discordant grains are most likely the result of Pb-loss along unavoidable cracks, the presence of inclusions, or sampling of multiple age domains during the ablation process and are not included in the interpretation. Grains mr02a26, mr02a45, mr04a52, mr02a54, mr02a86 (Appendix C) were considered unreliable because of their large uncertainty and were removed from the detrital zircon analysis.

The Nashoba Formation gneiss contained abundant grains (22) that were concordant, but had a low Th/U ratio (<0.1) which indicated that they were of metamorphic origin. The $^{206}Pb/^{238}U$ ages of these metamorphic zircons varied between 353±10 Ma and 429±12 Ma (Fig. 4.11). There are slight peaks in ages at ca. 360 Ma, and at ca. 400 Ma. It should be noted that zircon grains mr02a34, mr02a10, mr05a82, mr02a49, mr02a35, mr02a45, mr02a58, mr06a30 and mr04a61 (Appendix C) yielded $^{206}Pb/^{238}U$ ages between 477 Ma and 541 Ma. Because there are zircons of the same age in this and in other samples with Th/U ratio's > 0.1 and with high probability of concordance, it is reasonable to assume that these zircons could not be metamophically grown at the same time that others were depositing. Therefore, these grains must be detrital zircon grains derived from a metamorphic protolith. Zircons mr02a44, mr06a28 and mr02a17 (appendix C) have Th/U ratios > 0.1 but previous studies have shown that metamorphism was occurring during this time period (Hepburn *et al.,* 1995; Jerden *et al.,* 1997; Stroud *et al.,* 2004). Thus, these grains were included in the metamorphic population and were not included in this study.

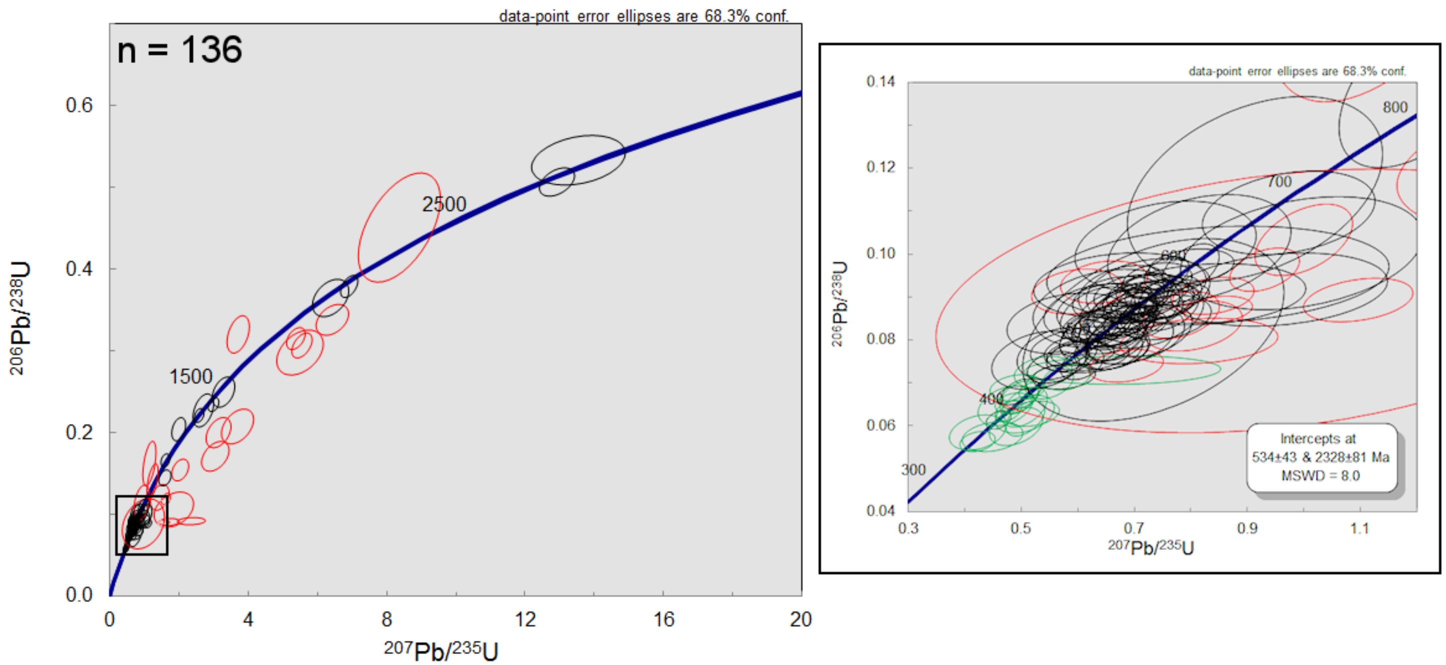

Figure 4.10A: Concordia diagram of all data from the Nashoba Formation gneiss (left). Enlarged image of Concordia diagram for youngest zircon ages between 300 Ma to 800 Ma (right). Black ellipses represent the data that met the criteria of this study and were included in the analysis. Red ellipses represent discordant data (< 0.05 probability of concordance) that was not included in this study. Green ellipses represent zircons with a low Th/U ratio (< 0.1) and a texture indicative of being metamorphically grown. The ages of the yellow ellipses were not included in the detrital zircon analysis but are interpreted in the section on metamorphism (See section 5.8).

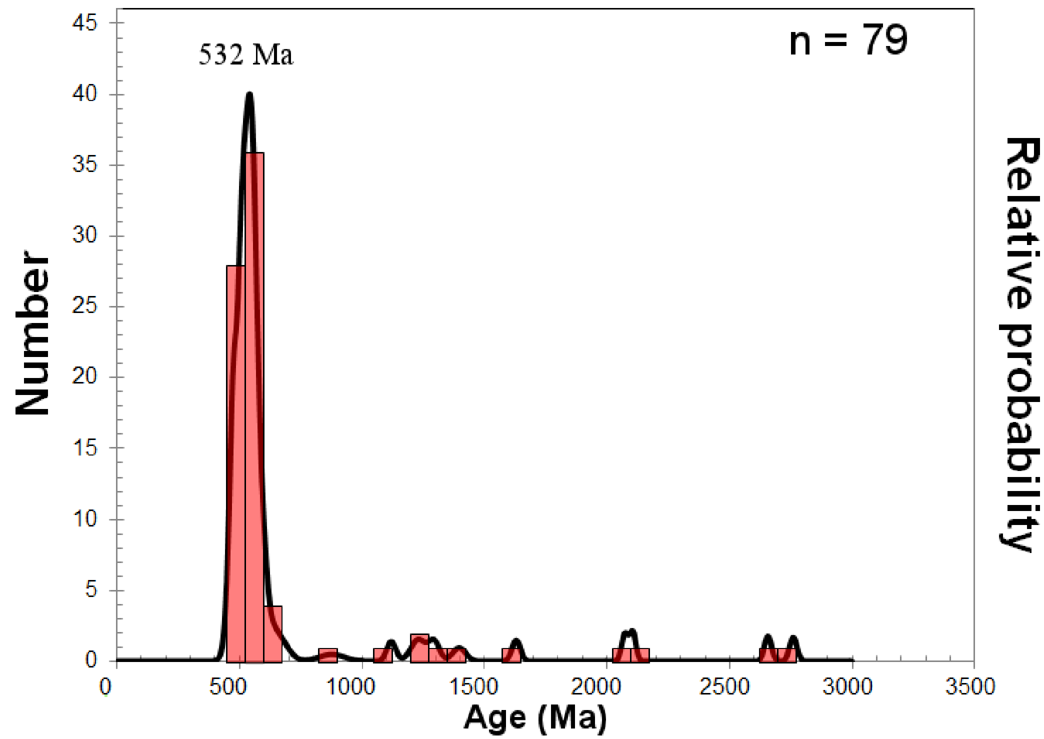

Figure 4.10 B: Probability density diagram of the concordant zircons (>0.05 probability of concordance) from sample the Nashoba Formation gneiss. The probability density diagram shows $^{206}Pb/^{238}U$ for zircons < 800 Ma and $^{207}Pb/^{206}Pb$ for zircons >800Ma. The diagram does not include discordant or young, metamorphically grown, zircons.

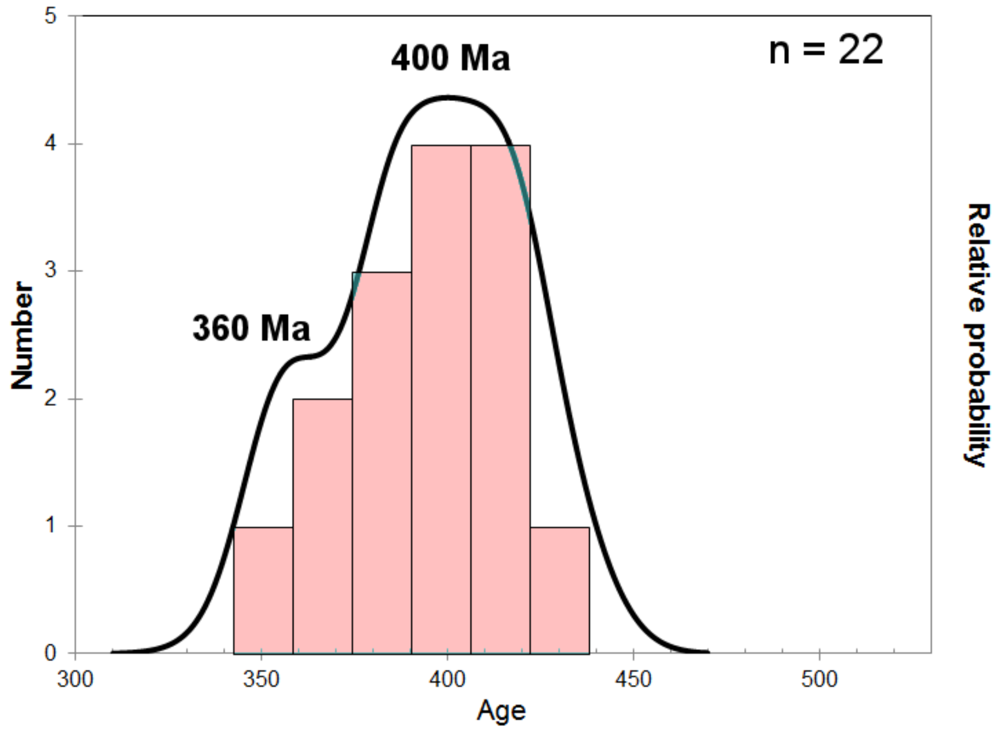

Figure 4.11: Probability density diagram of $^{206}Pb/^{238}U$ ages of metamorphic zircons (Th/U < 0.1) in the Nashoba Formation gneiss, excluding those that are older than ca. 461 Ma.

Table 4.12 **Calculated Ages** 1/3

MLNB1	207Pb/ 235U	1s error	206Pb/ 238U	1s error	207Pb/ 206Pb	1s error	Concordia age	2s error	Probability of concordance	Th/U
mr06a25	449	20	458	15	405	38	455	27	0.67	0.175
mr06a39	482	16	463	15	513	31	471	26	0.26	0.439
mr04a87	433	37	468	27	524	47	457	49	0.37	0.624
mr06a17	466	16	471	13	339	41	469	23	0.76	0.289
mr02a31	488	30	476	15	641	49	478	29	0.69	0.208
mr06a19	454	31	477	24	414	54	469	43	0.47	0.643
mr02a34	482	23	477	11	657	49	478	22	0.82	0.050
mr02a06	464	17	480	13	477	36	475	24	0.39	0.445
mr06a20	517	20	481	17	556	38	494	31	0.09	0.174
mr06a07	490	43	483	21	444	46	484	41	0.87	0.591
mr02a18	515	27	484	19	769	44	491	35	0.26	0.372
mr02a10	534	31	497	23	661	26	508	42	0.26	0.081
mr04a52	482	16	499	17	428	25	490	28	0.34	1.101
mr05a82	520	21	501	22	622	30	511	36	0.40	0.097
mr02a49	505	31	503	27	494	65	504	47	0.96	0.028
mr02a35	535	38	504	27	586	46	512	50	0.43	0.027
mr06a14	521	15	504	11	584	25	509	19	0.27	1.068
mr05a87	554	30	509	24	647	44	523	44	0.16	0.245
mr05a89	516	19	511	17	526	26	513	30	0.80	1.366
mr04a62	513	28	512	23	614	34	513	41	0.97	0.724
mr04a44	493	14	513	13	464	24	504	23	0.21	0.869
mr02a58	494	19	514	14	452	46	508	26	0.30	0.090
mr05a79	498	25	515	15	494	59	511	28	0.50	0.608
mr05a91	518	25	516	22	514	30	517	39	0.95	0.763
mr02a85	517	29	516	19	497	61	516	35	0.97	0.220
mr06a26	537	16	517	16	487	29	526	27	0.25	0.365
mr05a81	468	47	519	28	508	68	508	52	0.29	1.054

Table 4.12 **Calculated Ages** 2/3

MLNB1	207Pb/ 235U	1s error	206Pb/ 238U	1s error	207Pb/ 206Pb	1s error	Concordia age	2s error	Probability of concordance	Th/U
mr02a32	532	17	524	14	462	32	527	25	0.65	1.074
mr02a80	570	32	527	20	952	35	536	38	0.20	0.321
mr02a78	544	13	531	13	537	22	537	22	0.36	2.266
mr04a71	499	27	531	26	508	30	516	43	0.29	1.120
mr04a68	526	25	532	23	600	19	529	39	0.85	0.784
mr02a13	550	41	532	31	627	30	537	57	0.68	0.929
mr06a35	522	27	534	21	494	34	530	37	0.67	1.175
mr02a42	500	40	535	26	577	49	526	47	0.40	1.040
mr06a36	532	24	535	22	503	22	534	39	0.90	0.695
mr06a30	535	19	538	12	650	37	537	23	0.86	0.084
mr02a24	548	28	539	18	522	65	541	34	0.74	0.806
mr05a70	510	36	539	24	536	30	531	44	0.44	0.806
mr05a69	509	53	540	36	505	57	532	65	0.57	0.786
mr04a61	574	21	541	21	736	17	557	35	0.13	0.040
mr04a54	537	16	543	16	567	16	540	27	0.70	1.869
mr04a77	542	15	544	11	601	26	543	21	0.92	0.674
mr05a92	575	17	546	13	572	36	555	24	0.10	1.006
mr05a78	539	23	551	16	503	40	548	29	0.64	0.880
mr06a24	561	26	551	18	509	64	554	34	0.72	0.631
mr05a71	522	33	552	21	591	38	545	39	0.37	0.882
mr05a90	562	18	553	15	591	34	556	27	0.65	1.129
mr02a76	576	21	556	19	798	48	564	33	0.39	0.654
mr04a58	552	15	558	12	501	36	556	22	0.69	2.240
mr04a80	585	21	559	10	866	35	562	20	0.22	0.515
mr06a06	538	27	559	18	590	43	553	33	0.46	0.433
mr04a90	612	65	559	28	1196	65	564	54	0.43	0.839
mr02a36	529	33	562	24	471	55	552	43	0.33	1.760

Table 4.12 **Calculated Ages** **3/3**

MLNB1	207Pb/ 235U	1s error	206Pb/ 238U	1s error	207Pb/ 206Pb	1s error	Concordia age	2s error	Probability of concordance	Th/U
mr04a89	553	43	564	29	623	57	561	54	0.81	0.618
mr02a33	558	25	564	15	559	47	563	28	0.80	0.319
mr06a05	681	66	566	33	1226	42	578	65	0.10	0.371
mr02a25	554	17	572	11	509	38	567	20	0.33	0.781
mr04a78	523	61	572	29	813	71	565	56	0.43	0.796
mr02a86	562	24	577	17	526	45	573	30	0.55	1.024
mr04a63	624	110	586	44	1043	55	589	86	0.74	1.003
mr04a41	572	15	588	15	557	21	581	25	0.34	0.640
mr06a37	605	60	623	48	808	28	616	85	0.79	0.268
mr05a77	571	61	624	41	570	38	610	75	0.41	0.396
mr04a51	690	52	671	37	897	50	676	68	0.72	0.650
mr02a55	968	33	993	30	877	53	982	50	0.51	0.590
mr04a67	1110	46	1201	50	1119	19	1146	77	0.10	0.366
mr06a18	963	47	874	36	1226	27	900	66	0.08	0.139
mr02a87	1326	54	1322	71	1243	40	1325	101	0.95	0.201
mr05a80	1293	26	1291	29	1295	21	1292	46	0.94	0.371
mr02a16	1404	27	1360	30	1396	27	1385	46	0.18	0.315
mr04a42	1476	51	1439	63	1629	17	1463	93	0.57	0.272
mr04a88	2029	48	2007	71	2073	14	2025	92	0.75	1.028
mr04a82	2101	21	2073	42	2105	13	2100	43	0.45	0.950
mr02a41	2674	25	2644	49	2656	15	2673	49	0.50	0.846
mr04a49	2718	62	2757	84	2759	15	2730	112	0.66	0.898

Table 4.12: U-Pb data from detrital zircon grains of the Nashoba Formation gneiss with a probability of concordance >0.05 and a Th/U ratio >0.1. For a complete table of zircon analyses including discordant and metamorphic grains see Appendix C. The ages and associated error used in this study are highlighted in blue.

4.4 NW NASHOBA TERRANE: NASHOBA FORMATION SCHIST (MLNS1)

4.4.1 *Sample Location and description*

The Nashoba Formation schistose unit was collected from Green St. Northboro, MA (Appendix A). The sample is a garnet-muscovite-biotite-quartz-(±sillimanite) schist (Appendix B). Of the abundant schistose units in the Nashoba terrane this sample was selected because of its minimal quartz vein inclusions.

4.4.2 *Zircon Morphology*

The most abundant zircon morphology in the Nashoba Formation gneiss consisted of round, clear to cloudy grains (population F: Fig. 4.1 and Table 4.1) and constituted ~90% of this sample. The remaining grains were rounded with short aspect ratios (Population E: Fig. 4.1 and Table 4.1) and a single faceted grain within the large grains size fraction (Population B: Fig. 4.1 and Table 4.1).

4.4.3 *U-Pb Geochronology*

Of the 140 grains analyzed in this sample, 4 met the criteria for being included in the detrital zircon study (Section 4.0.1). The youngest detrital zircon in the Nashoba Formation schistose unit had a $^{206}Pb/^{238}U$ age of 477 ± 32 Ma. The remaining three detrital grains had $^{206}Pb/^{238}U$ ages of 538± 20 Ma, 611± 94 Ma, and a $^{207}Pb/^{206}Pb$ 1692 ± 32 Ma. Although a statistically representative sample for provenance studies (see above) could not be achieved for this unit, the Nashoba Formation schistose unit did provide abundant metamorphic data, which is helpful in understanding the ages of metamorphism experienced by the Nashoba terrane as a whole.

Of the 136 remaining grains, 18 were discordant. Age ranges for the metamorphic zircons of the Nashoba Formation schistose unit range from 327 Ma to 430 Ma. The relative probability curve of the data (Fig. 4.13) shows a single peak at 367 Ma. The single peak in the frequency curve of the data indicates that the uncertainty was too large to differentiate between closely spaced metamorphic events as are known based on the dating of metamorphic monazites (Stroud *et al.*, 2009).

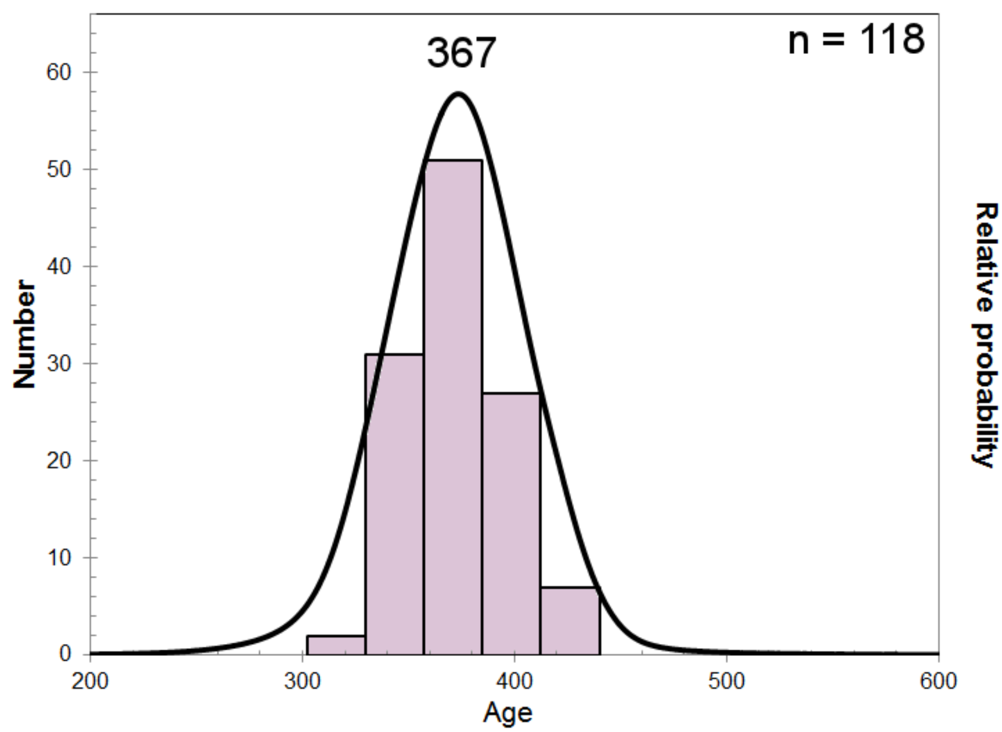

Figure 4.13 Probability Density diagram of concordant zircons (>0.05 probability of concordance) with a low Th/U ratio (<0.1) from the Nashoba Formation schist. The probability density diagram shows $^{206}Pb/^{238}U$ for zircons < 800 Ma

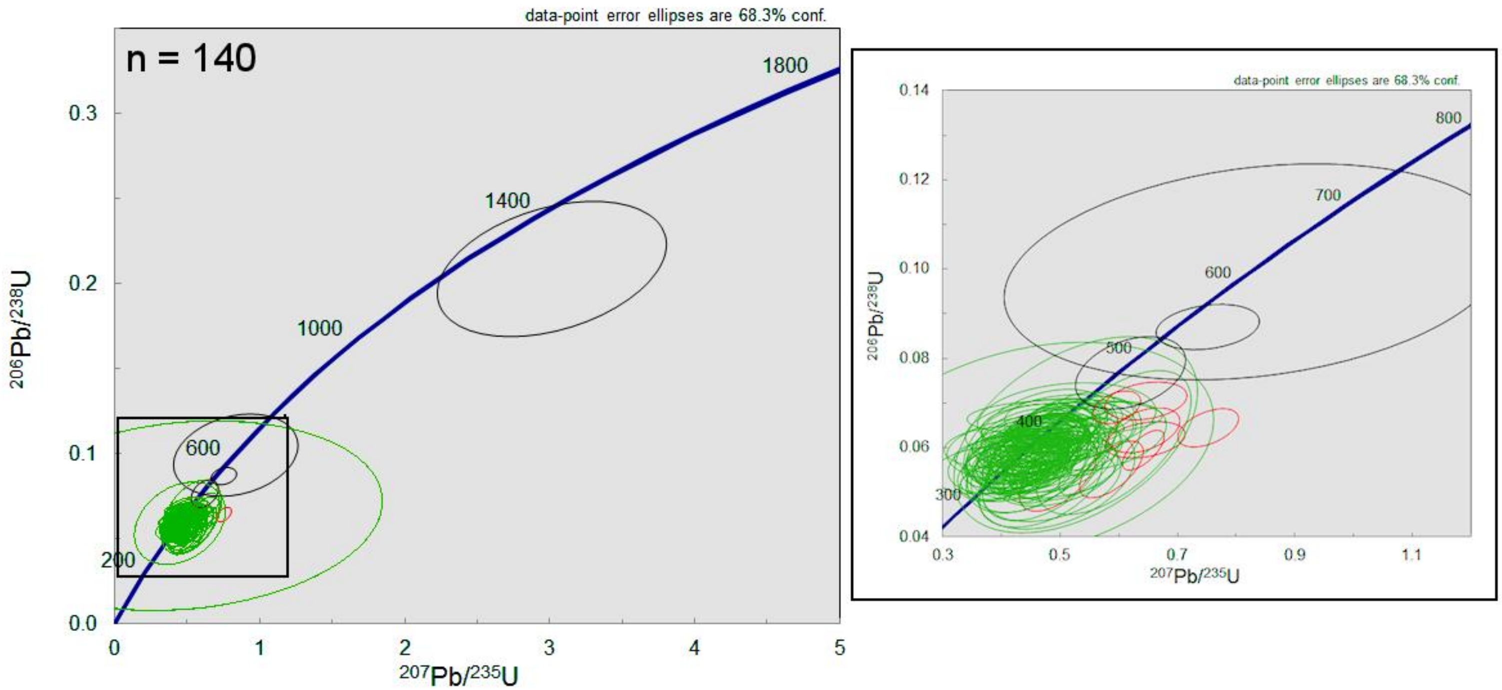

Figure 4.14.A: Concordia diagram of all data from the Nashoba Formation schist (left). Enlarged image of Concordia diagram for youngest zircon ages between 300 Ma to 800 Ma (right). Black ellipses represent the data that met the criteria of this study and were included in the analysis. Red ellipses represent discordant data (< 0.05 probability of concordance) that was not included in this study. Green ellipses represent zircons with a low Th/U ratio (< 0.1) and a texture indicative of being metamorphically grown. The ages of the green ellipses were not included in the detrital zircon analysis but are interpreted in the section on metamorphism (See section 5.8).

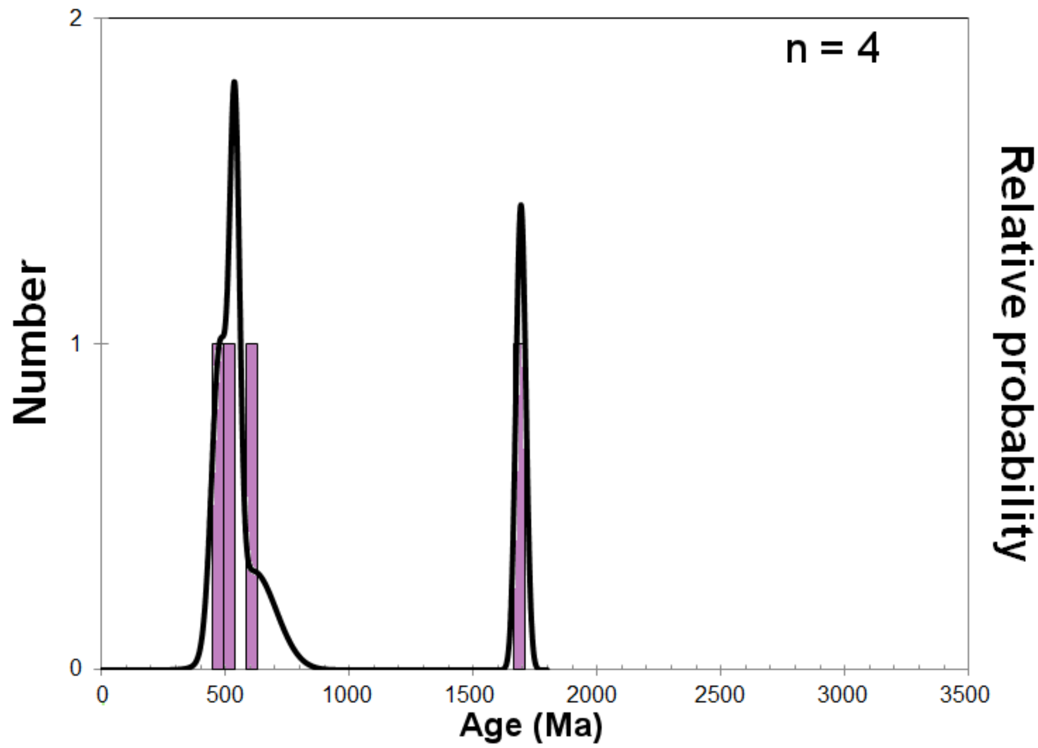

Figure 4.14.B: Probability density diagram of the concordant zircons (>0.05 probability of concordance) from the Nashoba Formation schistose unit. The probability density diagram shows $^{206}Pb/^{238}U$ for zircons < 800 Ma and $^{207}Pb/^{206}Pb$ for zircons >800Ma. The diagram does not include discordant or young, metamorphically grown, zircons.

MLNS1	207Pb/ 235U	1s error	206Pb/ 238U	1s error	207Pb/ 206Pb	1s error	Concordia Age	2s error	Probability of concordance	Th/ U
	Calculated Ages									1/1
se13a22	490	38.9	477	32.1	448	38.4	481	57.4	0.75	0.286
se10a164	569	33.7	538	19.9	739	38.2	544	37.7	0.37	1.161
se13a13	616	157.0	611	93.7	942	57.8	612	175.8	0.98	0.273
se10a209	1411	131.9	1223	140	1692	19.9	1312	233.8	0.23	0.546

Table 4.15: U-Pb data from detrital zircon grains of the Nashoba Formation schist with probability of concordance >0.05 and a Th/U ratio >0.1. For a complete table of zircon analyses including discordant and metamorphic grains see Appendix C. The ages and associated error used in this study are highlighted in blue.

4.5 NW NASHOBA TERRANE: NASHOBA FORMATION CALC-SILICATE (MLBM1)

4.5.1 *Sample Location and description*

The Nashoba Formation calc-silicate gneiss was collected from an outcrop in the spillway of a flood control dam in Berlin, MA (Appendix A). The outcrop contained rock types ranging from rusty garnet-bearing schist in the northern end, to calc-silicate gneiss, to amphibolite approximately 100m south of the main outcrop. The calc-silicate gneiss sample contains diopside, actinolite and phlogopite with abundant biotite and muscovite from the originally more dolomitic layers that are preserved as ca. 3 x 6 cm swirling lenses (Appendix B; Hepburn and Munn, 1984). It also contained abundant titanite. The unit is deformed with a zone of shearing separating the more calcareous layers of the outcrop from the northern schistose layers. Samples were taken away from the zone of shearing and included a mixture of rocks with or without the mica lenses.

4.5.2 *Zircon Morphology*

Approximately 56% of the zircons in the sample consisted of rounded, clear to cloudy grains that retain the typical igneous zircon 4:1 aspect ratio but without any clear faces (population E: Fig. 4.1 and Table 4.1). The second most abundant population was the well rounded, clear to cloudy grains (population F: Fig. 4.1 and Table 4.1), which account for ~31% of the entire zircon population. Many of the remaining grains were prismatic with both long and short aspect ratios (Populations A and B: Fig. 4.1 and Table 4.1). There is no clear correlation between morphology and the age of the grain, or the Th/U ratio. Abundant cracks are present in nearly every zircon grain.

4.5.3 *U-Pb Geochronology*

The $^{206}Pb/^{238}U$ ages of the zircons in the Nashoba terrane calc-silicate are much younger than adjacent units and range from 310 ± 35 Ma to 500 ± 21Ma (Fig. 4.16). However, unlike in MLNS1 the zircons of the calc-silicate unit have Th/U ratios > 0.1. If these grains are truly detritus from an igneous protolith, then deposition occurred at the same time as metamorphism only a few km away. This appears impossible given the temperature and burial pressure necessary for metamorphism to the amphibolite facies. Also, the Nashoba Formation is crosscut by several igneous rocks that are older than 310 Ma (Hepburn, 2004), also suggesting the age of deposition must be older than that.

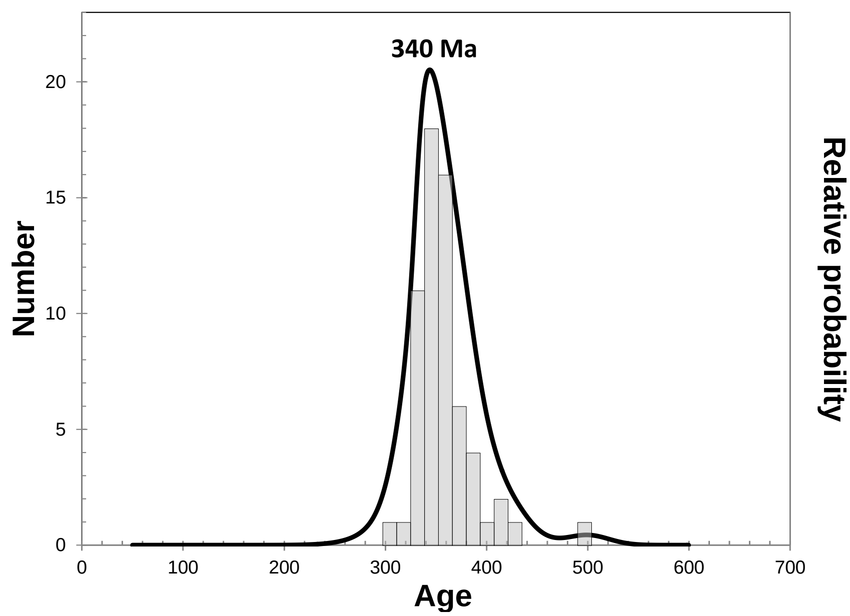

Figure 4.16: Probability density diagram of the concordant zircons (>0.05 probability of concordance) from the Nashoba Formation calc-silicate. The probability density diagram shows $^{206}Pb/^{238}U$ for zircons < 800 Ma and $^{207}Pb/^{206}Pb$ for zircons >800Ma.

The young ages for these grains can be explained if they grew hydrothermally, or if they experienced fluid-induced recrystallization that resulted in compositional changes including the lowering of Th/U ratios and U-Pb isotope resetting (Hoskin and Schaltegger, 2003). Typical igneous zircons have a Th/U ratio >0.5 and metamorphic zircons have a Th/U ratio <0.1 (Hoskin and Schaltegger, 2003). The zircon grains in MLBM1 have a Th/U ratio barely above 0.1. It is possible that these zircons underwent partial or full recrystallization or that they are hydrothermally grown. Hydrothermally grown zircons are typically associated with a brown, "spongey" or pitted appearance under reflected-light, and an unzoned slightly brighter BSE response then a typical igneous zircon and no response under CL (Hoskin, 2005)**.** Only some of the zircons in sample MLBM1 match this description. Partial recrystallization can be achieved through cracks, which are prevalent in the zircons of sample MLBM1, or through amorphous zoning due to metamictization. Cracks act as fluid conduits that allow hydrothermal fluids entry into the interior parts of the crystal. Zircons can be altered in the presence of fluids high in F, Cl or carbonate at temperatures well below the greenschist faces (Rizvanova, 2000; Hoskin and Schaltegger, 2003; Hoskin, 2005).

It is believed that water percolated into the calc-silicate unit through the shear zone within the outcrop during the (M3) period of retrograde greenschist facies metamorphism (see section 1.3). It is more reasonable for these grains to be altered by hydrothermal fluids that penetrated the zircons through the cracks, or have grown as a result of these fluids then it is for them to have been deposited during an age that corresponds with a period of known metamorphism in the area. Therefore, these grains are interpreted as hydrothermally altered and not will not be included in the detrital zircon analysis. The complete list of ages for this unit can be found in Appendix C.

4.6 NW NASHOBA TERRANE: TADMUCK BROOK SCHIST (MLTMBC)

4.6.1 *Sample Location and Description*

Only the high grade (SE) member (Jerden *et al.*, 1997) of the Tadmuck Brook Schist was sampled. MLTMBC is a combination of several samples taken within 50m along one continuous road outcrop in Littleton, MA (Appendix A). The Tadmuck Brook Schist is a rusty-weathering, sillimanite-bearing sulfidic mica schist that contains quartz-rich layers (Appendix B). The Tadmuck Brook Schist has unique mineralogy as it is the only unit found to contain scheelite, a fluorescent tungsten-bearing mineral with similar morphology to an igneous zircon. Scheelite, or $Ca(WO_4)$, is commonly associated with high-temperature hydrothermal veins, and contact metamorphism in skarns (Klein, 2001). The unit also contained abundant titanite.

4.6.2 *Zircon Morphology*

The sample was dominated by small (30-80 µm) well rounded, clear to cloudy grains (population F: Fig. 4.1 and Table 4.1) that constituted ~71% of the zircons of the sample. The remaining grains were prismatic-to-rounded and retained the typical igneous zircon 4:1 aspect ratio (population A and E: Fig. 4.1 and Table 4.1). The majority of the discordant grains were from populations A and E (Fig. 4.1 and Table 4.1). Due to the small grain size and the thin shape of the grain, crossing boundaries during the ablation process was more likely to occur. Abundant cracks are present in many zircon grains.

4.6.3 *U-Pb Geochronology*

Of the 68 grains that were analyzed in this sample, 34 met the criteria to be included in this study (see section 4.0.1). The youngest detrital zircon age of the Tadmuck Brook Schist, 463 ± 42 Ma, was determined by taking the weighted average of the youngest four grains (Table 4.17). In general, zircons of sample MLTMBC are small and morphologically indistinct. Zircons se10a41, se09b20, se10a72 and se10a27 formed a very tight age-group (Table 4.17). Given the number of grains that defined this age group and the large uncertainty on the individual $^{206}Pb/^{238}U$ ages, the weighted average the four youngest zircons formed the best interpretation. Zircon se10a71 (Appendix C) contained abundant unavoidable cracks and inclusions and its $^{206}Pb/^{238}U$ age of 424 ± 44 Ma coincided with a period of known metamorphism (See section 1.3), therefore, it was removed from the detrital zircon analysis.

The uncertainties on the Tadmuck Brook Schist zircons were consistently larger than any of the other units sampled. Due to the small grain size, all of the zircons of this sample were ablated using the 30x30 μm square raster, which decreased the sample size and duration of sampling and led to increased uncertainty. In order to gain any insight from this data, for this unit only, zircon grains were used only if their uncertainty was within 15% of their $^{206}Pb/^{238}U$ age, (e.g. a ca. 324 Ma zircon would be rejected if its uncertainty exceeded ± 48.6 Ma). Due to the small number of grains obtained from the sample and the large uncertainty associated with the grains this data is not a statistically representative sample for provenance studies of the Tadmuck Brook Schist. However, the data does provide a range of ages that can be compared other formations in the Nashoba terrane to test the provenance (See section 5.2).

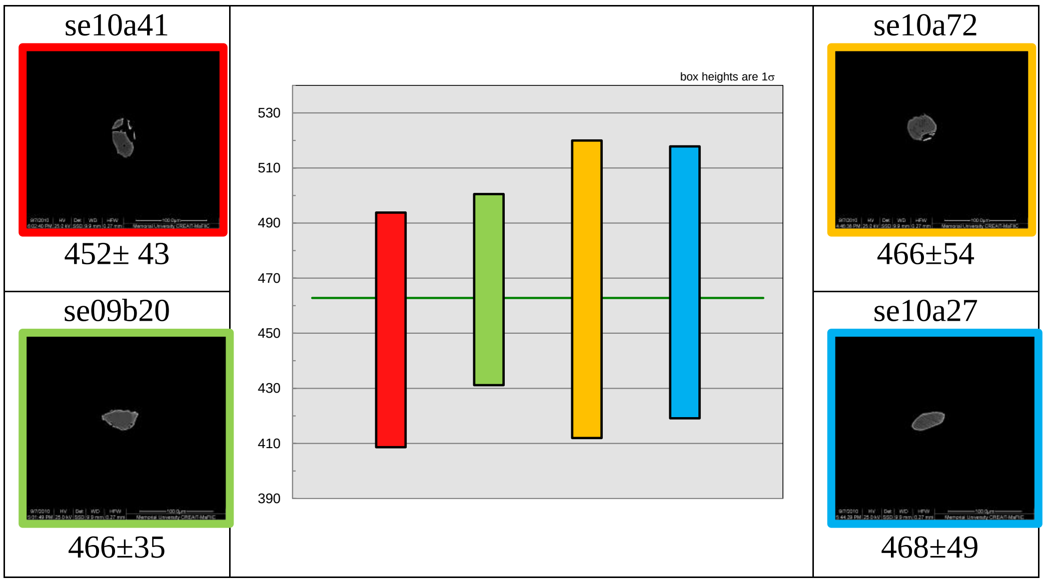

Fig. 4.17: Weighted average of the youngest four detrital zircon grains in the Tadmuck Brook Schist, se10a41 (red), se09b20 (green), se10a72 (orange) and se10a27 (blue). Mean= 463±42 (MSWD = 0.033, probability = 0.992)

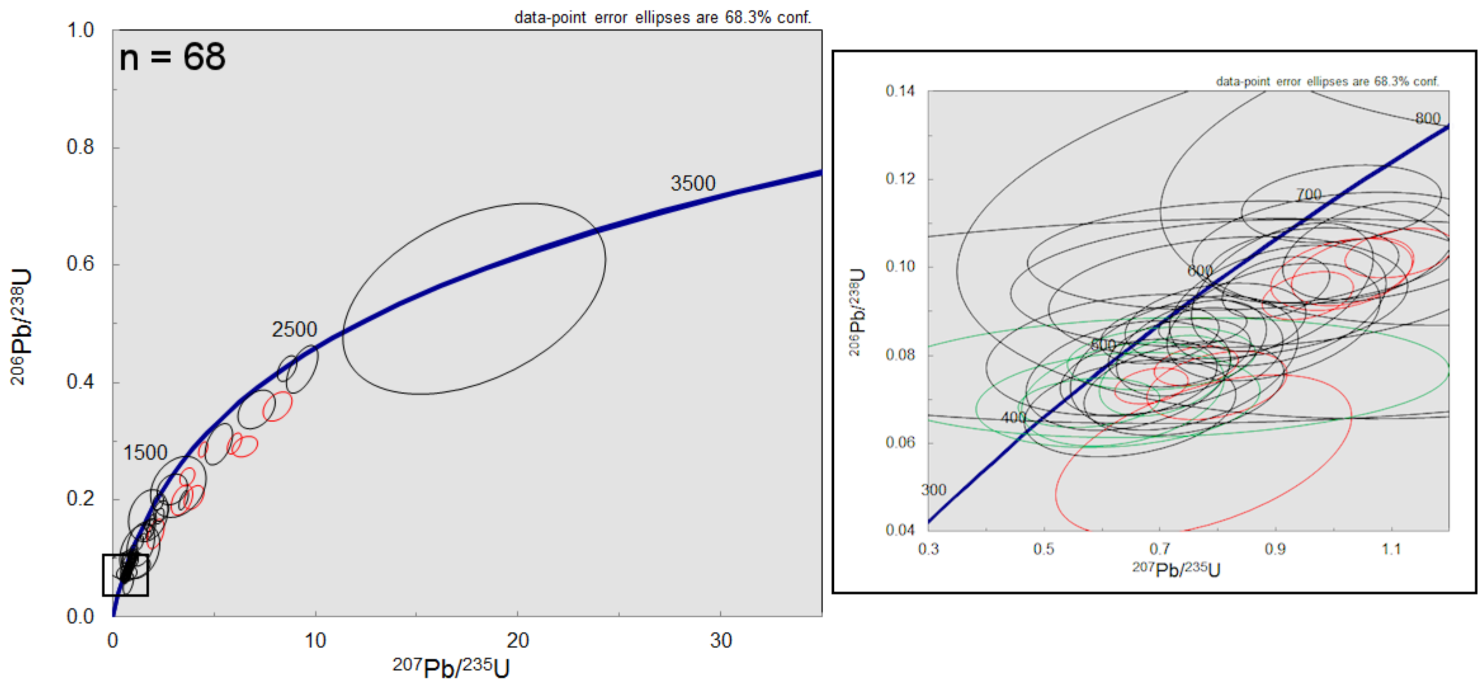

Figure 4.18 A: Concordia diagram of all data from the Tadmuck Brook Schist. (left). Enlarged image of Concordia diagram for youngest zircon ages between 300 Ma to 800 Ma (right). Black ellipses represent the data that met the criteria of this study and were included in the analysis. Red ellipses represent discordant data (< 0.05 probability of concordance) that was not included in this study. Green ellipses represent zircons with a low Th/U ratio (< 0.1) and a texture indicative of being metamorphically grown. The ages of the green ellipses were not included in the detrital zircon analysis but are interpreted in the section on metamorphism (See section 5.8).

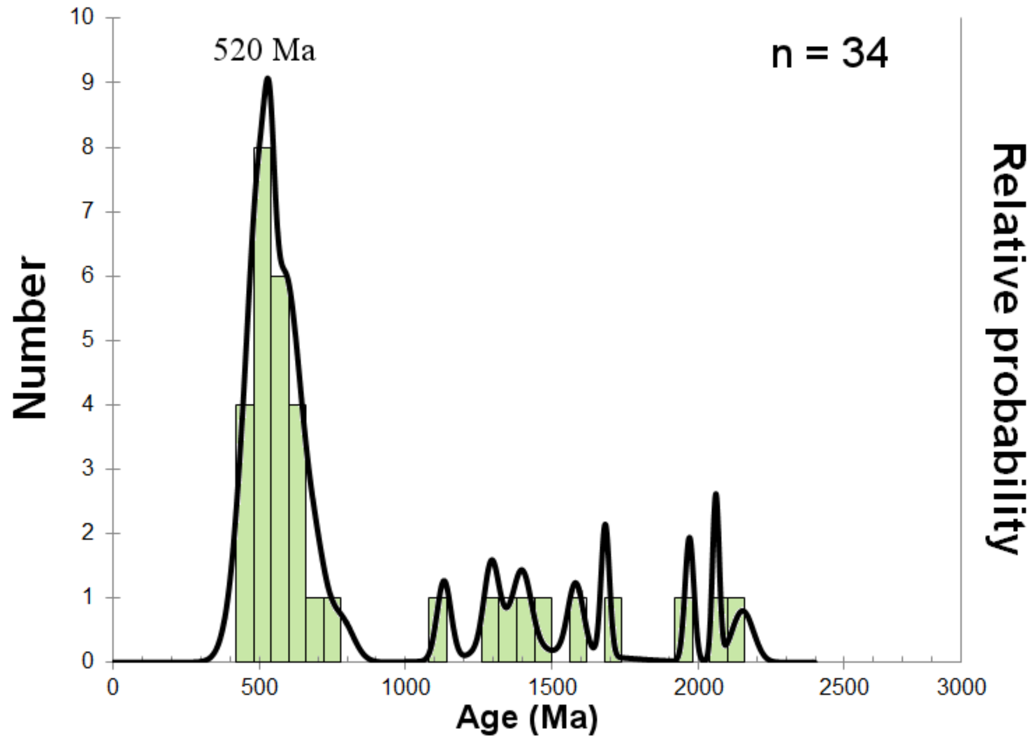

Figure 4.18 B: Probability density diagram of the concordant zircons (>0.05 probability of concordance) from the Tadmuck Brook Schist. The probability density diagram shows $^{206}Pb/^{238}U$ for zircons < 800 Ma and $^{207}Pb/^{206}Pb$ for zircons >800Ma. The diagram does not include discordant or young, metamorphically grown, zircons.

Table 4.19 **Calculated Ages** 1/2

MLTMBC	207Pb/ 235U	1s error	206Pb/ 238U	1s error	207Pb/ 206Pb	1s error	Concordia age	2s error	Probability of concordance	Th/U
se10a41	563	67	451	43	701	47	470	82	0.11	0.157
se09b20	516	55	466	35	555	38	476	66	0.37	0.239
se10a72	536	199	466	54	966	63	469	107	0.73	0.520
se10a27	505	72	469	49	495	51	477	92	0.62	0.198
se10a42	563	76	486	60	471	37	508	111	0.33	0.412
se10a67	540	64	492	28	566	37	497	55	0.47	0.081
se10a38	512	104	497	54	673	42	499	104	0.89	0.169
se10a11	558	48	500	31	626	43	511	58	0.23	0.373
se10a18	571	49	506	43	608	26	529	77	0.22	0.120
se10a22	538	40	524	26	564	28	527	48	0.73	0.366
se09b29	582	29	536	17	625	44	544	32	0.12	1.298
se09b08	594	58	540	36	687	49	550	68	0.37	0.627
se10a58	650	65	542	52	616	31	572	97	0.11	0.764
se09b19	654	66	564	54	694	28	591	98	0.20	0.185
se10a70	607	114	574	54	684	58	578	104	0.78	1.043
se10a17	652	33	588	27	745	25	609	49	0.07	0.189
se10a26	658	55	588	57	675	15	623	96	0.24	0.364
se10a39	626	149	593	56	1187	55	596	110	0.83	0.363
se09b21	677	57	617	33	769	45	627	63	0.32	0.431
se10a30	617	134	630	48	639	49	629	93	0.92	0.334
se10a78	734	48	637	43	688	27	672	77	0.06	0.495
se10a36	714	88	641	49	669	36	652	93	0.42	0.147
se10a10	710	57	699	34	682	30	701	63	0.84	0.409
se10a13	872	43	776	44	851	42	821	74	0.05	0.340

Table 4.19				**Calculated Ages**						2/2
MLTMBC	**207Pb/ 235U**	**1s error**	**206Pb/ 238U**	**1s error**	**207Pb/ 206Pb**	**1s error**	**Concordia age**	**2s error**	**Probability of concordance**	**Th/U**
se10a21	1196	55	1155	48	1131	24	1171	82	0.51	0.096
se10a60	1242	74	1073	64	1293	25	1128	115	0.05	0.221
se09b10	1052	55	937	40	1347	68	966	73	0.06	0.415
se09b10	1052	55	937	40	1347	68	966	73	0.06	0.415
se10a51	1393	127	1271	92	1399	30	1302	168	0.39	0.508
se10a12	1003	38	944	25	1498	209	958	47	0.15	0.346
se10a69	1467	217	1294	182	1581	27	1348	325	0.49	0.070
se10a76	1858	74	1667	116	1682	14	1827	148	0.07	0.652
se10a59	2124	76	1955	104	1970	15	2071	146	0.11	0.021
se10a57	2373	50	2273	122	2060	11	2382	98	0.32	0.571
se09b17	2297	34	2279	66	2152	37	2297	67	0.75	0.178

Table 4.19: U-Pb data from detrital zircon grains of the Tadmuck Brook Schist with probability of concordance >0.05 and a Th/U ratio >0.1. For a complete table of zircon analyses including discordant and metamorphic grains see Appendix C. The ages and associated error used in this study are highlighted in blue.

4.7 NEWBURY VOLCANIC COMPLEX SLATE- PHYLLITE (MLIS1)

4.7.1 *Sample Location and description*

The Newbury Volcanic Complex sample was collected adjacent to a parking lot area in Ipswich, MA (Appendix A). The sample was a fine-grained, red slate to phyllite that was metamorphosed no higher than the lower greenschist facies (Appendix B). The sample was heavily weathered and broke apart easily.

4.7.2 *Zircon Morphology*

More than half of the zircons in the sample (~56%) consisted of well rounded, clear to cloudy grains (population F: Fig. 4.1 and Table 4.1). The second most abundant population was faceted, clear to cloudy zircons, with a short aspect ratio (2:1) (population A: Fig. 4.1 and Table). The remaining zircon grains were prismatic-to-rounded with long aspect ratios (population B and E: Fig. 4.1 and Table). A few zircons of various morphologies appeared brown under reflected light.

4.3.3 *U-Pb Geochronology*

Of the 56 grains that were analyzed in this sample, only 23 met the conditions to be included in this study (Table 4.21). Due to the small number of grains obtained from the sample, it is not statistically representative for provenance studies of the Newbury Volcanic Complex. The $^{206}Pb/^{238}U$ age of the youngest detrital grain was 385±19 Ma. There is a cluster of 8 zircons with similar ages that are within error of each other and within less than 5 My from older zircon ages and correspond to a peak with a weighted mean of 418±18 Ma (MSWD = 0.073, probability = 0.999, n = 8).

The remaining 33 grains were all discordant. There were no metamorphic zircons (Th/U <0.1 found in this unit. This unit was unique in that the U concentrations in 18 of the discordant data were between 10,000 and 100,000 ppm. A typical metamorphic zircon has a U concentration of 100 ppm or less. A typical igneous zircon has a U value from several 100 to several 1000 ppm (Mezger *et al.*, 1997). Hydrothermally grown zircons can have U values of >10,000 ppm (Hoskin, 2005). Therefore, the Newbury volcanic complex contained abundant zircons that are likely hydrothermally grown.

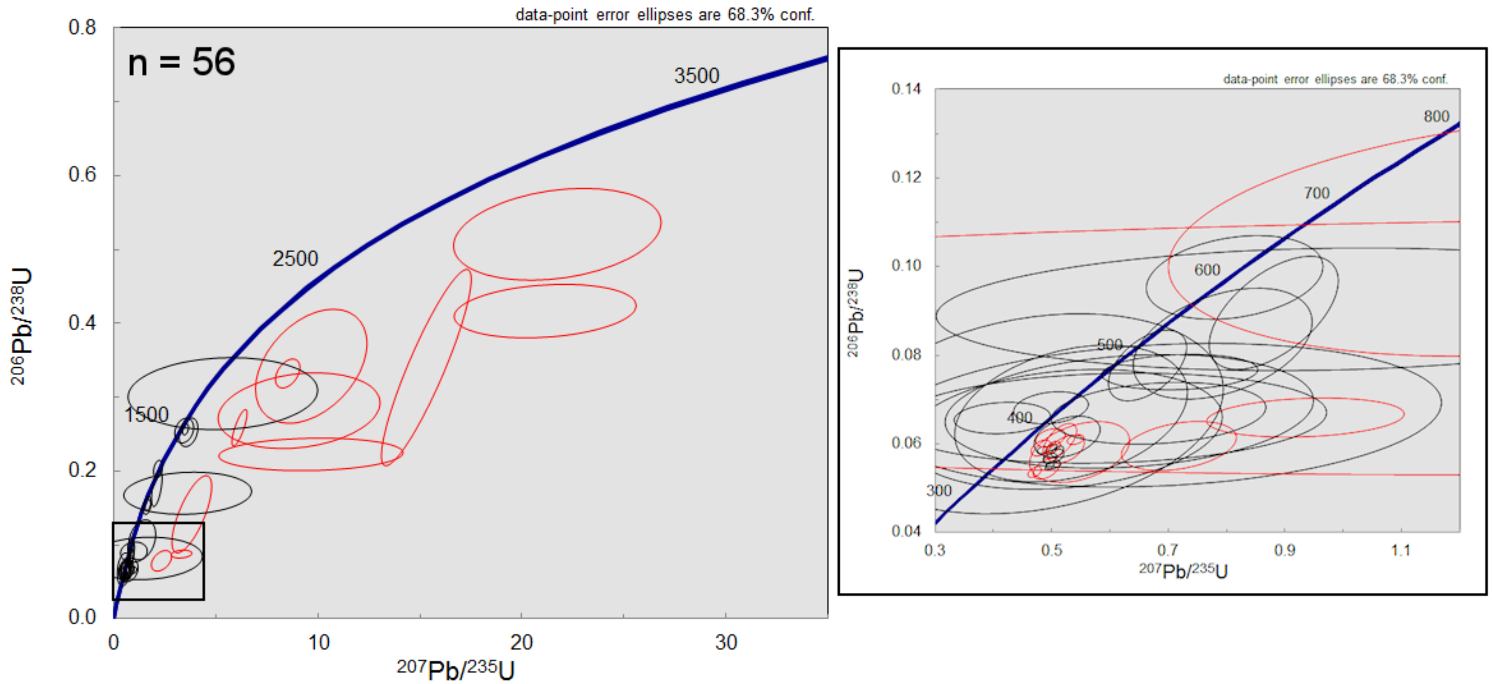

Figure 4.20 A: Concordia diagram of all data from sample the Newbury Volcanic Complex (left). Enlarged image of Concordia diagram for youngest zircon ages between 300 Ma to 800 Ma (right). Black ellipses represent the data that met the criteria of this study and were included in the analysis. Red ellipses represent discordant data (< 0.05 probability of concordance) that was not included in this study.

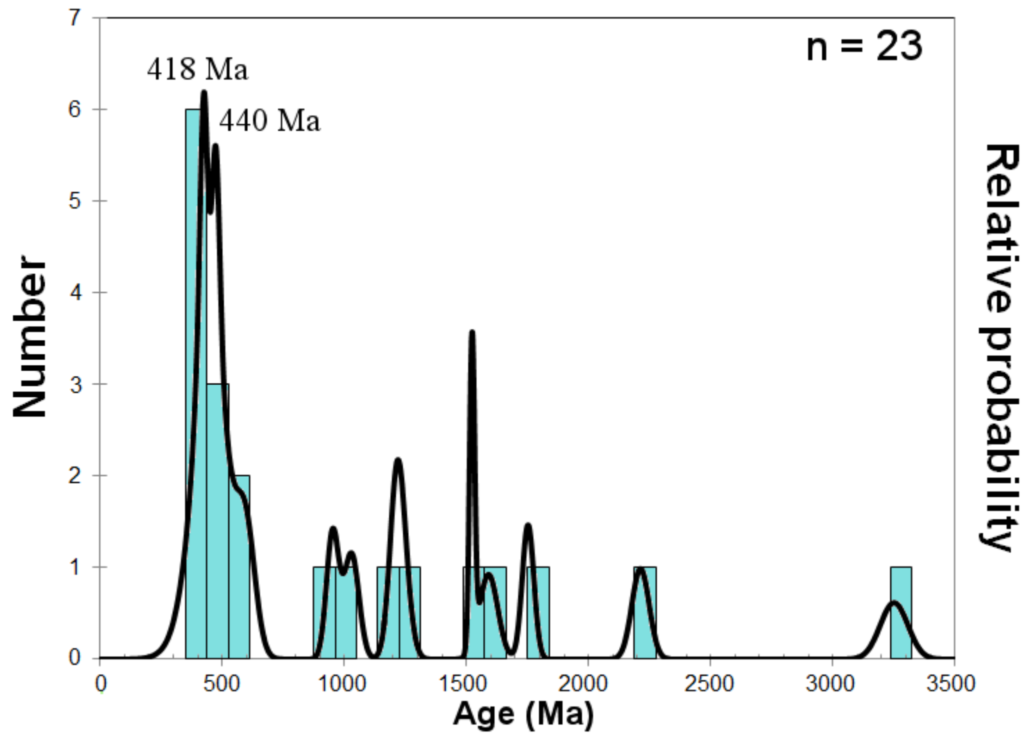

Figure 4.20 B: Probability density diagram of the concordant zircons (>0.05 probability of concordance) from the Newbury Volcanic Complex. The probability density diagram shows $^{206}Pb/^{238}U$ for zircons < 800 Ma and $^{207}Pb/^{206}Pb$ for zircons >800Ma. The diagram does not include discordant or young, metamorphically grown, zircons.

Table 4.21 **Calculated Ages** ½

MLIS1	207Pb/ 235U	1s error	206Pb/ 238U	1s error	207Pb/ 206Pb	1s error	Concordia age	2s error	Probability of concordance	Th/U
se08a16	429	25	385	19	478	24	397	35	0.0865	0.421
se09a43	427	119	396	54	764	72	399	105	0.800	0.636
se09a23	477	156	411	41	1319	85	413	81	0.683	0.811
se09a30	353	39	411	14	401	66	406	28	0.132	0.958
se08b29	533	189	415	65	1349	46	420	128	0.552	0.909
se09a72	390	149	417	90	481	73	411	168	0.862	0.611
se09a83	434	87	417	62	535	63	422	114	0.854	1.176
se08b27	529	73	418	28	909	99	424	55	0.147	0.920
se09a78	498	130	420	51	1250	71	425	101	0.563	0.742
se08a50	411	29	425	14	561	34	423	28	0.6269	1.207
se08a05	551	52	473	16	764	32	477	31	0.1554	0.311
se09a18	593	57	512	49	697	58	539	89	0.177	1.160
se09a67	684	225	558	54	1653	51	561	107	0.597	1.064
se08b16	605	56	600	37	567	54	601	68	0.940	1.462
se08a10	987	41	937	35	952	25	955	62	0.2672	0.264
se09a40	969	50	911	38	1029	30	928	68	0.290	0.132
se09a71	1164	47	1191	42	1214	29	1179	71	0.619	0.317
se09a79	1143	57	1048	89	1230	34	1135	114	0.197	0.549
se08a41	1525	23	1473	25	1523	10	1503	39	0.0572	0.728
se09a61	1512	71	1464	57	1590	38	1481	100	0.555	0.507
se09a70	1558	67	1452	67	1752	24	1501	110	0.18	0.582

Table 4.21			**Calculated Ages**							2/2
MLIS1	**207Pb/ 235U**	**1s error**	**206Pb/ 238U**	**1s error**	**207Pb/ 206Pb**	**1s error**	**Concordia age**	**2s error**	**Probability of concordance**	**Th/U**
se09a32	1873	493	1716	159	2212	35	1725	313	0.77	0.204
se08b26	1550	457	1013	104	3250	57	1016	208	0.36	0.352

Table 4.21: U-Pb data from detrital zircon grains of the Newbury Volcanic Complex with probability of concordance >0.05 and a Th/U ratio >0.1. For a complete table of zircon analyses including discordant and metamorphic grains see Appendix C. The ages and associated error used in this study are highlighted in blue.

5.0 DISCUSSION

5.1 Units Southeast of the Assabet River fault zone

Previous work on the Marlboro Formation has focused on ages for the felsic intrusions, such as the Grafton Granite (515 Ma), that cut the Marlboro Formation, rather than the age of the unit itself (Acaster and Bickford, 1999; Walsh *et al.*, 2009*).* Through these studies, researchers have determined that the Marlboro Formation is most likely Cambrian to Ordovician in age. The 470 Ma age of the youngest detrital zircon in this study is consistent with this assessment but the associated uncertainty is too large to constrain the age any further. A statistically representative data set for the provenance of the unit could not be obtained due to the scarcity of zircon in the samples. Therefore, it is possible that a younger detrital zircon could exist in the unit. The scarcity of zircon in the Marlboro Formation meta-sedimentary rocks can be attributed to the basaltic nature of the volcanics and may indicate that they are primarily sourced locally and derived mostly from the zircon-poor Marlboro Formation volcanics.

Geochemistry on Marlboro Formation has suggested that it may have formed over continental crust (Hepburn et al., 1995; Kay *et al.*, 2009). The Mesoproterozoic and Paleoproterozoic aged zircons in the Marlboro Formation, combined with the oldest detrital zircon that had a ca. 3.3 Ga core and a ca. 2.6 Ga rim, strongly supports this interpretation and that the Marlboro Formation meta-sedimentary rocks were likely sourced from, or incorporated, old continental material. If the Marlboro Formation was a primitive arc that built up on oceanic crust over a subduction zone (Hepburn et al., 1995), then it would be expected to have mainly Cambrian to Ordovician zircons and no Mesoproterozoic and Paleoproterozoic zircons. Thus, the Marlboro Formation must have formed on or in proximity to old continental material.

Previous attempts to date the Shawsheen Gneiss resulted in unreliable ages; however, a 2042± 52 Ma U-Pb zircon upper intercept age suggested a Paleoproterozoic source for the zircons (Olzewski, 1980). The Shawsheen Gneiss sample for this research provided a complete, statistically representative, suite of detrital zircon ages that ranged from ca. 470 Ma to ca. 2400 Ma. As with the Marlboro Formation, the Mesoproterozoic and Paleoproterozoic ages are consistent with the oldest zircons in the Shawsheen Gneiss being sourced from old continental material.

Similarities in the ca. 470 age of the youngest detrital zircons and the abundance of the Mesoproterozoic and Paleoproterozoic ages in both the Marlboro and the Shawsheen units suggests that they are related and are most likely conformable with each other, as was previously interpreted by Goldsmith (1991a).

5.2 Units Northwest of the Assabet River fault zone

The Nashoba Formation gneissose unit contained a complete, statistically representative, suite of detrital zircon ages that ranged from ca. 465 Ma to ca. 2800 Ma (Fig. 4.3A). Unlike the Marlboro Formation and Shawsheen Gneiss, the Nashoba Formation gneiss contained abundant metamorphic zircons, indicating that perhaps the northwestern portion of the Nashoba terrane experienced a higher degree of metamorphism than the southeastern part. Implications of the metamorphic ages of these zircons and those found in the other Nashoba units will be discussed below.

Although a sample that was statistically representative for provenance studies could not be achieved for the Tadmuck Brook Schist (see above), the largest zircon age population, at ca. 520-540 Ma (Fig. 5.1), matched well with the detrital zircon suite from the Nashoba Formation gneissose unit (MLNB1). Figure 5.1 is a probability density diagram of the Tadmuck Brook Schist (green) versus the Nashoba Formation gneissose unit (red) and with zircon suites from the Berwick (CT) and Hebron Formation (ME) of the Merrimack Belt (black) (Wintsch *et al.,* 2007). The large age uncertainty associated with the zircons of the Tadmuck Brook Schist widens the peak area that the data encompasses (Fig. 5.1). However, the peak in the Tadmuck Brook Schist data more closely resembles the Nashoba Formation gneissose unit than the Merrimack belt. In addition, the Tadmuck Brook Schist displayed a consistent progression of detrital zircon ages throughout the Mesoproterozoic and Paleoproterozoic (Fig. 5.1) consistent with the other sampled units of the Nashoba terrane. Therefore, it is concluded that the Tadmuck Brook Schist is part of the northwestern Nashoba terrane and is not part of the Merrimack belt.

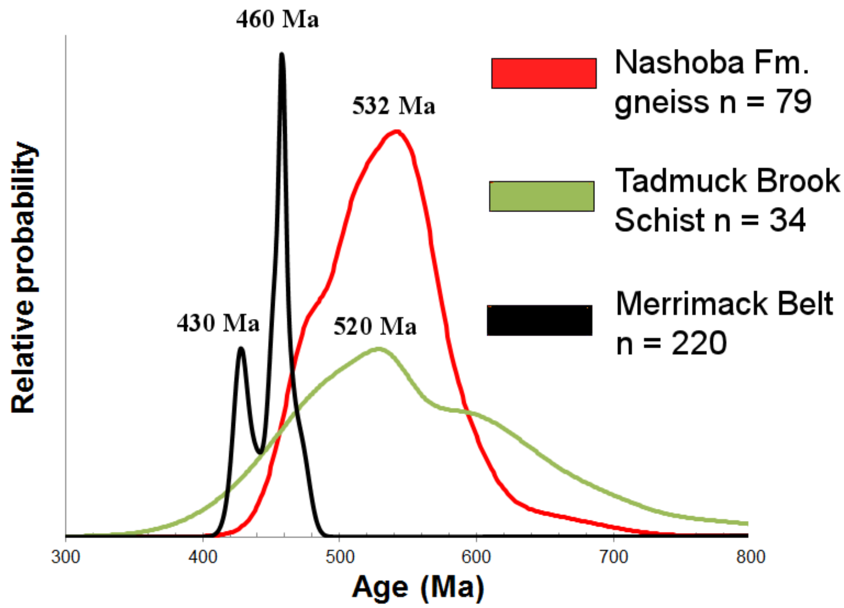

Figure 5.1: Probability density diagram shows frequency curves for concordant zircons (>0.05 probability of concordance) of the suites of zircon ages from the Tadmuck Brook Schist, the Nashoba Formation gneiss, and selected units of the Merrimack belt (Wintsch *et al.*, 2007) for the period between 300 to 800 Ma. The probability density diagram shows $^{206}Pb/^{238}U$ ages for zircons <800 Ma. The diagram does not include discordant or metamorphic zircons. The frequency curves are scaled on the y-axis to reflect the number of grains. The population sizes are based on the number of zircons sampled in total from each unit.

5.3 The Assabet River fault zone (ARFZ)

The Assabet River fault zone (Fig. 1) is a major intra-terrane fault zone that has been inferred to follow a curved path along the Andover Granite, separating the Fishbrook Gneiss from the Shawsheen Gneiss and the Nashoba Formation schist from the Marlboro Formation, and possibly continuing to Connecticut (Figure 2.0; Hepburn and DiNitto, 1978; Goldsmith, 1991a; Stroud *et al.*, 2009). One purpose of this study was to test the hypothesis that the ARFZ represents a major terrane boundary, similar to the Clinton-Newbury fault zone or the Bloody-Bluff fault zone, and that the Nashoba terrane represents two separate terranes. To test this hypothesis, all of the detrital zircon grains from the units southeast of the ARFZ (Marlboro and Shawsheen Gneiss) were plotted together in one color, and those from areas northwest of the ARFZ (Nashoba Formation and Tadmuck Brook Schist) in another, on probability density diagrams and histograms (Fig. 5.2).

Samples from either side of the ARFZ show a peak at ca. 540 Ma with a similar peak width (Figs. 5.2 and 5.2 C). Older age data show similar distributions with age clusters in the Mesoproterozoic and Paleoproterozoic. The data indicate that, at the resolution obtained for this study, there is no significant difference in detrital age populations across the Assabet River Fault Zone. Thus, it is interpreted that the fault zone does not represent a terrane boundary and the Nashoba terrane as mapped represents a single terrane rather than a composite of multiple terranes.

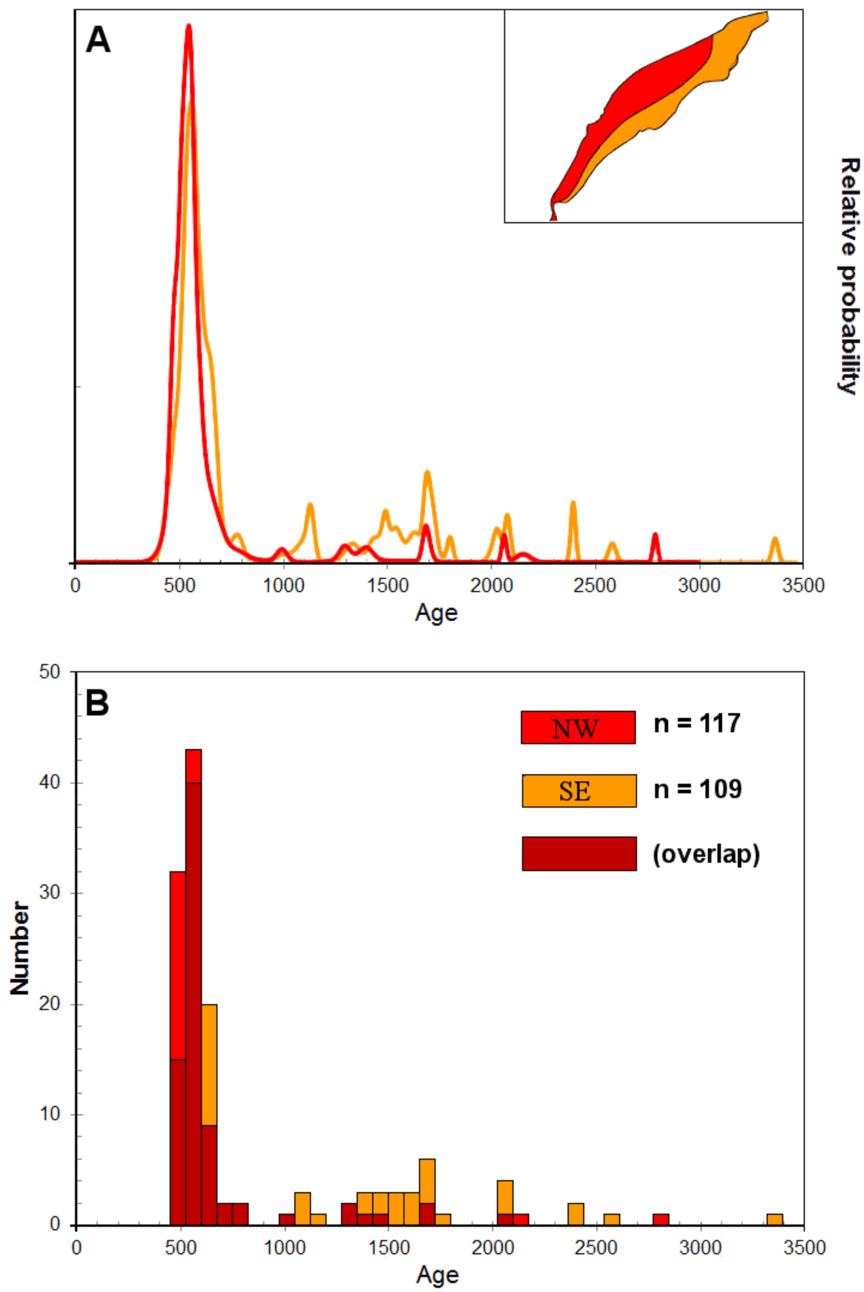

Figure 5.2: A probability density diagram and histogram of the concordant zircons (>0.05 probability of concordance) from the suites of zircon ages of units southeast and northwest Nashoba terrane. The probability density diagram shows $^{206}Pb/^{238}U$ ages for zircons < 800 Ma and $^{207}Pb/^{206}Pb$ ages for zircons >800 Ma. The diagram does not include discordant or metamorphic zircons. The frequency curves (A) are scaled on the y-axis to reflect the number of grains.

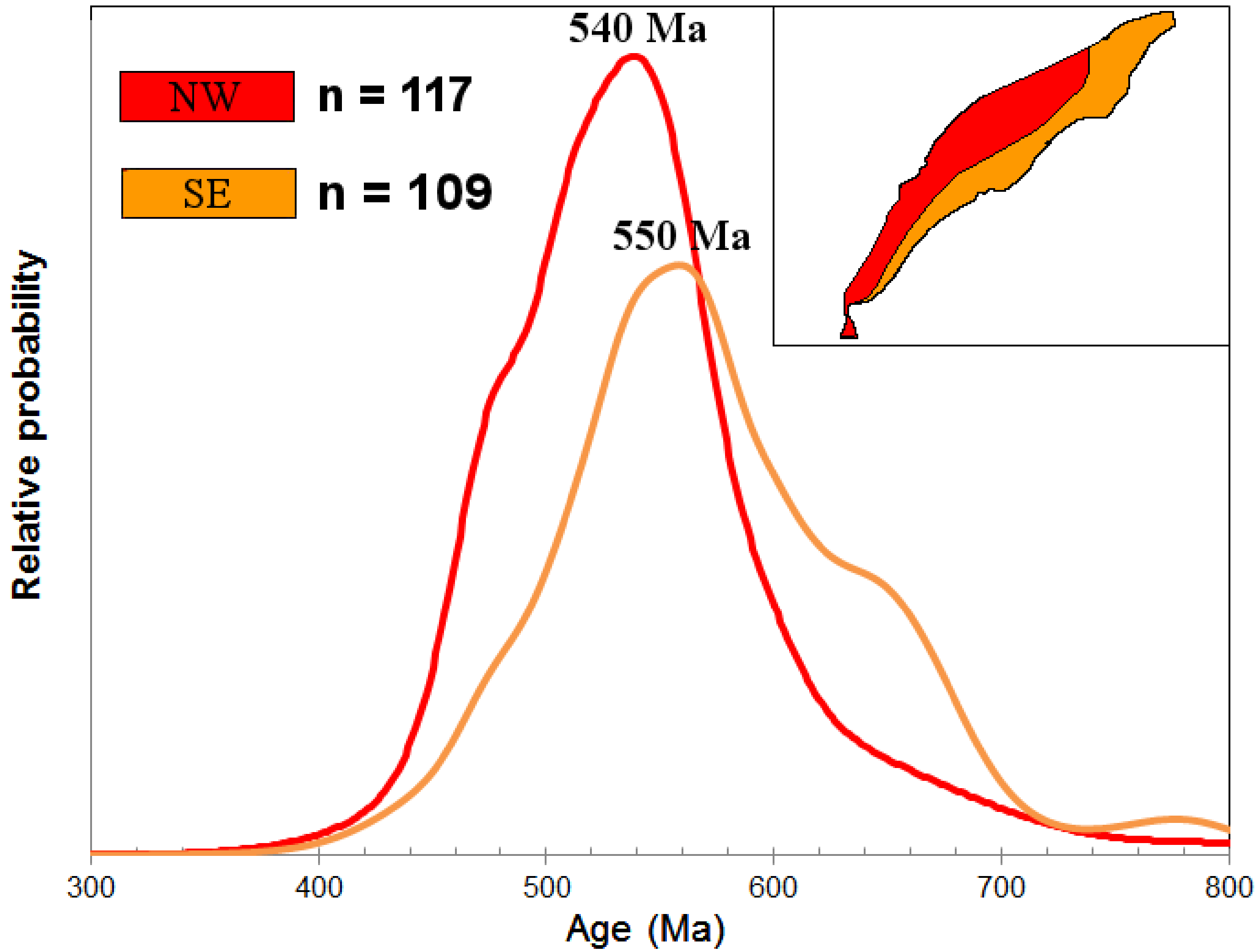

Figure 5.2C: Enlarged version of Figure 5.2A.

5.4 Comparison of the Nashoba terrane and Avalonia

Global tectonic reconstructions of Avalonia and its neighboring peri-Gondwanan terranes show Avalonia and the other peri-Gondwanan terranes, including Ganderia, as having rifted from Gondwana in the Neoproterozoic as (1) a single super-terrane that later accreted to Laurentia (Hatcher, 2010), (2) separate, but adjacent, micro-continents that then amalgamated outboard of Laurentia (or were very close) and docked as a single unit (Nance and Murphy, 1994; Keppie *et al.*, 1996; 1998; Nance *et al.*, 2002) or (3) separate, but adjacent, micro-continents that docked to the Laurentian margin individually (Nance *et al.*, 2008; van Staal *et al.*, 2009). These hypotheses were tested in eastern Massachusetts in this study by comparing the detrital zircon suite of the Nashoba terrane to detrital zircon suites of Avalonia from the literature.

For Avalonia, detrital data was taken from Pollock *et al.*, (2009), Hepburn *et al.*, (2008) and Thompson and Bowring (2000). Pollock *et al.*, (2009) took samples across Avalonia in Newfoundland and reported the youngest detrital zircon ages of formations including the Mall Bay Formation (ca. 581 Ma), the Briscal Formation (ca. 562 Ma), the Cuckold Formation (ca. 555 Ma), the Crown Hill Formation (ca. 557 Ma), the Random Formation (ca. 542 Ma), and the Redman Formation (ca. 535 Ma). Pollock (2009) suggested that the Redman Formation, which has a youngest detrital zircon age of ca. 535 Ma but was deposited in the Arenig, might have a different provenance then all other Avalonian units and include Cadomian input. However, the data was included in this study in order to incorporate data from Avalonian formations deposited in the

Ordovician. Hepburn *et al.*, (2008.) sampled a younger portion of the Westboro Formation of the Avalon terrane in Massachusetts (at ca. 590 Ma). Thompson and Bowring, (2000) sampled the older portion of Westboro Formation of the Avalon terrane (at ca. 1000 Ma).

Figure 5.3 is the combination of the Avalonian detrital zircon ages from the literature and the Nashoba terrane detrital zircon ages from this study. The Mesoproterozoic and Paleoproterozoic data is very similar for both the Avalon and Nashoba terrane, suggesting that they may have similar provenance areas. However, Figure 5.3 C shows a distinct difference between the zircon age populations for the two terranes. The Nashoba terrane has a distinct age peak at ca. 540 Ma and lacks any indication of the ca. 610 Ma age population that is dominant in the Avalon terrane. The opposite is true in Avalonia. If the two terranes had docked, or come close enough to have transported sediment from one to the other in the Neoproterozoic or early Paleozoic, or were connected throughout their geologic history, zircon provenance from these critical periods of Neoproterozoic tectonic activity should appear in both terranes. Based on the difference in zircon provenance, combined with (1) the existence of a major fault zone separating the Nashoba terrane and the Avalon terrane, (2) the distinct change in metamorphic grade across the fault zone, and (3) the difference in geochemical signatures, it is interpreted that the Nashoba terrane and the Avalon terrane may have formed in close proximity to each other, but had separate geologic histories and arrived at the Laurentian margin as two distinct tectonic blocks.

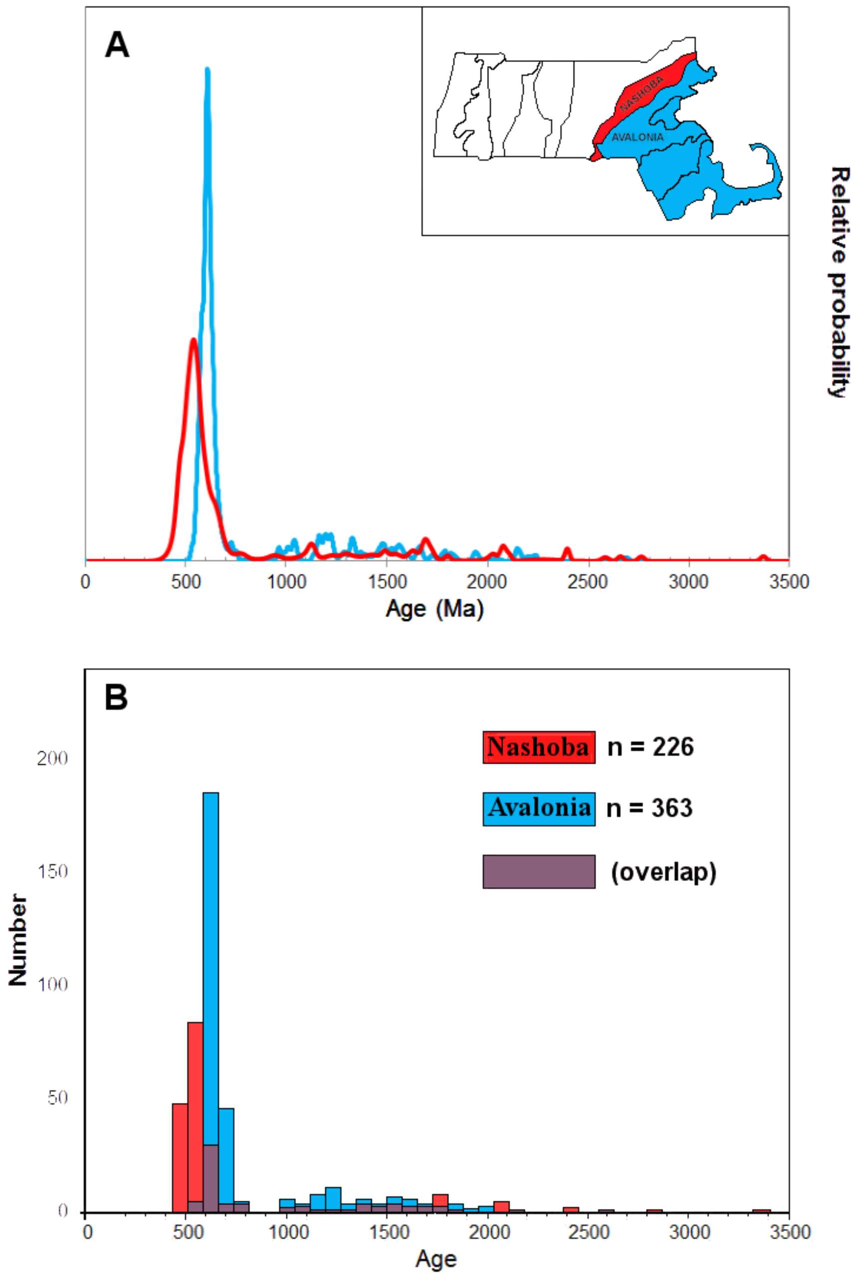

Figure 5.3 A and B: Probability density diagram of the concordant zircons (>0.05 probability of concordance) from the suites of zircon ages from meta-sedimentary rocks of the Nashoba terrane and Avalonia. The probability density diagram shows $^{206}Pb/^{238}U$ ages for zircons < 800 Ma and $^{207}Pb/^{206}Pb$ ages for zircons >800 Ma. The diagram does not include discordant or metamorphic zircons. The frequency curves (A) are scaled on the y-axis to reflect the number of grains. Data for Avalonia from Pollock *et al.*, (2009) Hepburn, (2008), and from Thompson and Bowring, (2000)

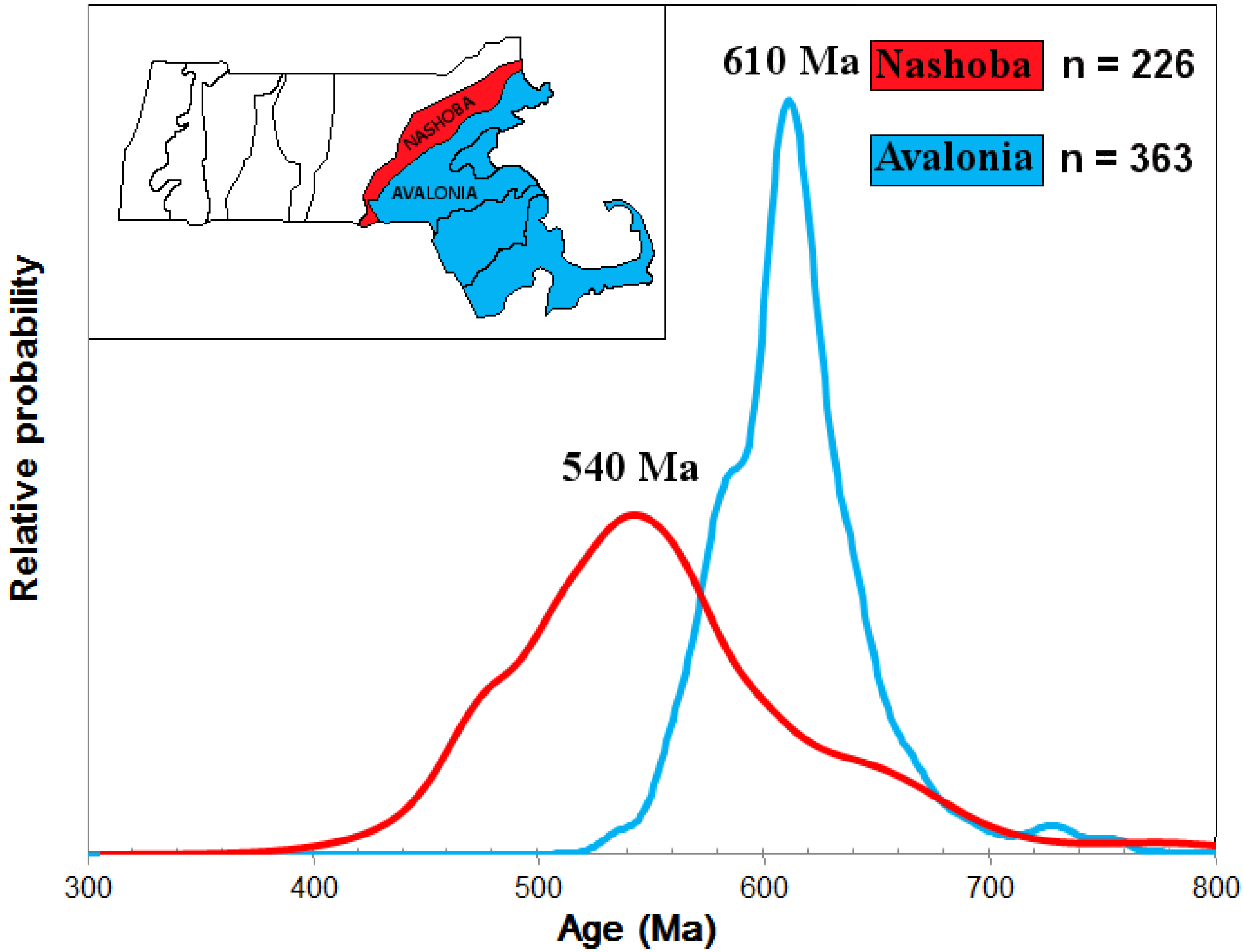

Figure 5.3 C: Enlarged version of Figure 5.3.

5.5 Comparison of the Nashoba terrane and the Merrimack Belt

The Merrimack terrane has previously been investigated by Wintsch *et al.,* (2007) who dated detrital zircons of metasedimentary rocks in the Hebron and Berwick Formations. These units showed Silurian-aged sediments with a large input of what the authors interpreted to be Laurentian-derived sediments, specifically of Grenvillian age. Wintsch *et al.,* (2007) argued that the similarities in provenance between the Hebron Formation of Connecticut and the Berwick Formation of Maine suggested that these two end member units fairly represented the geologic history of the entire Merrimack belt. Although the Merrimack units in Massachusetts are in the process of being dated by U-Pb zircon methods, Wintsch's interpretation is assumed here in to be correct.

Detrital zircon ages from the Merrimack belt and the Nashoba terrane are plotted on a probability density diagram (Fig. 5.4). The age of the Merrimack belt zircons are somewhat younger than that of the Nashoba terrane zircons and are Ordovician to Silurian in age (cf. Goldsmith, 1991a; Wintsch *et al.,* 2007) The large Grenvillian-aged zircon populations, (at ca. 0.9 Ma to 1.3 Ma), described by Wintsch *et al.* (2007) in the Merrimack belt are not as prominent in the Nashoba terrane, and the Nashoba terrane has three minor peaks between 1600 and 2400 Ma that are not present in the Merrimack belt data.

The Merrimack belt lacks any peak at ca. 540 Ma, the age that is most dominant in the Nashoba terrane (Fig. 5.4C). Based on the difference in zircon provenance, combined with (1) the existence of a major fault zone separating the Nashoba terrane and the Merrimack belt, and (2) the distinct change in metamorphic grade across the fault zone, it is interpreted that the Nashoba terrane and the Merrimack belt had separate geologic histories.

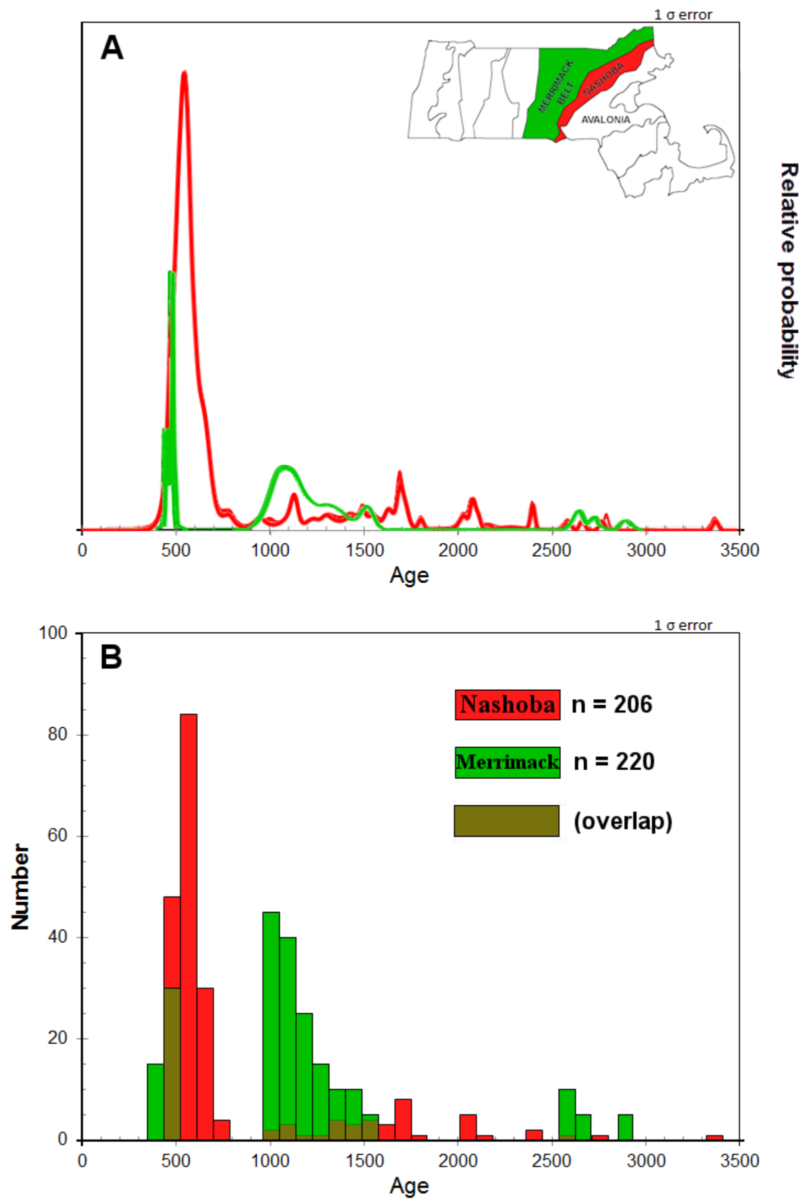

Figure 5.4: A probability density diagram and histogram of the concordant zircons (>0.05 probability of concordance) from the suites of zircon ages from meta-sedimentary rocks of the Nashoba terrane and the Merrimack belt. The probability density diagram shows $^{206}Pb/^{238}U$ ages for zircons < 800 Ma and $^{207}Pb/^{206}Pb$ ages for zircons >800 Ma. The frequency curves (A) are scaled on the y-axis to reflect the number of grains. Data for the Merrimack belt from Wintsch *et al.*, (2007).

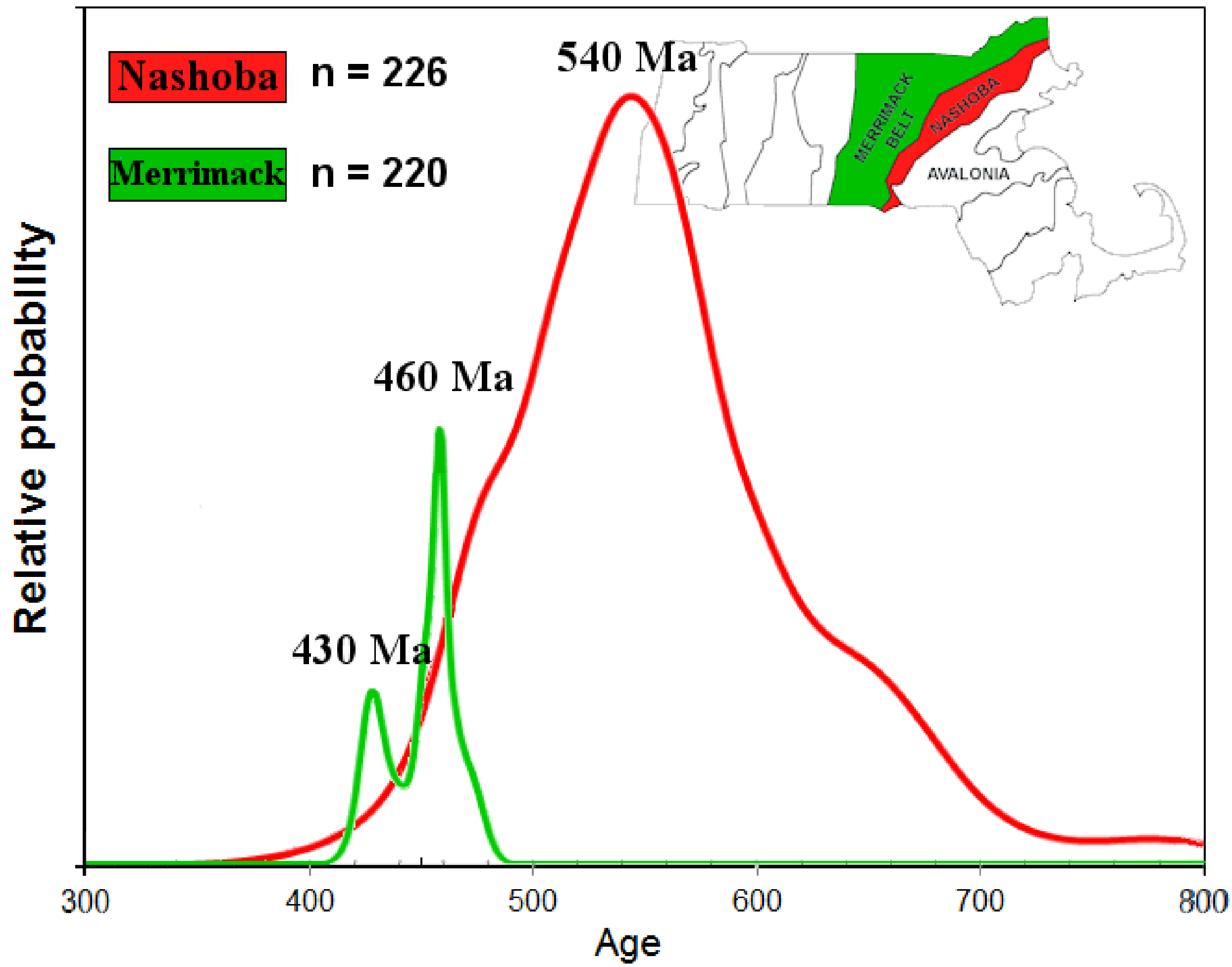

Figure 5.4 C: Enlarged version of Figure 5.6.

5.6 Comparison of the Nashoba terrane and Ganderia

The Avalon terrane and the adjacent Gander terrane in Newfoundland have been established as two separate microcontinents for many years (van Staal *et al.*, 2005; 2009; 2011). Differences in detrital zircon age populations and the negative εNd values associated with Gander terrane rocks (Whalen *et al.* 1996; Samson *et al.*, 2000; Rodgers *et al.*, 2006), versus the positive εNd values in Avalonian rocks (Samson *et al.*, 2000) suggests that these two peri-Gondwanan blocks have different geologic histories and are therefore distinct terranes. The Gander terrane of Newfoundland directly abuts the Avalon terrane, just as the Nashoba terrane is adjacent to the Avalon terrane of New England. Several studies have correlated the Nashoba terrane to the Gander terrane (e.g. van Staal *et al.*, 2009; Walsh, 2011). To date, there has not been any study that has compared a detrital zircon suite of the Nashoba terrane with the detrital zircon suite of Ganderia.

Detrital zircon information for Ganderia was taken from Fyffe *et al.*, (2009), who sampled in New Brunswick and Maine, and from Pollock *et al.*, (2009), who sampled from units southeast of the Dog Bay Line in Newfoundland (Figure 1.0). The information from Ganderia is overlain by the data from the Nashoba terrane in Figures 5.5 and 5.5C. The ca. 540 Ma peak in the ages for both terranes is nearly identical. This is a strong indication that either: (1) the Nashoba terrane and Ganderia received sediment from a similar source, or (2) the Nashoba terrane is sourced from Ganderia. Given the age of the Nashoba terrane and the fact that the sediments are not significantly younger than the Ganderian sediments, the first scenario is thought to be more likely. Thus, this study provides strong evidence that the Nashoba terrane of Massachusetts is part of composite Ganderia and shared a similar sedimentary source as Ganderian fragments in Newfoundland, Maritime Canada, and Maine.

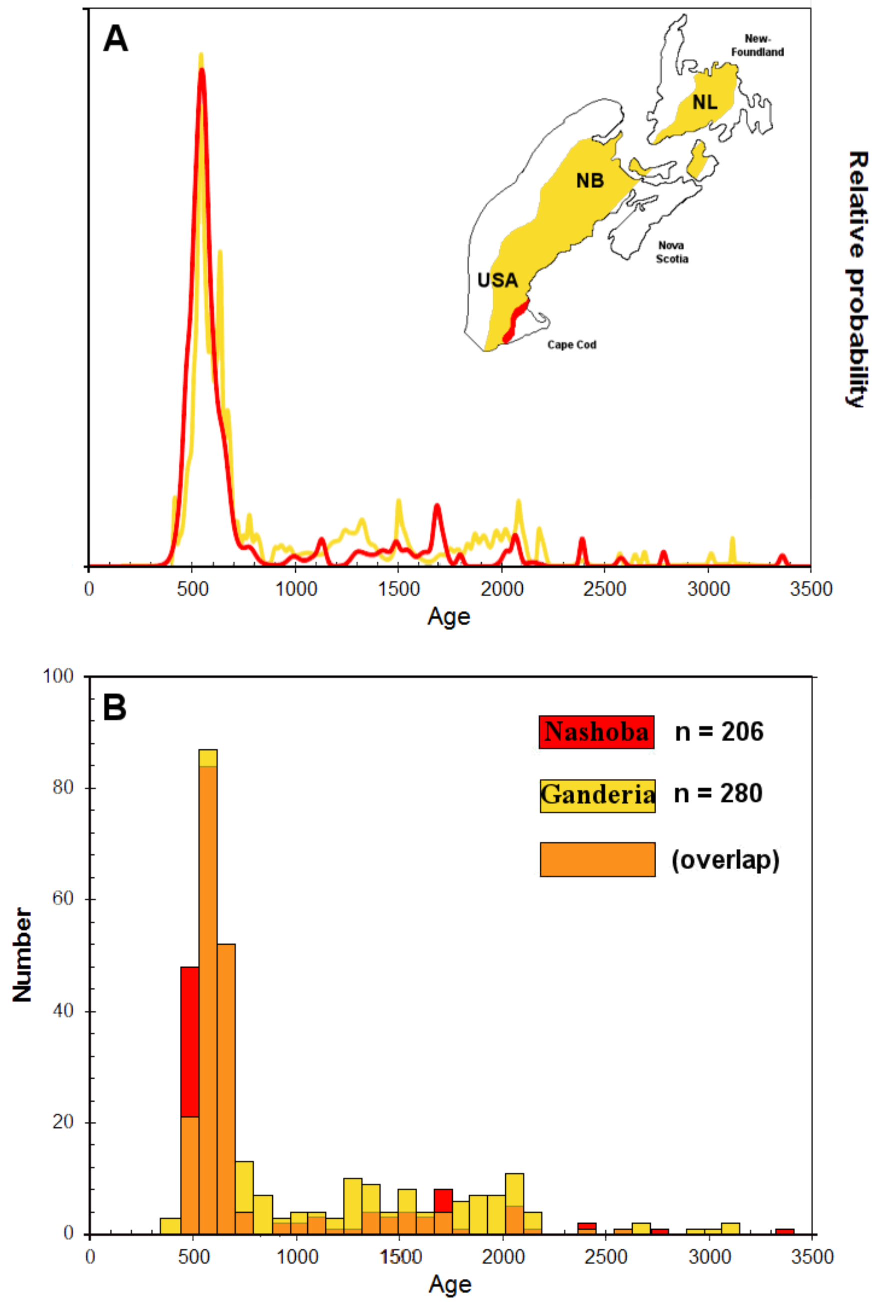

Figure 5.5: A probability density diagram and histogram of the concordant zircons (>0.05 probability of concordance) from the suites of zircon ages from meta-sedimentary rocks of the Nashoba terrane and Ganderia. The probability density diagram shows $^{206}Pb/^{238}U$ ages for zircons < 800 Ma and $^{207}Pb/^{206}Pb$ ages for zircons >800 Ma. The diagram does not include discordant or metamorphic zircons. The frequency curves (A) are scaled on the y-axis to reflect the number of grains. Data for Ganderia from Fyffe *et al.*, (2009) and Pollock *et al.*, (2009).

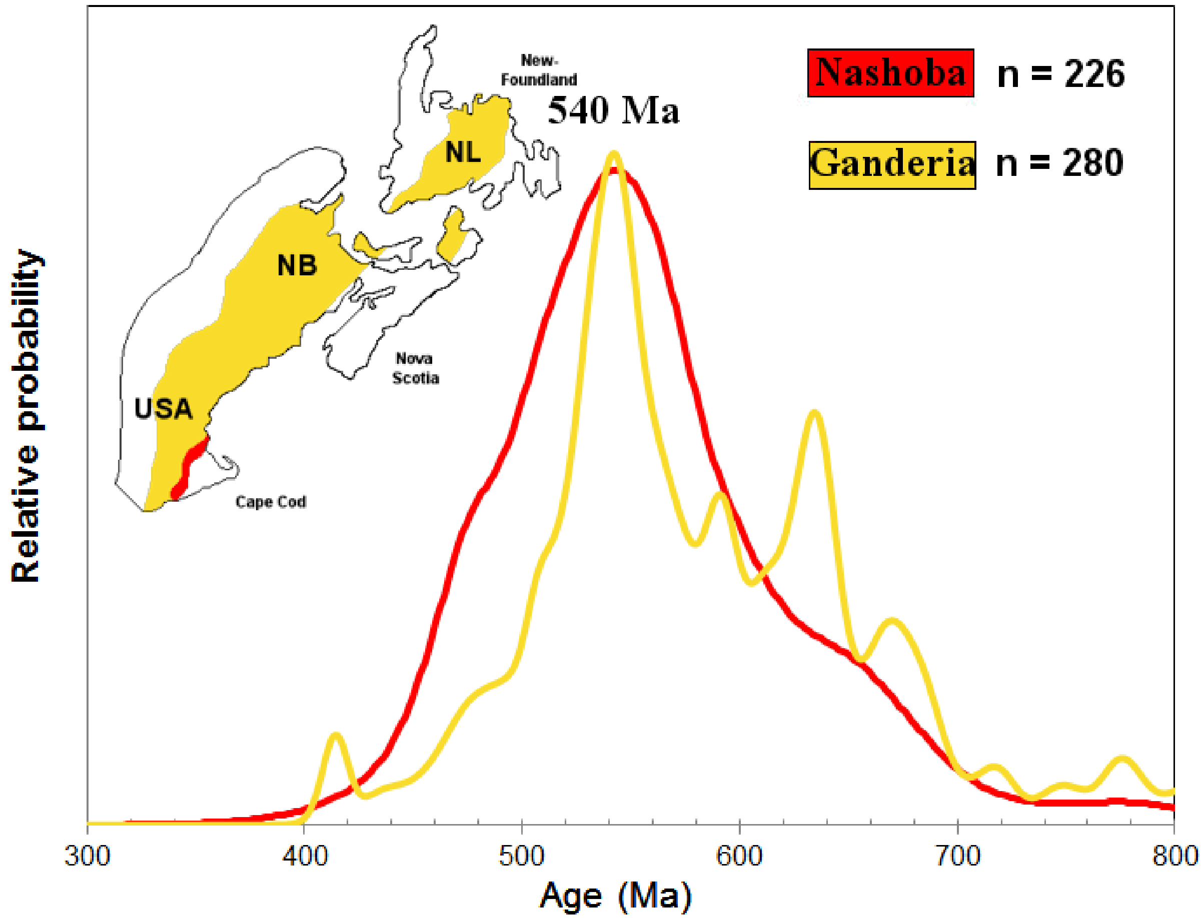

Figure 5.9: Enlarged version of Figure 5.6.

5.7 Provenance of the Nashoba terrane

The provenance of the sediments in the Nashoba terrane can be established by comparing the age populations of the Nashboa terrane (Fig. 5.10, red) to periods of tectonic activity (and of quiescence) in Laurentia, Baltica, and the West African and Amazonian shields of Gondwana based on data collected by multiple Appalachian researchers (Fig. 5.10; cf. Nance and Murphy, 2008). The Nashoba terrane as a whole exhibits a steady record of zircon ages from the Paleoproterozoic to the Neoproterozoic. Thus, by comparing these ages to the periods of activity in the four cratons, the detrital zircon suite of the Nashoba terrane is most consistent with a source along the Amazonian craton.

In general, the Amazonian craton was assembled through a complex orogenic history involving Archean orogens (3200-2600 Ma), the Trans-Amazonian orogeny (2200-1900 Ma), the Jurena/Rio Negro (1750-1500 Ma), the Rondonian/San Ignacio (1550-1250 Ma), and the Sunsas/Aguapei orogenies (1100-900 Ma) (Chew *et al.*, 2007; Pollock *et al.*, 2007). The age of these tectonic events agrees well with the age clusters of the Nashoba terrane established in this study. This result is also consistent with previous interpretations of the provenance of Ganderia from Amazonia (Nance *et al.*, 2010). It eliminates the need for transport of sediments from Laurentia (another potential source of Grenvillian-aged zircons). Finally, the provenance of the sediments in the Nashoba terrane in Amazonia supports its connection to Ganderia.

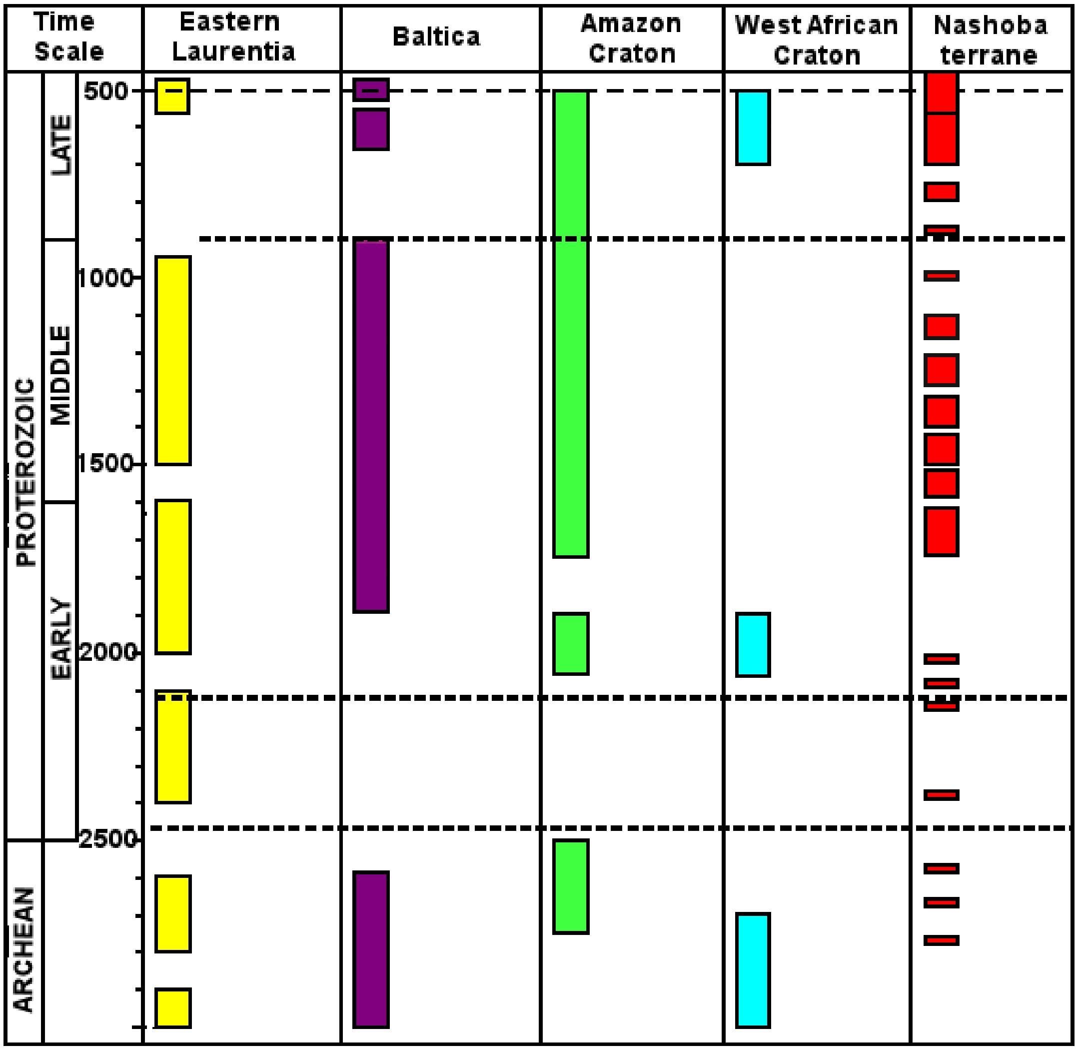

Figure 5.10: U/Pb zircon age data from the early Paleozoic to the Archean for cratonic provinces in Eastern Laurentia (yellow), Baltica (purple), Amazonia (green), and West Africa (blue). U/Pb ages (1σ error) of zircons from the Nashoba terrane (red) in this study were added for provenance comparison. The zircon suite of the Nashoba terrane most closely resembles the Amazonian craton of Gondwana. Modified from Nance and Murphy (2008).

Many researchers have generated global tectonic reconstructions based on paleomagnetic, isotopic, and detrital zircon studies in order to determine the exact location of Ganderia in the Neoproterozoic. All of these reconstructions place Ganderia, and neighboring Avalonia, somewhere along the coast of the Amazon craton (Murphy *et al*., 2010, Nance *et al.,* 2010; Keppie *et al.,* 2011). These reconstructions either treat Ganderia and Avalonia as a single microcontinent (Nance and Murphy 1994; Keppie et al. 1996, 1998; Murphy et al. 2000; Nance et al. 2002; Hatcher, 2010), as two distinct microcontinents with Avalonia bridging the gap that separates Amazonia from West Africa (van Staal *et al.,* 1996; Rogers *et al*., 2006), or most recently, as two distinct microcontinents that were located along what is now the northwestern margin of Amazonia (Murphy *et al*., 2010, Nance *et al.,* 2010; Keppie *et al.,* 2011).

The northwestern portion of South America and southern Mexico are composed of multiple terranes, such as the Chibcha and Oaxaquia (Fig. 5.10 A), that were thought to have once formed a perimeter around the (present location) northwestern portion of Amazonia, known as the "Oaxaquia margin" (Fig 5.10 B). The Oaxaquia margin is characterized by ca. 1.0-1.3 Ga zircon ages (Cordani *et al.,* 2010) and depleted Nd mantle model ages (T_{DM}) of 1.35-1.77 Ga (Keppie *et al.,* 2011). Researchers suggest that Oaxaquia-type basement underlies Avalonia and Ganderia (Figure 5.10 B; Nance *et al.,* 2010; Keppie *et al.,* 2011). If this is the case, then the Nashoba terrane may have originated from the (modern orientation) northwestern portion of Amazonia along the Oaxaquia margin.

A

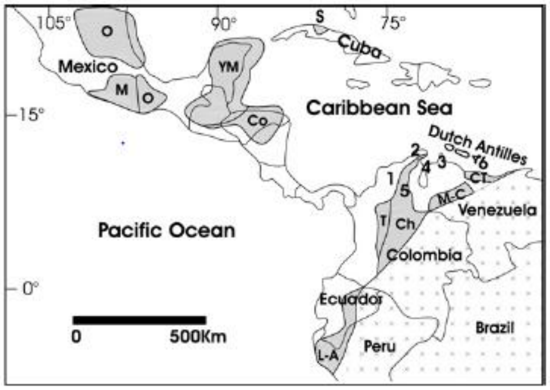

B

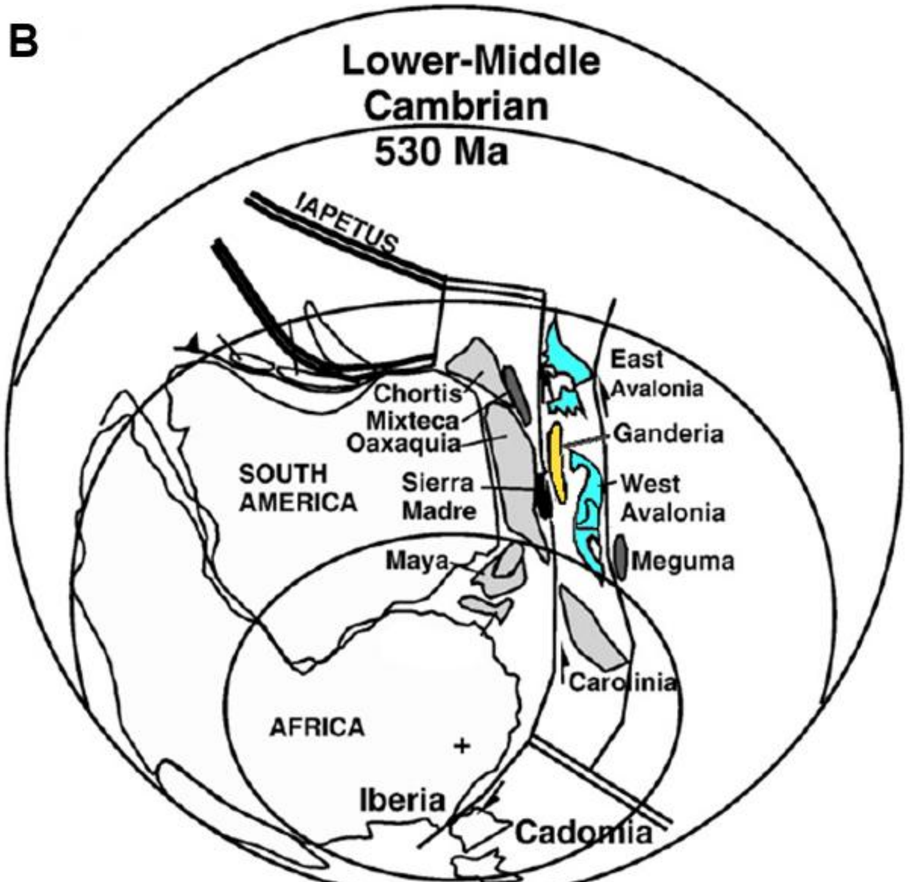

Figure 5.10 A and B: (A) Modern geographic localities of Oaxaquia margin terranes. Ch, Chibcha; C-T, Caucagua-Tinaco; Co, Chortis; LA, Loja-Amotape; M-C, Merida Caparo; M Mixteca; O, Oaxaquia; S, Socorro Complex; T, Tahamı; Y-M, Yucatan-Maya. From Molina *et al.* (2006). (B) Approximate location of Ganderia and Avalonia at ca. 530 Ma. Modified from Keppie *et al.*, (2011).

5.8 Tectonic Reconstruction of the Nashoba terrane

Ediacaran to Cambrian

Both Avalonia and at least part of Ganderia experienced active magmatism between ca. 650-610 Ma (van Staal, 2011). For Ganderia, this abundant arc magmatism continued until the Early Cambrian, whereas Avalonian Neoproterozoic magmatic history ceases at ca. 590 Ma (Barr *et al.*, 2003; Murphy *et al.*, 2004; Samson *et al.*, 2005; van Staal *et al.*, 2009; 2011). Ganderian rocks in the Grand Manan Island and New River belts of New Brunswick both record these two distinct periods of Neoproterozoic arc magmatism; one at ca. 629 to 611 Ma (the age group shared with Avalonia) and another at ca. 553 to 535 Ma (the age group unique to Ganderia) (Fyffe *et al.*, 2009). However, some areas of Ganderia, such as the Brookville belt (New Brunswick) only experienced a single period of arc magmatism lasting from ca. 553 to 528 Ma (Fyffe *et al.*, 2009). During the Neoproterozoic to Cambrian, the Brookville belt has been suggested to be located in a more stable inboard position within the Ganderian segment of the Amazonian upper-plate hinterland relative to the active outboard margin represented by the Grand Manan Island and New River belts (Fyffe *et al.*, 2009). Similarly, >600 Ma plutons occur in the Ganderian Aspy belt in northwestern Cape Breton Island but are absent in the Bras d'Or belt to the southeast (Barr and Raeside, 1989; Fyffe *et al.*, 2009). Based on the detrital zircon data presented above, the Nashoba terrane lacks abundant zircons from the ca. 630-610 Ma magmatic event. Thus, it only recorded input from plutonic rocks during the ca. 550- 528 period indicating it may be derived from a source similar to the

Brookville and Bras d' Or belts of New Brunswick and Cape Brenton Island, and may also have been located in a more stable inboard portion of Ganderia.

In Newfoundland it is seen that, the ca.553 to 528 Ma period of magmatism in Ganderia was followed by rifting at ca. 520 to 500 Ma (Fyffe *et al.,* 2009; van Staal *et al.,* 2009; 2011). Ganderia is thought to have completely rifted off of Gondwana by 500 Ma (van Staal *et al.* 2009; 2011) opening the Rheic ocean behind it (Fig. 5.11). Continued slab roll back, combined with the heat generated by the Penobscot arc (ca. 515 to 495) along the leading edge of Ganderia and produced a second spreading center within Ganderia itself, at ca. 495 Ma, forming the Penobscot backarc basin. This separated Ganderia into an active leading edge (Penobscot arc) and a passive trailing edge known as the Gander margin (van Staal *et al.* 2009; 2011). Volcanic rocks in the Marlboro Formation and the Fishbrook Gneiss (ca. 499 Ma) of the Nashoba terrane formed within the time frame of active magmatism and rifting associated with the Penobscot arc back-arc basin.

By the Early Ordovician, at ca. 485-480 Ma, the two halves of Ganderia were pushed back together temporarily closing the Penobscot back-arc basin due to the shallowing of the subducting Iapetan slab (Zagorevski *et al.,* 2010; van Staal *et al.,* 2011). The closure of the Penobscot back-arc is marked by obducted ophiolite sequences onto the trailing Gander margin and is known as the Penobscot orogeny (van Staal *et al.* 2009; 2011). This time period is related to orogenesis, uplift, and erosion in Newfoundland (van Staal *et al.* 2009; 2011; Zagorevski *et al.,* 2010). There are many detrital zircons, within error, of this age in the Nashoba terrane. In addition, this time frame is also marked by the presence of detrital zircons with low Th/U ratios. These zircon grains were interpreted as being detrital but with a metamorphic origin (Fig. 5.12). The weighted average of these zircon ages is 484 ± 15 Ma. It is possible that these low Th/U zircons formed as a result of the short lived Penobscot orogeny.

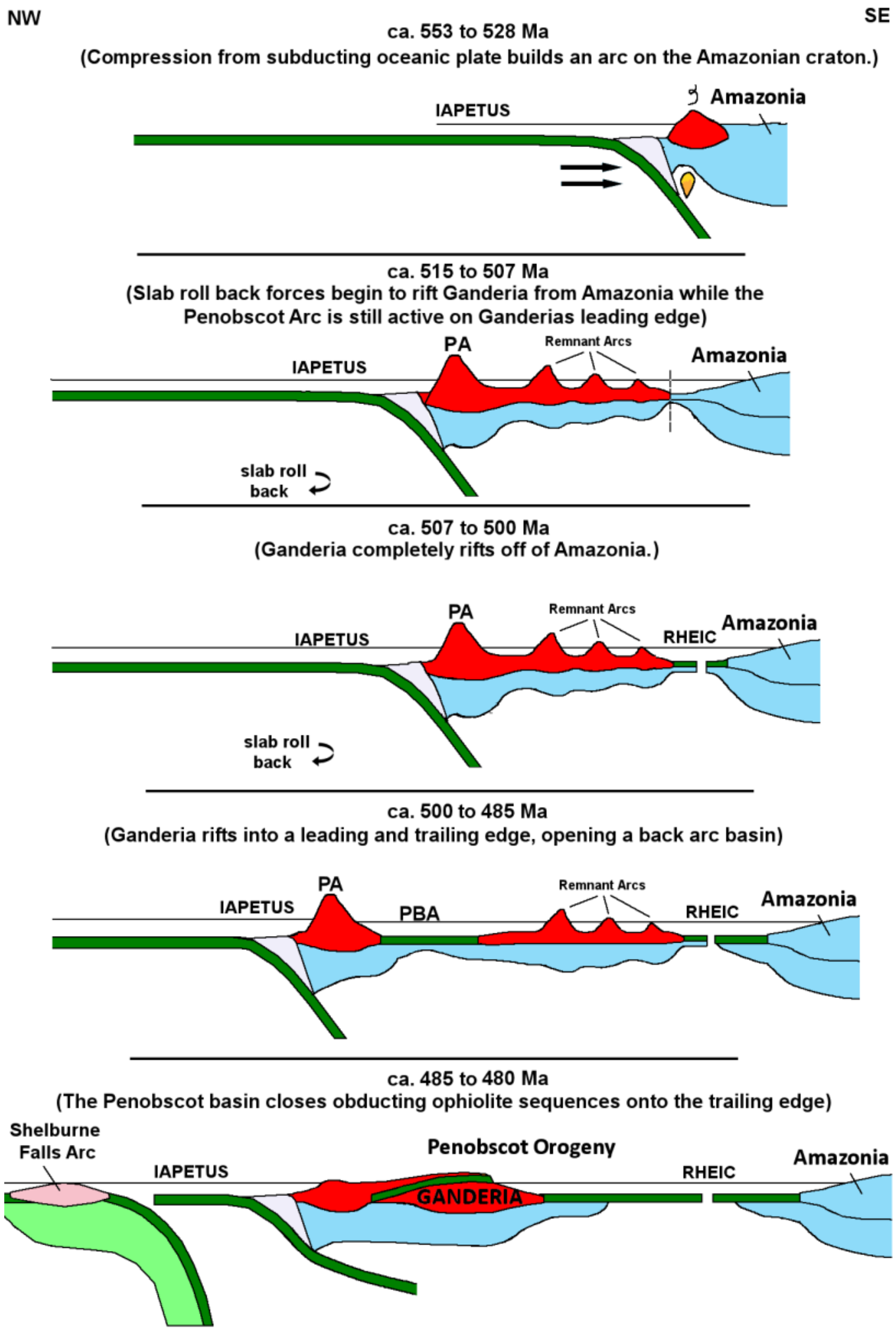

Figure 5.11: A tectonic reconstruction of Ganderia from the Ediacaran through the Ordovician. Modified from van Staal *et al.,* (2009; 2011). PA = Penobscot arc. PBA = Penobscot Back Arc Basin.

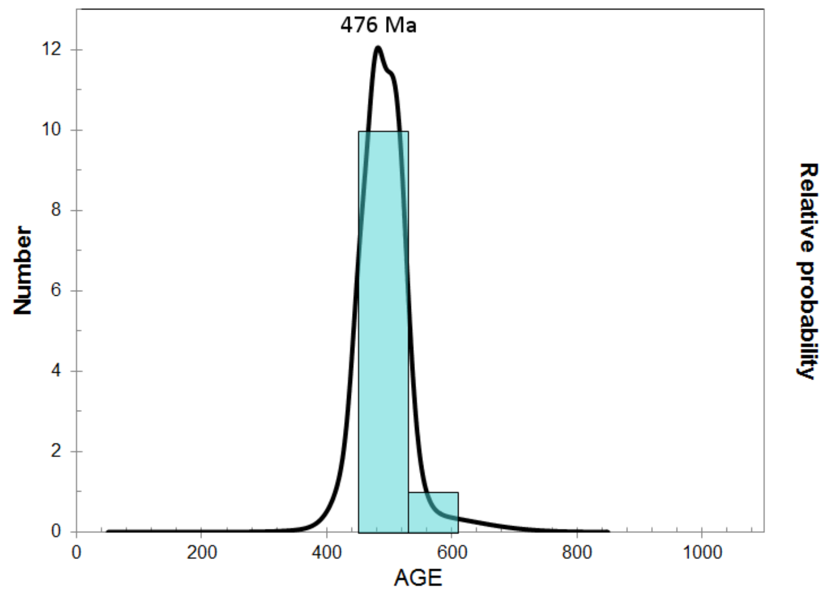

Figure 5.12: Probability density diagram of the concordant zircons (>0.05 probability of concordance) from the Nashoba terrane that were interpreted to be detrital zircons with a metamorphic protolith (low Th/U ratios of <0.1) . The probability density diagram shows $^{206}Pb/^{238}U$ ages from the Shawsheen Gneiss, the Nashoba Formation gneiss, and the Tadmuck Brook Schist.

After the Penobscot orogeny a new arc, the Popelogan-Victoria arc (Fig. 5.13), was built on the remnants of the Penobscot arc (van Staal *et al.* 2009; 2011). Due to differences in the rate of plate motion (van Staal *et al.*, 2011) the Popelogan-Victoria arc rifted from Ganderia resulting into a leading edge and trailing edge for a second time at ca. 475 Ma and formed a wide back-arc basin known as the Tetagouche-Exploits basin and separated the passive Gander margin (trailing edge) from the Popelogan-Victoria arc on the leading edge. The Tetagouche-Exploits basin sediments are dominated by Grenvillian aged zircons, interpreted to be derived from a Laurentian source, and by late-Ordovician to early-Silurian aged zircons (Pollock *et al.*, 2007).

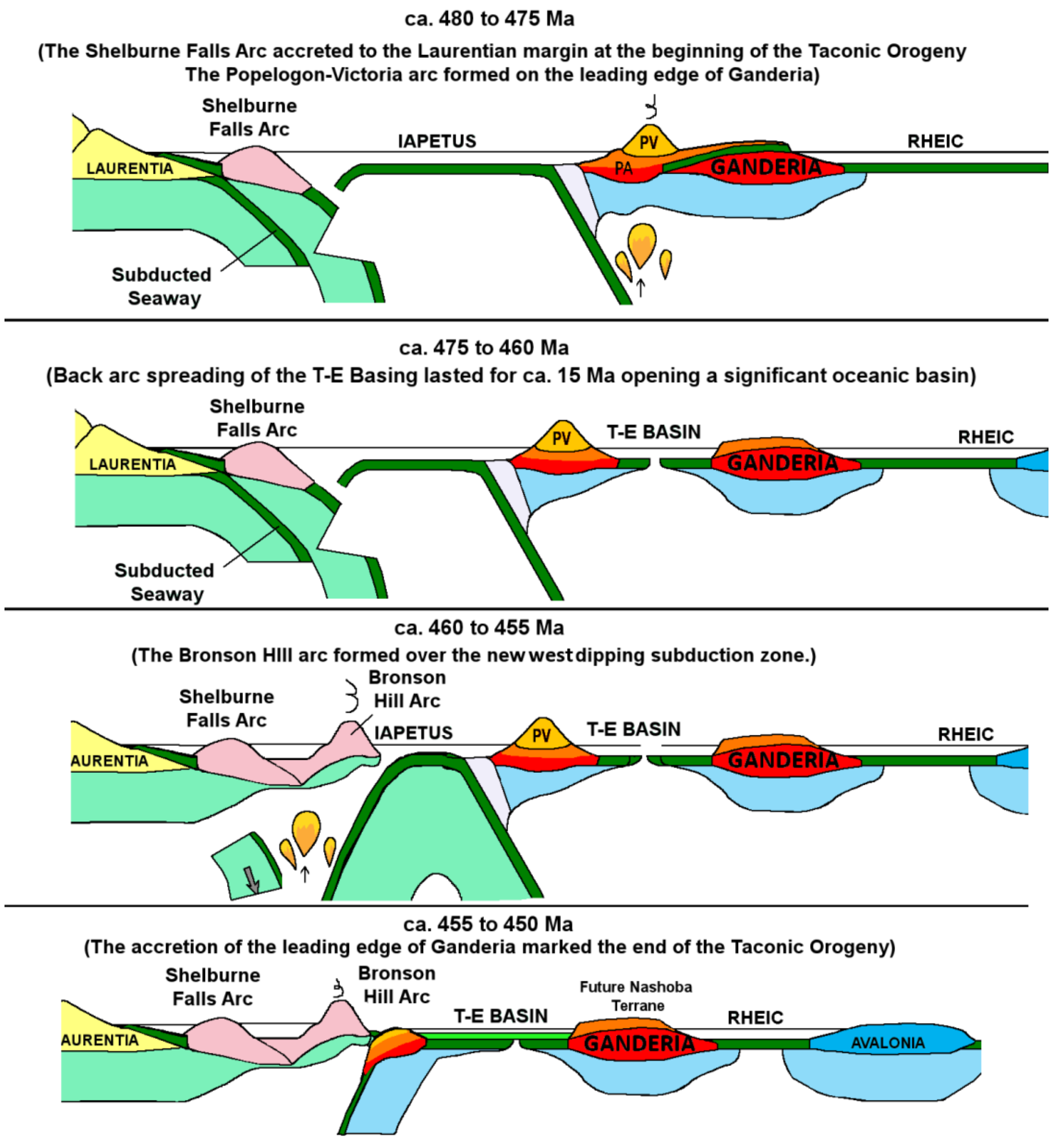

Figure 5.13: A tectonic reconstruction Ganderia during the Ordovician. Here the Nashoba terrane can be directly substituted for “Ganderia”. Modified from van Staal *et al.*, (2009; 2011). PV = Popelogan Victoria Arc. T-E Basin = Tetagouche-Exploits Basin

The Popelogan-Victoria arc accreted to the Laurentian margin at ca. 455 to 450 Ma during the final stages of the Taconic orogeny (van Staal *et al.*, 2011). This time period marks the maximum age of deposition of the Nashoba terrane meta-sediments and the end of the Nashoba terrane's detrital zircon record. After this point in time the zircon record changes to metamorphic, beginning with the closure of the Tetagouche-Exploits basin during the Salinic orogeny.

There are complications, however, to this scenario. As discussed above, the detrital zircon suite of the Nashoba terrane closely matches the detrital zircon suite of the Gander terrane in Newfoundland, Ganderia's passive trailing margin. However, the Marlboro Formation of the Nashoba terrane has a distinct arc-like geochemical signature (DiNitto *et al.*, 1984; Kay *et al*., 2009). If the Nashoba terrane was similar to the Gander terrane then the Nashoba terrane should be the passive trailing edge of Ganderia as well and should not have an arc. In addition, the arcs of the leading edge of Ganderia, the Penobscot/ Popelogon-Victoria are not visible in Massachusetts, presumably having been subducted or are covered by the Merrimack belt sediments or younger cover. Because the leading edge of Ganderia cannot be seen in SE New England this hypothesis is difficult to test.

Based only on the zircon data from this study, it is not possible to determine if the Gander margin of SE New England experienced an additional arc building stage beyond what is seen in Maine through Newfoundland, or if the geometry of the suduction zones differs in Massachusetts versus the northern Appalachians. However, another solution to the apparent "reverse geometry" of the Marlboro Formation is that multiple periods of deformation have compressed

Massachusetts and truncated Ganderia. The Marlboro Formation arc could be a Penobscot arc back-arc remnant that was obducted onto the Gander margin during the Penobscot orogeny and has been translated to the east in subsequent deformations (Fig. 11). As stated earlier, the reported ages of the Marlboro Formation volcanics range between ca. 501 Ma and 540 Ma (Walsh *et al.*, 2011) and, in general, become younger northward (modern orientation). This is a long time-span for a single arc/back-arc as most are considered to have an average lifespan of approximately 11 Ma (cf. Schmidt and Poli, 2003). It is possible that, with continued slab roll-back, the Penobscot arc rifted several times into remnant arcs with ages spanning between 540 to 500 Ma (Fig. 11A). The Penobscot orogeny may have compressed these remnant arcs and translated them onto the Gander margin. If true, the Marlboro Formation and the meta-sedimentary rocks of the Nashoba terrane as a whole are translated portions of the Penobscot arc/back-arc system.

Ordovician to Carboniferous

In addition to detrital zircons, the Nashoba terrane has produced abundant metamorphic zircons. Metamorphic zircons in the Nashoba terrane span an age range from ca. 450 Ma to ca. 310 Ma (See section 5.3). The oldest age of metamorphism in the Nashoba terrane is constrained by the ca. 423 Ma age of monazites (Stroud *et al.*, 2009) and a metamorphic monazite age of 425 Ma in the Fish Brook Gneiss (Hepburn *et al.*, 1995). There is some evidence to suggest that the Salinic orogeny is recorded in the Nashoba terrane metamorphic record based on the zircon data in this study; however, the relationship is tenuous due to the large error associated with the data in this study. The single Gaussian curve of the data (Fig. 5.8A) is interpreted to mean that the resolution of the LA-ICP-MS data was too low to differentiate between different age populations that are apparent from other studies (Hepburn *et al.*, 1995; Jerden *et al.*, 2007; Stroud *et al.*, 2009). Without distinguishable peaks in the data it is not possible to interpret multiple metamorphic events. However, the data from the Nashoba terrane metamorphic zircons does show a peak at 370 Ma, which coincides with the Neoacadian orogeny and the (M3) metamorphic event of Stroud *et al.*, (2009). The (M3) metamorphic event was interpreted by them as a period of fluid infiltration along shear zones and was identified only in metamorphic rims on monazite grains. Zircon grains in the Nashoba terrane fall within this same age period (i.e. sample MLBM1) indicating that the zircon may have also experienced hydrothermal alteration that resulted in compositional changes including the lowering of the

Th/U ratios and the resetting of the U-Pb isotopes (Hoskin and Schaltegger, 2003).

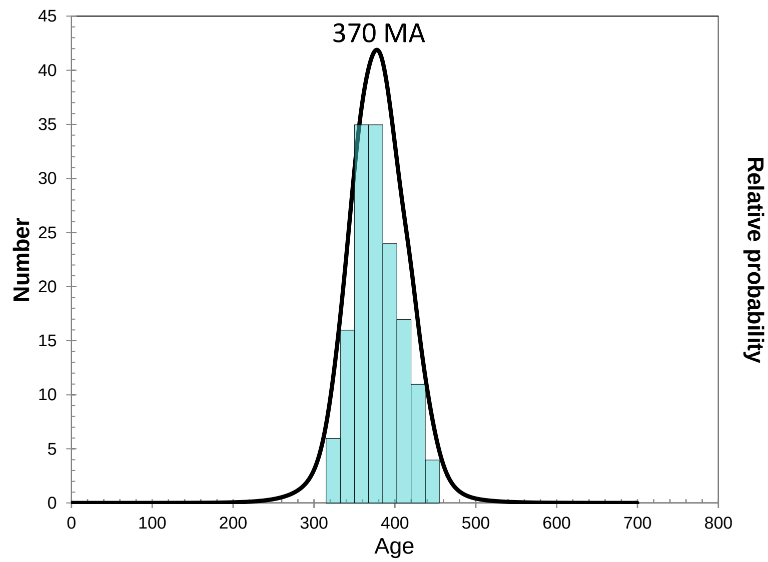

Figure 5.14: Probability density diagram of concordant (>0.05 probability of concordance) metamorphic zircons (Th/U <0.1) of the Nashoba terrane. The probability density diagram shows $^{206}Pb/^{238}U$ ages.

5.9 Newbury Volcanic Complex

The Newbury Volcanic Complex slate-phyllite was the only unit with zircons that were significantly different in age from the other units sampled. There were no metamorphic grains in the Newbury Volcanic Complex, which was expected due to the low grade of metamorphism of the formation. The youngest detrital zircon was Devonian in age, whereas the units in the Nashoba terrane had youngest detrital zircons that were Ordovician in age. There are peaks in the zircon ages at ca. 420 Ma and 440 Ma, which do not correspond to either the Avalonian peak, (ca. 610 Ma) or to the Nashoba peak (ca.540 Ma). It cannot be ignored that these ages are similar, within error, to the ages of the Merrimack belt sediments (Wintsch, 2007). However, there were not enough grains obtained from this sample to statistically represent the Newbury Volcanic Complex; as a result, it is unclear whether the Newbury Volcanic Complex should be considered part of, or whether it received sediment from, the Nashoba, Avalon, or the Merrimack terrane. However, the ca. 420 Ma peak in the data corresponds to the beginning of the Acadian orogeny and the subduction of the oceanic tract separating Avalonia from Ganderia (Van Staal *et al*., 2009). Therefore, there is a strong correlation between the Newbury Volcanic Complex and the convergence between Avalonia and Ganderia.

In Newfoundland, the convergence of Avalonia is responsible for the Acadian orogeny (Dunning *et al.,* 1990; van Staal *et al.*, 2009). The timing of the Acadian orogeny is constrained by the presence of a Silurian arc and backarc magmatism on the trailing edge of Ganderia facing Avalonia, at ca. 423 to 442 Ma (van Staal *et al.,* 2009; Barr *et al.*, 2002; Hepburn *et al.*, 1995). While there is some evidence to suggest that Avalonia was still outboard of the New England Laurentian margin during the Devonian (Wintsch *et al.,* 1992, 1993; Walsh *et al.*, 2011), this study proposes that the Newbury Volcanic Complex formed as a Siluro-Devonian arc in response to the convergence of Avalonia and the subduction of the oceanic tract separating the two terranes.

6.0 CONCLUSIONS

The maximum ages of deposition of metasedimentary rocks of the Nashoba terrane, based on the age of the youngest detrital zircons and known stratigraphic relationships (Goldsmith, 1991a) are (from oldest to youngest): the Marlboro Formation at ca. 470 Ma, the Shawsheen Gneiss at ca. 470 Ma, the Nashoba Formation at ca. 465 Ma, and the Tadmuck Brook Schist at ca. 463 Ma. The Ordovician age of the units is consistent with the original Cambrian to Ordovician formation of the terrane. The lack of a significant difference in zircon ages or depositional history across the Assabet River fault zone indicates that the ARFZ does not represent a major terrane boundary.

The dominant detrital zircon age population in the Nashoba terrane is ca. 540 Ma, which is consistent with Ganderia. The data presented here supports the interpretation that the Nashoba terrane is now a part of Ganderia's passive trailing margin and was by at least the Acadian orogeny. The Cambrian volcanic rocks of the Nashoba terrane may have formed during a period of widespread igneous activity in Ganderia at ca. 540 Ma. This period of magmatism was followed shortly after by the rifting of the Penobscot arc and opening of the Penobscot back-arc basin at ca. 500 Ma (Fyffe et al. 2009; van Staal et al. 2009). The ca. 500 Ma time period is coincident with the ages of both the Marlboro Formation volcanics (Walsh et al., 2011) and with the age of the Fishbrook Gneiss (Hepburn et al., 1995). The oldest ages of the detrital zircon suite of the Marlboro Formation indicate that it formed over continental crustal material, and not as an isolated oceanic arc in a supra-subduction zone setting.

Following rifting, the Penobscot back-arc temporarily closed. This time period coincides with the age of detrital zircons with low Th/U ratios in the Nashoba terrane. At ca. 475 Ma a new arc, the Popelogan-Victoria had built on the remnant of the Penobscot arc and opened the Tetagouche-Exploits basin. The Popelogan-Victoria arc accreted to the Laurentian margin at ca. 455 to 450 Ma during the final stages of the Taconic orogeny. This time period coincides with the youngest detrital zircon grains of the Nashoba terrane meta-sediments and marks the maximum age deposition and the end of the Nashoba terrane's detrital zircon record. The Taconic orogeny was followed by the Salinic orogeny when the trailing edge of Ganderia accreted to composite Laurentia closing the Tetagouche-Exploits basin at ca. 450 to 425 Ma. There is some evidence to suggest that the Salinic orogeny is recorded in the Nashoba terrane metamorphic zircon record, however the relationship is tenuous due to the large error associated with these grains.

The continuous succession of detrital zircons ages in the Nashoba terrane that range from 500 Ma to 1.7 Ga is consistent with its origin along the peri-Gondwanan Oaxaquia margin of Amazonia (Murphy *et al*., 2010; Nance *et al*., 2010; Keppie *et al*., 2011). If this is the case, then this relationship could account for the population of Grenville-aged zircon grains found in the Nashoba terrane and the older Paleoproterozoic to Archean aged zircon grains without having to rely on distant transport from the Laurentia margin by the recycling of Ganderian crust. Metasedimentary units of the Nashoba terrane show no indication of receiving sediment from Avalonia or the Merrimack belt, suggesting that it docked as a separate tectonic block.

Based on U-Pb ages of monazite (Stroud *et al.,* 2009) the Nashoba terrane underwent at least three distinct periods of metamorphism. The detrital zircon data of this study are not precise enough to differentiate between the different periods of metamorphism; however, the largest peak in the metamorphic zircon data is associated with the Neoacadian orogeny and the docking of the Meguma terrane. The Neoacadian metamorphic event was interpreted as a period of fluid infiltration along shear zones and was responsible for the alteration and resetting of Nashoba terrane zircons that were located adjacent to these shear zones

7.0 WORKS CITED

Acaster, M., and Bickford, M. E., 1999, Geochronology and geochemistry of Putnam-Nashoba Terrane metavolcanic and plutonic rocks, eastern Massachusetts; constraints on the early Paleozoic evolution of eastern North America: Geological Society of America Bulletin, v. 111, p. 240–253.

Aleinikoff, J. N., Schenck, W. S., Plank, M. O., Srogi, L., Fanning, C. M., Kamo, S. L., and Bosbyshell, H., 2006, Deciphering igneous and metamorphic events in high-grade rocks of the Wilmington Complex, Delaware: Morphology, cathodluminescence and backscattered electron zoning, and SHRIMP U-Pb geochronology of zircon and monazite: Geological Society of America Bulletin v. 118, no. 1-2 , p. 39-64.

Aleinikoff, J. N., Wintsch, R. P., Tollo, R. P., Unruh, D. M., Fanning, C. M., and Schmitz, M.D., 2007, Ages and origins of rocks of the Killingworth dome, south-central Connecticut: Implications for the tectonic evolution of southern New England: American Journal of Science, v. 307, p. 63– 118.

Andersen, T., 2005, Detrital zircons as tracers of sedimentary provenance: limiting conditions from statistics and numerical simulation: Chemical Geology, v. 216, p. 249–270.

Barr, S. M., and Raeside, R. P., 1989, Tectono-stratigraphic terranes in Cape Breton Island, Nova Scotia.implications for the configuration of the northern Appalachian orogen: Geology v. 17, p. 822–825.

Barr, S. M., White, C. E., and Miller, B. V., 2002, The Kingston Terrane, southern New Brunswick, Canada: Evidence for a Silurian volcanic arc: Geological Society of America, Bulletin v. 114, p. 964–982.

Barr, S. M., Davis, D. W., Kamo, S., and White, C. E., 2003, Significance of U-Pb detrital zircon ages in quartzite from peri-Gondwanan terranes, New Brunswick and Nova Scotia, Canada: Precambrian Research, v. 126, p. 123-145.

Bell, K. G. and Alvord, D. C., 1976, Pre-Silurian stratigraphy of northeastern Massachusetts, *in* Page L.R., ed., Contributions to the Stratigraphy of New England: Geological Society of America, memoir 148, p. 179-216.

Bennett, V. and Michael T., 2009, U-Pb isotopic age dating by LAM ICP-MS, INCO Innovation Centre, Memorial University: sample preparation methodology and analytical techniques, *in* MacFarlane, K.E., E Weston, L.H., and L.R. Blackburn, eds., Yukon Exploration and Geology p. 47-55

Billings, M. P., 1976, Geology of the Boston Basin, *in* Lyons, P.C., and Brownlow, A.H., eds., Studies in New England Geology: Geological Society of America Memoir 146, p. 5–28.

Cameron, B., and Naylor, R.S., 1976, General geology of southeastern New England. *In* Geology of southeastern New England. *Edited by* B. Cameron: New England Intercollegiate Geological Conference Guidebook, 68th Annual Meeting, Science Press, Princeton NJ, p. 13-27

Cordani, U. G., Teixeira, W., DÁgrella-Filho, M.S., Trindade, R.I., 2009. The position of the Amazon Craton in Supercontinents: Gondwana Research v. 115, p. 396–407.

Cawood, P. A., McCausland, P. J. A., and Dunning, G. R., 2001, Opening Iapetus; constraints from the Laurentian margin in Newfoundland: Geological Society of America Bulletin, v. 113, p. 443–453.

Chew, D. M., Kirkland, C. L., Schaltegger, U., Goodhue, R., 2007, Neoproterozoic glaciation in the Proto-Andes: tectonic implications and global correlation: Geology v. 35, p. 1095–1099.

Cherniak, D. J., Watson, E. B., 2003, Diffusion in Zircon: Reviews in Mineralogy and Geochemistry, v. 53, p. 113-143.

Corfu, F., Hanchar, J. M., Hoskin, P. W. O., and Kinny, P. D., 2003, Atlas of zircon textures. Zircon: Reviews in Mineralogy and Geochemistry, v. 53, p. 469-500

Cox, R. A., Wilton, D. H. C. and Košler J., 2003, Laser ablation U-Th-Pb in-situ dating of zircon and allanite: An example from the October Harbour granite, central coastal Labrador, Canada: The Canadian Mineralogist v. 41, p. 273-291

DiNitto, R., Hepburn, J.C., Cardoza, K.D. and Hill, M., 1984, The Marlboro Formation in its type area and associated rocks just west of the Bloody Bluff Fault Zone, Marlborough area, Massachusetts, *in* Hanson, L., ed., Geology of the Coastal Lowlands: Boston, MA to Kennebunk, ME: New England Intercollegiate Geological Conference, 76th Annual Meeting, Salem State College, Salem, Massachusetts, p. 271-291

Dorais, M. J., and Wintsch, R. P., 2001, A Laurentian provenance of the Merrimack Belt, New England Appalachians: Geological Society of America, Abstracts with Programs, v. 33, p. 261.

Emerson, B.K., 1917, Geology of Massachusetts and Rhode Island: U.S. Geological Survey Bulletin v. 597, no. 289

Faure, G. and Mensing, T. M., 2005, Isotopes, principles and applications. Chapter 10: John Wiley and Sons Inc., Hoboken, NJ.

Fedo, C.M., Sircombe, K.N. & Rainbird, R.H. 2003. Detrital zircon analysis of the sedimentary record. In: Hanchar, J.M. & Hoskin, P., eds., Zircon: Experiments, Isotopes, and Trace Element Investigations: Mineralogical Society of America, Reviews in Mineralogy, v. 53, p. 277–303.

Fyffe, L.R., Barr, S.M., Johnson, S.C., McLeod, M.J., McNicoll, V.J., Valverde-Vaquero, P., van Staal, C.R., and White, C.E., 2009, Detrital zircon ages from Neoproterozoic and Early Paleozoic conglomerate and sandstone units of New Brunswick and coastal Maine: implications for the tectonic evolution of Ganderia: Atlantic Geology v. 45, p. 110–144

Gates, O., Moench, R.H., 1981, Bimodal Silurian and Lower Devonian volcanic rock assemblages in the Eastport-Machias area, Maine: US Geological Survey Professional Paper v. 1148, p. 32

Goldsmith, R., 1991a, Stratigraphy of the Nashoba Zone, eastern Massachusetts: an enigmatic terrane, *in* Hatch, N.L., Jr., ed., The Bedrock Geology of Massachusetts: United States Geological Survey, Professional Paper 1366 E-J, p. F1-F22.

Goldsmith, R., 1991b, Structural and metamorphic history of eastern Massachusetts, *in* Hatch, N.L., Jr., ed., The Bedrock Geology of Massachusetts: United States Geological Survey, Professional Paper 1366 E-J, p. H1-H63.

Goldstein, A., and Hepburn, J.C., 1999, Possible correlations of the Norumbega fault system with faults in southeastern New England, *in* Ludman, A., and West, D.P., Jr., eds, Norumbega Fault System of the Northern Appalachian: Boulder, Colorado: Geological Society of America Special Paper, v. 331, p. 73-82.

Hatcher, R.D., Jr., 2010, The Appalachian orogen: A brief summary, *in* Tollo, R.P. Bartholomew, M.J., Hibbard, J.P., and Karabinos, P.M., eds., From Rodinia toPangea: The Lithotectonic Record of the Appalachian Region: Geological Society of America, Memoir 206, p. 1–19

Hepburn, J.C., and Munn, B., 1984, A geologic traverse across the Nashoba block, eastern Massachusetts, *in* Hanson, L.S., ed., Geology of the Coastal lowlands: Boston, MA to Kennebunk, ME: New England Intercollegiate Geological Conference, 76th Annual Meeting, Salem State College, Salem, Massachusetts, p. 103-114.

Hepburn, J.C., Hon, R., Dunning, G.R., Bailey, R.H., and Galli, K., 1993, The Avalon and Nashoba terranes (eastern margin of the Appalachian orogen in southeastern New England), in Cheney, J.T., and Hepburn, J.C., eds., Field trip guidebook for the Northeastern United States: Boulder, Colorado, Geological Society of America, Annual Meeting, Boston, v. 2, p. X1–X31.

Hepburn, J. C., Dunning, G. R., Hon, R., 1995, Geochronology and Regional Tectonic Implications of Silurian Deformation in the Nashoba Terrane, Southeastern New England, U.S.A., *in* Hibbard, J.P., van Staal, C.R., and Cawood, P.A., eds. Current Perspectives in the Appalachian-Caledonian Orogen: Geological Association of Canada, Special Paper 41, p. 349-366.

Hepburn, J. C., Fernandez-Suarez, J., Jenner, G. A., and Belousova, E.A., 2008,Significane of Detrital Zircon Ages from the Westboro Quartzite, Avalone terrane, Eastern Massachusetts: Geological Society of America, *Abstracts with Programs*, Vol. 40, No. 2, p. 14.

Hon, R., Hepburn, J. Christopher and Laird, Jo, 2007, Siluro-Devonian Igneous Rocks of the Easternmost Three Terranes in Southeastern New England: Examples from NE Massachusetts and SE New Hampshire, in Thompson, Peter, J., ed., Guidebook to Field Trips in New Hampshire, Adjacent Maine and Massachusetts: Geological Society of America, Northeastern Section, Univ. of New Hampshire p.23-43.

Horn, I., Rudnick R.L., McDonough, W.F., 2000, Precise elemental and isotope ratio determination by simultaneous solution nebulization and laser ablation-ICP-MS: application to U-Pb geochronology: Chemical Geology v. 167, p. 403-423.

Jerden, J.L., Jr., 1997, Polyphase Metamorphism and Structure of the Tadmuck Brook Schist, Eastern Massachusetts [M.S. thesis]: Chestnut Hill, Massachusetts, Boston College, 250

Hoskin, P. W. O., and Schaltegger, U., 2003, The composition of zircon and igneous and metamorphic petrogenesis, *in* Hanchar, J. M., and Hoskin, P. W. O., editors, Zircon: Washington, D. C., Mineralogical Society of America, Reviews in Mineralogy and Geochemistry, v. 53, p. 27–62.

Hoskin P.W.O., 2005, Trace-element composition of hydrothermal zircon and the alteration of Hadean zircon from the Jack Hills, Australia: Geochimica et Cosmochimica Acta 69, p. 637-648.

Karabinos, P., Samson, S. D., Hepburn, J. C., and Stoll, H. M., 1998, Taconian orogeny in the New England Appalachians: Collision between Laurentia and the Shelburne Falls arc: Geology, v. 26, p. 215–218.

Kay, A., Hepburn, J. C., Kuiper, Y. D., 2009., Nd Isotopic Constrains on the origin of the Nashoba terrane, Eastern Massachusetts: Geological Society of America *Abstracts with Programs*, Vol. 41, No. 3, p. 98.

Keppie J.D., Murphy, J.B., and Nance, R.D., 1996, Terrane transfer between eastern Laurentia and western Gondwana in the early Paleozoic: Constraints on global reconstructions. *In* Avalonian and Related peri-Gondwanan Terranes of the Circum-North Atlantic. *Eds.* R.D. Nance and M.D. Thompson: Geological Society of America, Special Paper v. 304, p. 369–380.

Keppie J.D., Davis, D.W., and Krogh, T.E., 1998. U-Pb geochronological constraints on Precambrian stratified units in the Avalon composite terrane of Nova Scotia, Canada. Tectonic implications: Canadian Journal of Earth Sciences 35, p. 222–236.

Keppie, J.D. Murphy, J.B., Nance, R.D**.** and Dostal, J. 2011. Mesoproterozoic Oaxaquia-type basement in peri-Gondwanan terranes of Mexico, the Appalachians and Europe: TDM age constraints on extent and significance: International Geology Review, v. 54, *in press*.

Klein, Cornelis, and Dutrow, Barbara, 2007, Manual of Mineral Science, 23rd edition, John Wiley & Sons.

Košler, J., Fonneland, H., Sylvester, P., Tubrett, M., Pedersen, R., 2002, U–Pb dating of detrital zircons for sediment provenance studies—a comparison of laser ablation ICPMS and SIMS techniques: Chemical Geology v. 182, p. 605-618.

Košler, J, and Sylvester, P.J., 2003, Present trends and the future of zircon in geochronology; laser ablation ICPMS: Zircon: Reviews in Mineralogy and Geochemistry v. 53, p. 243-275.

Ludwig, K. L., 1998, On the Treatment of Concordant Uranium-Lead Ages: Geochimica et Cosmochimica Acta, v. 62, issue 4, p. 665-676.

Ludwig K.L., 2008, *Isoplot 3.7.* A geochronological toolkit for Microsoft Excel: Berkeley Geochronology Center Special Publication, No. 4, rev. August 26, p.77.

Markwort, R.J., 2007, Geology of the Shrewbury Quadrangle, East-Central Massachusetts [M.S. thesis]: Chestnut Hill, Massachusetts, Boston College, 208.

Mezger K, Krogstad E.J., 1997, Interpretation of discordant U-Pb zircon ages: an evaluation: Journal of Metamorphic Geology v. 15, p. 127-140.

Moench, R., and Aleinikoff, J. N., 2003, Stratigraphy, geochronology, and accretionary terrane settings of two Bronson Hill arc sequences, northern New England: Physics and Chemistry of the Earth, v. 28, p. 113–160.

Molina, A.C., Cordani, U. G., McDonald, William D., 2006, Tectonic correlations of pre-Mesozoic crust from the northern termination of the Colombian Andes, Caribbean region: Journal of South American Earth Sciences, v. 21, p. 337–354.

Murphy, J.B., Strachan, R.A., Nance, RD., Parker, K.D., and Fowler, M.B. 2000. Proto-Avalonia: A 1.2 – 1.0 Ga tectonothermal event and constraints for the evolution of Rodinia: Geology v. 28, p. 1071–1074.

Murphy, B. J., Fernandez-Suarez, J., Jeffries, T. E, and Strachan, R. A., 2004, U-Pb (LA-ICP-MS) dating of detrital zircons from Cambrian clastic rocks in Avalonia: erosion of a Neoproterozoic arc along the northern Gondwanan margin: Journal of the Geological Society, London, v.161, p. 243-254.

Murphy, J.B., Keppie, J.D., Nance, R.D. and Dostal, J., 2010, Comparative evolution of the Iapetus and Rheic Oceans: A North America perspective: Gondwana Research, v. 17, p. 482-499.

Nance, R.D.**,** Gutiérrez-Alonso, G., Keppie, J.D. Linnemann, U., Murphy, J.B., Quesada, C., Strachan, R.A. and Woodcock, N.H., 2010, Evolution of the Rheic Ocean. *Gondwana Research*, v. 17, p. 194-222Olszewski, W.J., Jr., 1980, The geochronology of some stratified metamorphic rocks in northeastern Massachusetts: Canadian Journal of Earth Sciences, v. 17, p. 1407-1416.

Nance, R.D., Murphy, J.B., and Keppie J.D., 2002, A Cordilleran model for the evolution of Avalonia: Tectonophysics, v. 352, p. 11–31.

Nance, R. D., Murphy, B.J., Strachan, R.A., Keppie, J.D.,Gutiérrez-Alonso, G., Fernández-Suárez, J., Quesada, C., Linnemann, U., D'lemos R., and Pisarevsky, P.A., 2008. Neoproterozoic-early Palaeozoic tectonostratigraphy and palaeogeography of the peri-Gondwanan terranes: Amazonian v. West African connections: Geological Society of London, Special Publications, v. 297, p. 345-383.

Parrish, R., and Noble, Stephan R., 2003, Zircon U-Th-Pb Geochronology by Isotope Dilution—Thermal Ionization Mass Spectrometry: Zircon: Reviews in Mineralogy and Geochemistry, v. 53, p. 183-210.

Pe-Piper, G. and Jansa, 1999, Pre-Mesozoic basement rocks offshore Nova Scotia, Canada: new constraints on the origin and Paleozoic accretionary history of the Meguma terrane: Bulletin of the Geological Society of America, v. 111, p. 1773-1791.

Pollack, J. C., Wilton, D. H. C., van Staal, C. R., and Morrissey, K. D., 2007, U-Pb zircon geochronological constraints on the Late Ordovician-Early Silurian collision of Ganderia and Laurentia along the Dog Bay Line: The terminal Iapetan suture in the Newfoundland Appalachians: American Journal of Science, v. 307, p. 399–433.

Pollock, J.C., Hibbard, J.P., and Sylvester, P.J., 2009, Early Ordovician rifting of Avalonia and birth of the Rheic Ocean; U-Pb detrital zircon constraints from Newfoundland: Journal of the Geological Society of London, v.166, no.3, p.501-515.

Rast, N. and Skehan, J.W., 1993, Mid-Paleozoic orogenesis in the North Atlantic: The Acadian Orogeny, *in* Roy, D.C. and Skehan, J.W., eds., The Acadian Orogeny: Recent Studies in New England, Maritime Canada and the Autochthonous Foreland: Geological Society of America, Special Paper v. 275, p. 1-25.

Reynolds, E., Kuiper, Y. D., Hepburn, J. C., Olszewski, W. J., 2010, New ^{40}Ar/Ar age constraints on the timing of metamorphism and deformation in the western Nashoba terrane, eastern Massachusetts. Geological Society of America *Abstracts with Programs*, Vol. 42, No. 1, p. 24

Rivers, T., 1997, Lithotectonic elements of the Grenville Province: review and tectonic implications: Precambrian Research, v. 86, p. 117–154.

Rizvanova , N.G., Levchenkov, O.A., Belous, A. E., Bezmen, N.I. Maslenikov, A.V., Komarov, A.N., Makeev, A.F., and Levskiy, L.K. 2000. Zircon reaction and stability of the U-Pb isotope system during interaction with carbonate fluid: experimental hydrothermal study: Contributions to Mineralogy and Petrology, v. 139, p. 101-114

Robinson, P., Tucker, R.D., Bradley, D., Berry, H.N., IV, and Osberg, P.H., 1998, Paleozoic orogens in New England, USA: Geologiska Föreningensi Stockholm Förhandlingar, v. 120, p. 119–148.

Rodgers, N., van Staal, C., McNicoll, V., Pollock, J., Zagorevski, A. & Whalen, J., 2006, Neoproterozoic and Cambrian arc magmatism along the eastern margin of the Victoria Lake Supergroup: A remnant of Ganderian basement in central Newfoundland? :Precambrian Research, v. 147, p. 320-341.

Samson, S.D., Barr, S.M., and White, C.E., 2000, Nd isotopic characteristics of terranes within the Avalon Zone southern New Brunswick: Canadian Journal of Earth Sciences v. 37, p.1039-1052.

Samson, S. D., D'Lemos, R. S., Miller, B. V. & Hamilton, M., A. 2005, Neoproterozoic palaeogeography of the Cadomia and Avalon terranes: constraints from detrital zircon U–Pb ages: Journal of the Geological Society, London, v. 162, p. 65–71.

Schmidt, M.W., Poli, S., 2003, Position and Life Span of Volcanic Arcs - What Link to Present-day Kinematic Parameters in Subduction Zones?: American Geophysical Union, Fall Meeting, abstracts with program

Shride, A. F., 1976, Stratigraphy and correlation of the Newbury Volcanic Complex, northeastern Massachusetts, *in* Page, Lincoln R. Contribution to the Stratigraphy of New England: Geological Society of America, Memoir v. 148, p. 147-179.

Sircombe, K., 2000, The usefulness and limitations of binned frequency histograms and probability density distributions for displaying absolute age data: Geological Survey of Canada, Current Research 2000-F2; Radiogenic Age and Isotopic Studies, Report 13, 11.

Sircombe, K., and Richard A. Stern, 2002, An investigation of artificial biasing in detrital zircon U-Pb geochronology due to magnetic separation in sample preparation: Geochimica et Cosmochimica Acta, v. 66, no. 13, p. 2379-2397.

Stanley, R. S., and Ratcliffe, N. M., 1985, Tectonic synthesis of the Taconian orogeny in western New England: Geological Society of America Bulletin, v. 96, p. 1227–1250.

Stroud, M.M., Markwort, R.J., and Hepburn, J.C., 2009, Refining temporal constraints on metamorphism in the Nashoba terrane, southeastern New England, through monazite dating: Lithosphere, v. 1, no. 6, p. 337–342

Sylvester , P.J. and Ghaderi, M., 1997, Trace element analysis of scheelite by excimer laser ablation–inductively coupled plasma–mass spectrometry (ELA–ICP–MS) using a synthetic silicate glass standard: Chemical Geology, v. 141, p. 49–65.

Thompson, M. D., Hermes, O. D., Bowring, S. A., Isachsen, C. E., Besancon, J. R. & Kelly, K. L., 1996, Tectonostratigraphic implications of Late Proterozoic U–Pb zircon ages in the Avalon Zone of southeastern New England: In: Nance, R. D. & Thompson, M. A. (eds) Avalonian and Related Peri- Gondwanan Terranes of the Circum-North Atlantic. Geological Society of America, Special Papers, v. 304, p. 179–191.

Thompson, M. D. & Bowring, S. A., 2000, Age of the Squantum 'Tillite', Boston Basin, Massachusetts: U–Pb zircon constraints on terminal Neoproterozoic glaciation: American Journal of Science, v. 300, p. 630–655.

Thompson, M.D., Grunow, A.M., and Ramezani, J., 2003, New paleomagnetic pole from the Late Cambrian Nahant Gabbro, Nahant, Massachusetts: Implicationsfor drift history of the Southeastern New England Avalon Zone: Geological Society of America Abstracts with Programs, v. 35, no. 3, p. 18.

Thompson, M.D., 2007, Late Neoproterozoic paleogeography of the Southeastern New England Avalon Zone: Insights from U-Pb geochronology and paleomagnetism: Geological Society of America Bulletin, v. 119, p. 681-696

Valverde-Vaquero, P., van Staal, C. R., McNicoll, V., and Dunning, G. R., 2006, Mid-Late Ordovician magmatism and metamorphism along the Gander margin in central Newfoundland: London, Journal of the Geological Society, v. 163, p. 347–362.

van Staal, C. R., McNicoll, V., Valverdee-Vaquero, P., Barr, S., Fyffe, L. R. & Reusch, D. N., 2004, Ganderia, Avalonia, and the Salinic and Acadian orogenies: Abstracts with Programs, 314 C. R. van Staal *et al.* Geological Society of America, 39th Annual Meeting, NE-section, 128–129.

van Staal, C. R., 2005, The Northern Appalachians. In: Selley, R. C., Cocks, L. R. & Plimer, I. R. eds., Encyclopedia of Geology, Elsevier, Oxford, v. 4, p. 81–91.

van Staal, C. R., Whalen, J. B., Valverde-Vaquero, P., Barr, S., Zagorevski, A. & Rodgers, N., 2009. Pre-Carboniferous, episodic accretion-related, orogenesis along the Laurentian margin of the northern Appalachians: Geological Society, London, Special Publications, v. 327, p. 271-316.

van Staal, C. R., Barr, S., Fyffe, L.R., Johnson, S.C., Park, A.F., White, C.E., and Wilson, R.A., 2011, The Defining Tectonic Elements of Ganderia in New Brunswick: Geological Association of Canada – Mineralogical Association of Canada – Society of Economic Geologists – Society for Geology Applied to Mineral Deposits Joint Annual Meeting, Ottawa 2011, Guidebook to Field Trip 1B, 30p.

Vermeesch, P., 2004. How many grains are needed for a provenance study? : Earth and Planetary Science Letters, v. 224, p. 441-451.

Walsh, G. J., Aleinikoff, John N., and Dorais, Michael J., 2009, Tectonic history of the Avalon and Nashoba terranes along the western flank of the Milford Antiform, Massachusetts: Geological Society of America, Abstracts with Programs, v. 41, p.98.

Walsh, G. J., Wintsch, R.P., 2011, Origin of the Quinebaug-Marlboro Belt in Southeastern New England: Northeastern (46th Annual) and North-Central (45th Annual) Joint Meeting (20–22 March 2011),Geological Society of America *Abstracts with Programs*, v. 43, no. 1, p. 158.

Whalen, J. B., Fyffe, L.R., Longstaffe, F.J., and Jenner, G.A., 1996, The position and nature of the Gander-Avalon boundary, southern New Brunswick, based on geochemical and isotopic data from granitoid rocks: Canadian Journal of Earth Sciences v. 33, p. 129–139.

Wintsch, R. P., Kunk, M. J., Boyd, J. L., and Aleinikoff, J. N., 2003, P-T-t paths and differential Alleghanian loading and uplift of the Bronson Hill terrane, south-central New England: American Journal of Science, v. 303, p. 410-446.

Wintsch, R. P., Aleinikoff, J.N., Walsh, G.J., Bothner, W.A., and Hussey, A.M., II., 2007, Provenance and metamorphic implications of zircon and monazite U-Pb ages of rocks of the Merrimack and Putnam-Nashoba terranes, eastern New England: American Journal of Science, v. 307, p.63-118.

Wintsch, R.P., Aleinkoff, J. N., and Walsh, G.J., 2009, Late Silurian Deposition and Late Devonian Metamorphism of Gander Cover at the Southern End of the Central Maine Terrane: Evidence from SHRIMP Analysis of Detrital Zircons: 44th Annual Meeting Northeastern Section Geological Society of America, Portland Maine.

Zartman, R.E. and Naylor, R.S., 1984, Structural implications of some radiometric ages of igneous rocks in southeastern New England: Geological Society of America Bulletin, v. 95, p. 539-552.

Zen, E-an, ed., Goldsmith, R., Ratcliffe, N.M., Robinson, P. and Stanley, R.S., compilers, 1983, Bedrock geologic map of Massachusetts: United States Geological Survey, Reston, Virginia, scale 1:250,000

APPENDIX A: GPS COORDINATES FOR SAMPLE LOCATIONS

Marlboro Formation	MLMR1	42°19'56.21"N, 71°36'01.70"W
	MLMR2	42°20'49.35"N, 71°32'52.56"W
	MLMR3	42°19'11.02"N, 71°29'27.32"W
	MLMR5	42°23'45.65"N, 71°28'24.11"W
	MLMR6	42°21'35.19"N, 71°31'30.10"W
Shawsheen Gneiss	MLSG1	42°31'34.98"N, 71°15'17.17"W
Nashoba Formation	MLNB1	42°19'50.51"N, 71°40'15.87"W
	MLBM1	42°22'50.87"N, 71°38'43.12"W
	MLNS1	42°20'25.45"N, 71°39'48.17"W
Tadmuck Brook Schist	MLTMBC	42°31'55.27"N, 71°31'30.25"W
Newbury Volcanic Complex	MLIS1	42°41'11.49"N, 70°54'58.47"W

APPENDIX B: THIN SECTION IMAGES

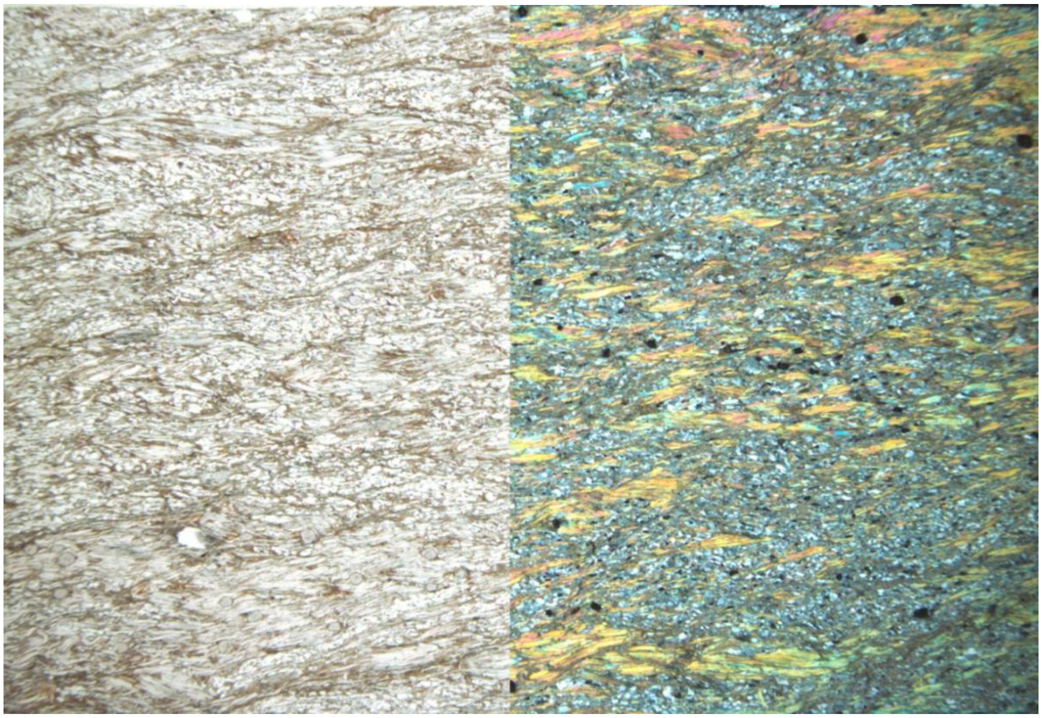

Photographs of thin sections for MLMR1 (Top) MLMR2 (Bottom). The right hand side of the image is with crossed polars.

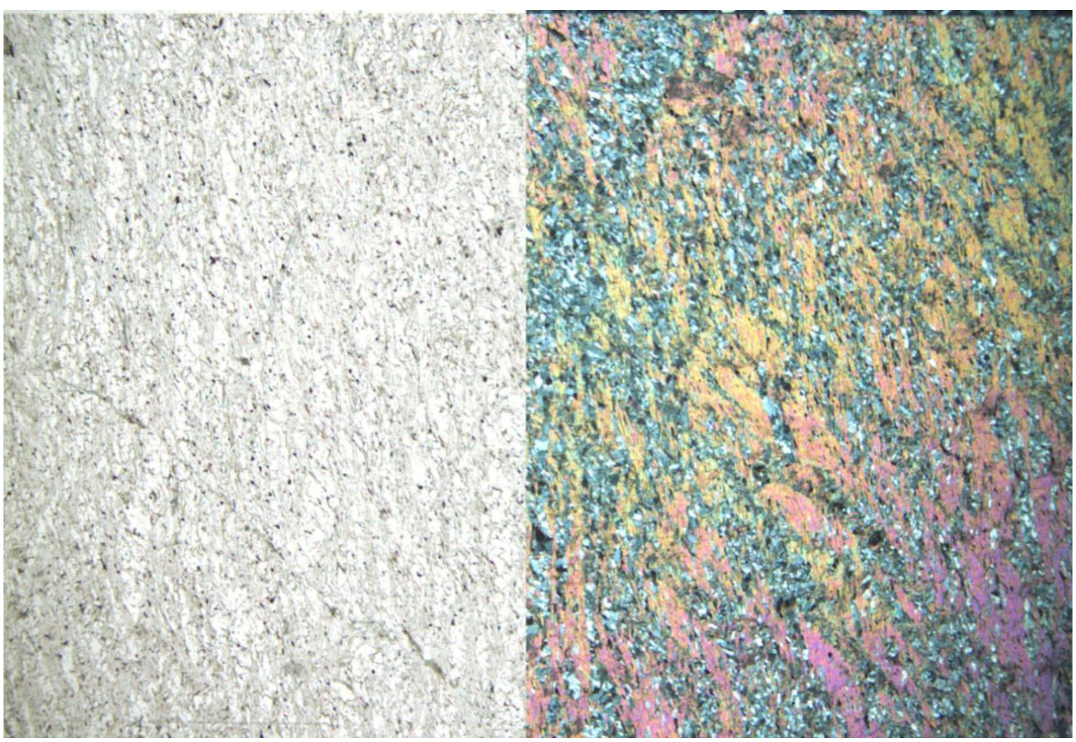

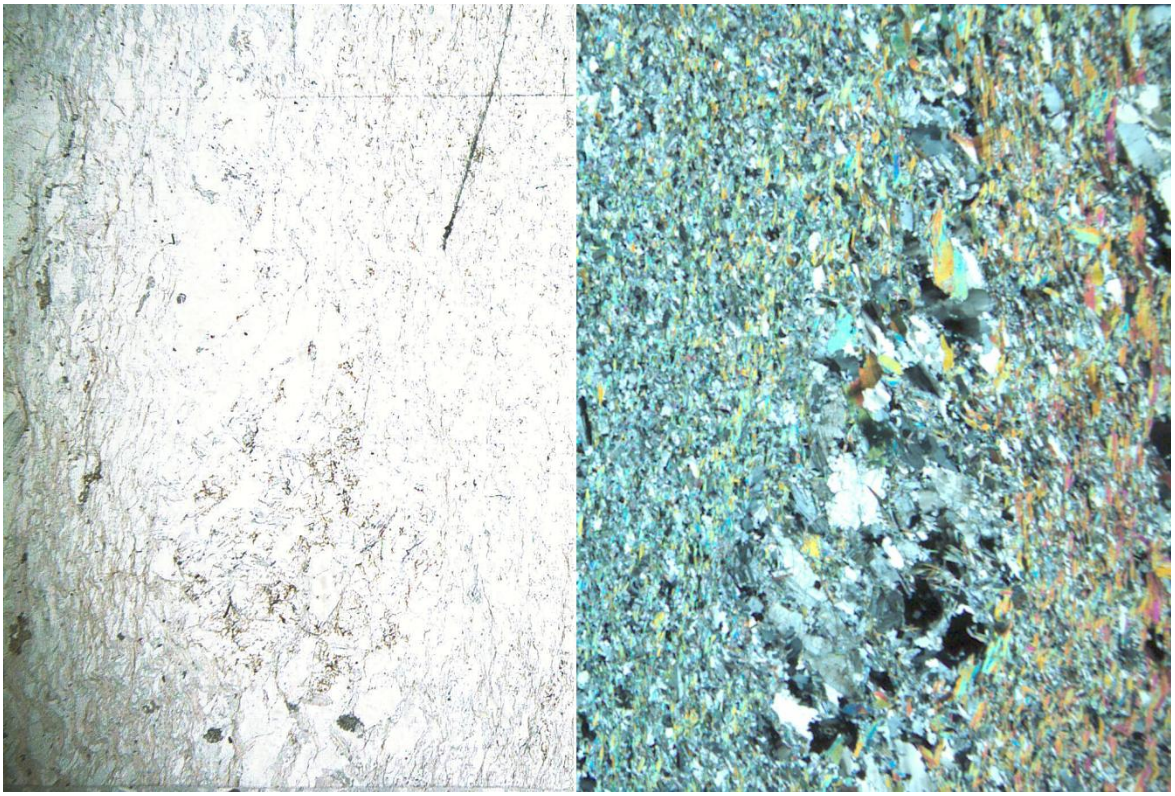

Photographs of thin sections for MLMR5 (Top) MLMR6 (Bottom). The right hand side of the image is with crossed polars.

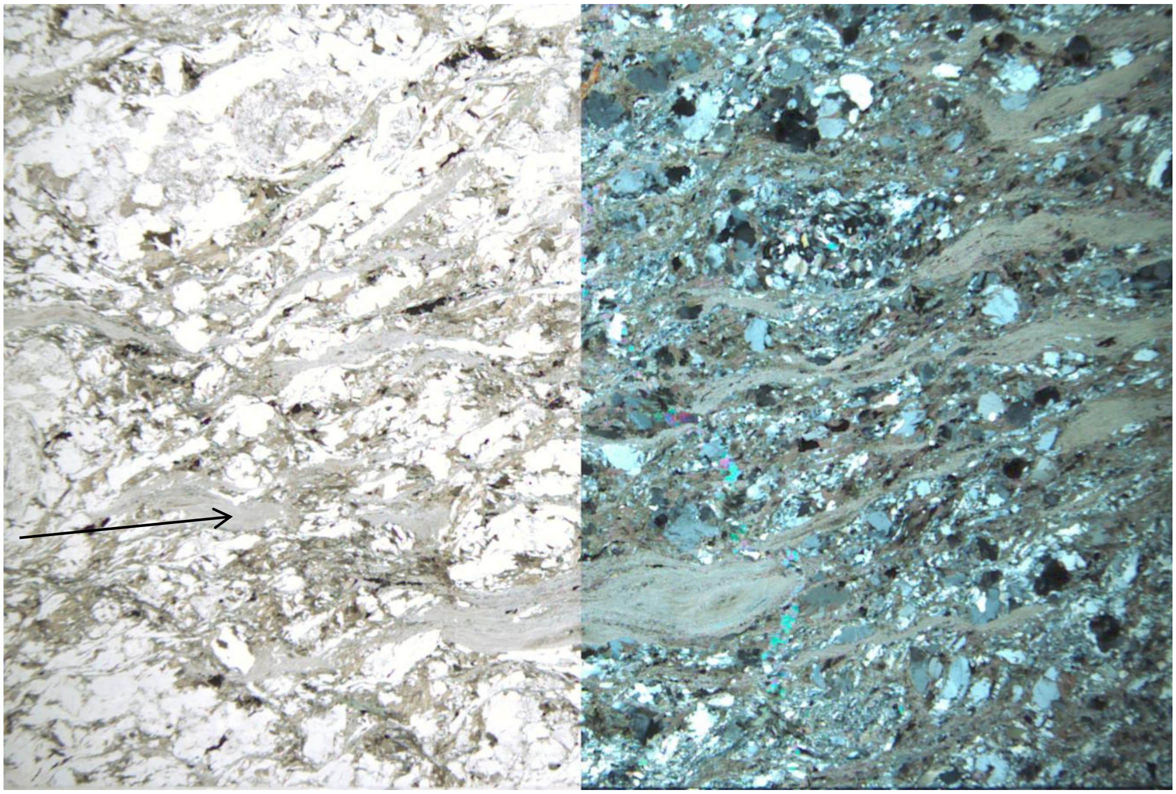

Photographs of thin sections for MLNB1 (Top) MLNS1 (Bottom). The right hand side of the image is with crossed polars.

Appendix B

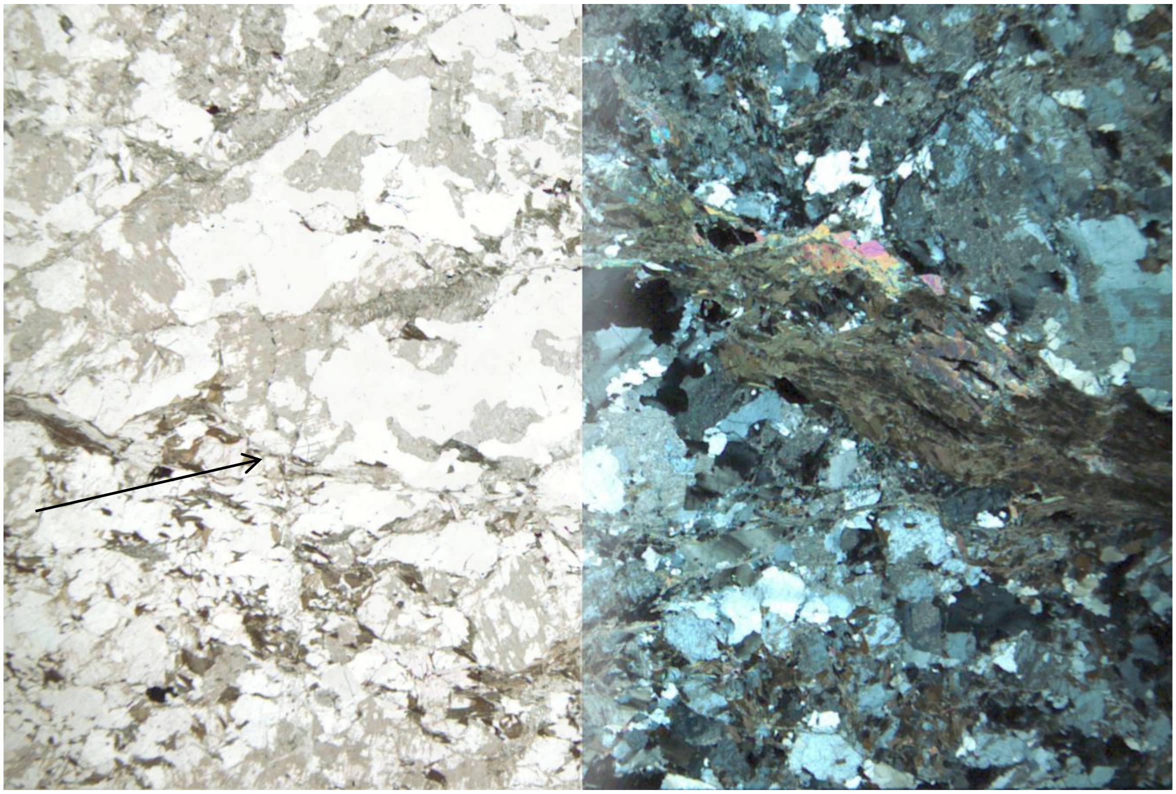

Photographs of thin sections for MLSG1 (Top) MLTMBC (Bottom). The right hand side of the image is with crossed polars.

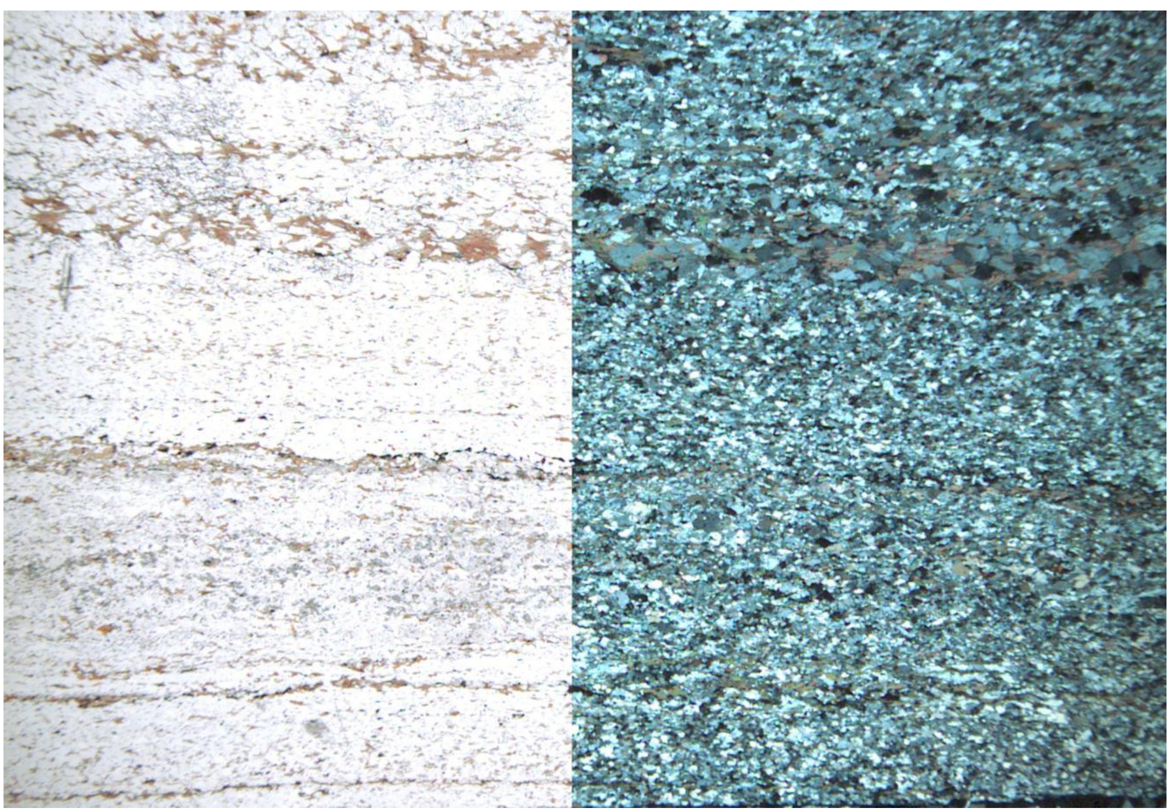

Appendix B

Photographs of thin sections for MLBM1 (Top) MLIS1 (Bottom). The right hand side of the image is with crossed polars.

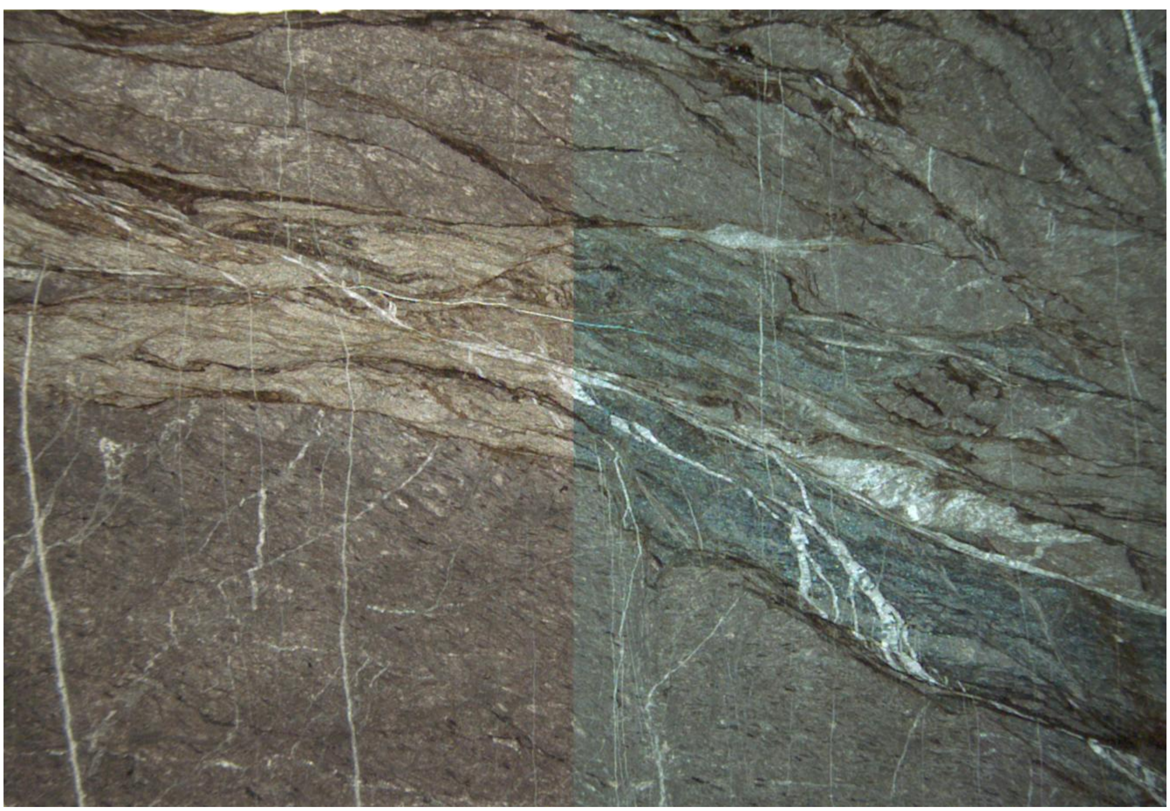

Appendix B

APPENDIX C: COMPLETE LIST OF ZIRCON AGES

Marlboro Formation Combined	Measured Isotopic Ratios 207Pb /235U	1s error	206Pb /238U	1s error	Rho	207Pb/ 206Pb	1s error	Calculated Ages 207Pb /235U	1s error	206Pb /238U	1s error	207Pb/ 206Pb	1s error	Concordia age	2s error	Probability Of Concordance	Th/ U
mr04a20	0.442	0.031	0.047	0.004	0.669	0.068	0.001	372	22	293	27	857	23	353	43	0.00	0.014
mr04a26	0.452	0.078	0.052	0.009	0.500	0.055	0.001	379	55	324	55	415	50	350	96	0.32	0.033
mr04a19	0.508	0.038	0.058	0.005	0.593	0.063	0.001	417	26	361	31	719	29	401	50	0.03	0.023
mr04a16	0.481	0.015	0.061	0.002	0.456	0.058	0.000	399	10	379	10	525	14	389	18	0.07	0.011
mr04a35	0.497	0.048	0.061	0.003	0.298	0.055	0.001	410	33	381	21	428	53	387	40	0.39	0.035
mr04a10	0.529	0.044	0.062	0.005	0.516	0.062	0.000	431	29	386	32	660	16	412	53	0.14	0.006
mr04a24	0.519	0.015	0.063	0.001	0.367	0.062	0.000	424	10	397	8	666	16	406	15	0.01	0.008
mr04a18	0.562	0.273	0.065	0.025	0.391	0.061	0.001	453	177	404	148	653	35	420	270	0.79	0.055
mr04a08	0.542	0.033	0.065	0.005	0.609	0.061	0.001	440	22	408	29	639	20	435	43	0.18	0.086
mr04a14	0.586	0.095	0.066	0.010	0.464	0.065	0.001	468	61	411	60	771	26	437	105	0.36	0.111
se14a97	0.507	0.080	0.068	0.004	0.183	0.060	0.003	417	54	424	24	617	96	423	46	0.89	0.023
mr04a31	0.562	0.053	0.070	0.004	0.322	0.060	0.001	453	35	434	26	594	44	439	47	0.61	0.611
mr04a09	0.531	0.028	0.071	0.004	0.521	0.056	0.000	432	19	440	23	453	20	434	35	0.73	0.005
mr04a17	0.598	0.055	0.071	0.007	0.511	0.062	0.001	476	35	443	40	665	24	464	65	0.39	0.039
mr04a06	0.589	0.061	0.076	0.008	0.483	0.058	0.002	470	39	470	46	515	93	470	72	1.00	0.182
se14a99	0.755	0.092	0.081	0.005	0.247	0.063	0.003	571	53	504	29	715	87	514	56	0.22	2.968
mr04a05	0.715	0.033	0.086	0.003	0.386	0.059	0.001	548	19	529	18	551	41	537	31	0.37	0.889
mr04a27	0.784	0.052	0.086	0.005	0.413	0.060	0.001	588	30	531	28	586	29	555	49	0.07	0.922
mr04a07	0.793	0.062	0.088	0.004	0.273	0.068	0.001	593	35	545	22	879	37	555	42	0.20	0.871
se14a98	0.898	0.084	0.104	0.007	0.337	0.062	0.001	651	45	640	39	679	23	644	68	0.83	0.240
mr04a28	3.142	0.310	0.189	0.017	0.461	0.110	0.002	1443	76	1115	93	1796	25	1296	153	0.00	0.455
mr04a34	5.856	0.301	0.318	0.011	0.344	0.126	0.002	1955	45	1778	55	2044	23	1885	83	0.00	0.207
mr04a33	5.980	0.272	0.318	0.012	0.412	0.129	0.001	1973	40	1780	58	2083	17	1927	78	0.00	0.620
mr04a32	10.966	0.283	0.466	0.010	0.424	0.154	0.001	2520	24	2467	45	2393	11	2516	48	0.19	0.364
se14a95	12.946	0.337	0.511	0.013	0.493	0.172	0.002	2676	25	2661	56	2581	18	2676	49	0.77	0.595
se14a94	30.084	0.955	0.745	0.020	0.418	0.280	0.003	3490	31	3588	73	3364	15	3490	62	0.14	0.356

Shawsheen Gneiss	Measured Isotopic Ratios							Calculated Ages									
	207Pb /235U	**1s error**	**206Pb /238U**	**1s error**	**Rho**	**207Pb/ 206Pb**	**1s error**	**207Pb /235U**	**1s error**	**206Pb /238U**	**1s error**	**207Pb/ 206Pb**	**1s error**	**Concordia age**	**2s error**	**Probability Of Concordance**	**Th/ U**
mr05a31	0.509	0.025	0.054	0.002	0.330	0.072	0.001	418	16	338	10	980	29	352	20	0.00	0.322
mr06a155	0.545	0.050	0.063	0.005	0.429	0.062	0.001	442	33	395	30	666	33	414	53	0.17	0.044
mr06a71	0.604	0.135	0.066	0.006	0.203	0.081	0.002	480	85	414	36	1213	42	419	71	0.45	0.049
se13a67	0.493	0.084	0.068	0.005	0.222	0.059	0.001	407	57	423	31	570	52	420	59	0.78	0.120
mr05a27	0.550	0.023	0.068	0.002	0.415	0.058	0.001	445	15	426	14	534	20	435	25	0.24	0.007
mr06a120	0.788	0.039	0.069	0.003	0.445	0.083	0.001	590	22	428	18	1260	24	467	34	0.00	1.083
mr06a128	0.587	0.064	0.069	0.003	0.217	0.068	0.002	469	41	429	20	881	50	433	38	0.34	0.019
mr06a130	0.610	0.048	0.071	0.004	0.320	0.064	0.001	483	30	441	21	757	37	452	40	0.17	0.125
se13a69	0.710	0.084	0.072	0.004	0.213	0.070	0.002	545	50	446	22	941	54	454	42	0.06	0.193
mr05a29	0.582	0.052	0.073	0.005	0.364	0.060	0.001	466	33	452	28	613	28	457	50	0.69	0.342
mr06a41	0.624	0.065	0.074	0.005	0.326	0.061	0.001	492	41	458	30	631	42	467	55	0.42	0.062
mr04a87	0.532	0.056	0.075	0.004	0.283	0.058	0.001	433	37	468	27	524	47	457	49	0.37	0.624
se13a56	0.593	0.035	0.076	0.002	0.243	0.059	0.001	473	22	474	13	566	43	474	25	0.96	0.113
se13a57	0.554	0.040	0.078	0.003	0.250	0.058	0.001	448	26	484	17	523	46	475	31	0.18	0.537
mr05a10	0.799	0.033	0.078	0.003	0.442	0.071	0.001	597	19	486	17	963	31	527	31	0.00	0.621
mr06a47	0.620	0.054	0.080	0.005	0.342	0.054	0.001	490	34	494	28	384	48	492	50	0.91	0.362
se13a60	0.633	0.147	0.080	0.012	0.317	0.059	0.001	498	91	497	70	549	43	498	127	1.00	0.582
mr05a48	0.616	0.057	0.081	0.003	0.230	0.060	0.001	487	36	503	21	616	52	500	39	0.67	0.306
se13a71	0.650	0.059	0.081	0.004	0.259	0.059	0.001	508	36	505	23	555	51	505	43	0.92	1.096
mr06a119	0.741	0.086	0.082	0.003	0.147	0.077	0.002	563	50	508	17	1117	52	511	33	0.29	0.108
mr06a140	0.686	0.044	0.082	0.003	0.251	0.060	0.001	530	27	510	16	612	50	514	30	0.47	0.731
mr06a77	0.845	0.084	0.083	0.005	0.276	0.072	0.002	622	46	512	27	995	67	528	52	0.02	0.534
mr05a39	0.750	0.023	0.083	0.002	0.351	0.064	0.001	568	13	515	11	737	25	532	20	0.00	0.326
mr06a137	0.695	0.035	0.083	0.003	0.403	0.056	0.001	536	21	516	20	449	35	525	34	0.37	0.528
mr06a85	0.712	0.082	0.084	0.009	0.476	0.059	0.001	546	49	517	55	563	46	535	88	0.59	0.406
mr05a51	0.682	0.045	0.085	0.003	0.272	0.061	0.001	528	27	526	18	633	42	527	34	0.96	0.580
mr05a18	0.762	0.061	0.085	0.004	0.280	0.059	0.001	575	35	526	23	553	49	536	42	0.18	0.929
mr06a66	0.788	0.031	0.086	0.002	0.351	0.065	0.001	590	17	530	14	787	30	548	25	0.00	0.762
mr06a111	0.746	0.041	0.086	0.003	0.303	0.067	0.001	566	24	530	17	825	43	539	31	0.15	0.585
se13a72	1.002	0.047	0.086	0.003	0.384	0.074	0.001	705	24	533	19	1047	38	571	35	0.00	0.189
mr06a141	0.859	0.062	0.087	0.004	0.303	0.071	0.002	630	34	535	22	964	46	554	43	0.01	0.622

	Measured Isotopic Ratios							Calculated Ages									
Shawsheen Gneiss	**207Pb /235U**	**1s error**	**206Pb /238U**	**1s error**	**Rho**	**207Pb/ 206Pb**	**1s error**	**207Pb /235U**	**1s error**	**206Pb /238U**	**1s error**	**207Pb/ 206Pb**	**1s error**	**Concordia age**	**2s error**	**Probability Of Concordance**	**Th/ U**
mr06a117	0.703	0.023	0.087	0.002	0.326	0.058	0.001	541	14	535	11	531	26	537	20	0.70	0.597
mr06a100	0.684	0.042	0.087	0.004	0.335	0.058	0.001	529	25	536	21	525	34	534	37	0.79	0.789
mr06a75	0.779	0.074	0.087	0.006	0.351	0.063	0.002	585	42	538	34	716	54	553	62	0.29	0.744
mr06a139	0.731	0.040	0.087	0.003	0.308	0.060	0.001	557	24	540	18	606	41	545	32	0.49	0.655
mr06a89	1.068	0.090	0.088	0.003	0.201	0.084	0.003	738	44	541	18	1297	58	551	35	0.00	0.262
mr06a126	0.705	0.076	0.088	0.006	0.311	0.062	0.001	542	45	542	35	671	45	542	63	1.00	0.656
mr06a131	0.748	0.039	0.088	0.003	0.368	0.061	0.001	567	22	543	20	632	36	552	35	0.32	0.599
mr06a65	0.760	0.025	0.088	0.002	0.356	0.060	0.001	574	14	544	12	600	26	555	22	0.05	0.886
se13a79	1.132	0.044	0.089	0.003	0.371	0.080	0.001	769	21	547	15	1197	25	582	29	0.00	0.333
mr06a97	0.750	0.060	0.089	0.004	0.285	0.061	0.002	568	35	548	24	654	54	553	44	0.58	0.772
mr05a30	0.654	0.052	0.089	0.004	0.270	0.058	0.001	511	32	550	23	537	47	538	41	0.25	0.560
mr06a149	0.702	0.077	0.089	0.004	0.230	0.064	0.002	540	46	550	26	754	50	548	50	0.83	1.559
mr04a86	0.960	0.403	0.089	0.020	0.271	0.108	0.002	683	209	550	120	1768	31	568	232	0.55	0.179
mr06a118	0.726	0.067	0.089	0.004	0.246	0.062	0.001	554	39	551	24	670	51	552	45	0.94	0.337
mr06a56	0.823	0.088	0.089	0.006	0.300	0.070	0.001	610	49	552	34	916	43	566	63	0.26	0.633
mr06a96	0.699	0.050	0.090	0.003	0.229	0.060	0.001	538	30	556	18	591	50	553	33	0.57	0.651
mr05a13	1.076	0.037	0.090	0.002	0.372	0.086	0.001	742	18	558	14	1340	21	596	26	0.00	0.153
mr04a90	0.827	0.116	0.091	0.005	0.185	0.080	0.003	612	65	559	28	1196	65	564	54	0.43	0.839
mr06a76	0.904	0.076	0.091	0.012	0.764	0.063	0.001	654	41	561	69	712	42	676	77	0.04	0.875
mr06a125	0.732	0.074	0.091	0.005	0.259	0.063	0.002	558	44	561	28	693	67	560	52	0.94	0.608
mr05a32	0.752	0.039	0.091	0.002	0.253	0.063	0.001	569	23	562	14	695	44	564	26	0.76	0.383
se13a80	0.804	0.048	0.091	0.003	0.263	0.062	0.001	599	27	563	17	685	39	570	32	0.20	0.688
mr06a99	0.817	0.046	0.091	0.003	0.322	0.065	0.001	607	26	563	19	784	29	575	36	0.11	0.551
mr06a50	0.795	0.032	0.092	0.002	0.304	0.062	0.001	594	18	564	13	675	32	573	24	0.12	0.631
mr04a89	0.724	0.072	0.091	0.005	0.271	0.061	0.002	553	43	564	29	623	57	561	54	0.81	0.618
mr06a81	2.014	0.134	0.092	0.003	0.277	0.151	0.004	1120	45	567	20	2353	43	562	40	0.00	1.099
mr06a51	0.747	0.070	0.093	0.003	0.183	0.060	0.002	566	41	571	19	604	66	570	36	0.92	0.724
mr05a53	0.864	0.064	0.093	0.003	0.202	0.071	0.002	632	35	572	16	958	55	578	32	0.10	1.059
mr06a48	0.740	0.058	0.093	0.004	0.247	0.062	0.002	562	34	573	21	660	64	570	40	0.77	0.818
mr05a43	0.743	0.037	0.093	0.003	0.270	0.059	0.001	564	22	574	15	561	40	572	27	0.65	0.487
mr06a156	0.810	0.050	0.093	0.003	0.293	0.061	0.001	603	28	576	20	628	42	583	37	0.37	0.565

Shawsheen Gneiss	Measured Isotopic Ratios 207Pb /235U	1s error	206Pb /238U	1s error	Rho	207Pb/ 206Pb	1s error	Calculated Ages 207Pb /235U	1s error	206Pb /238U	1s error	207Pb/ 206Pb	1s error	Concordia age	2s error	Probability Of Concordance	Th/U
mr06a135	0.799	0.060	0.093	0.003	0.218	0.067	0.002	596	34	576	18	824	55	579	35	0.57	0.610
mr05a21	0.741	0.038	0.094	0.002	0.225	0.060	0.001	563	22	579	13	608	41	576	24	0.49	0.461
mr06a59	0.774	0.067	0.094	0.004	0.268	0.060	0.002	582	38	581	26	602	60	581	47	0.98	1.541
se13a70	1.094	0.145	0.095	0.010	0.407	0.079	0.001	750	70	583	60	1163	20	632	111	0.02	0.216
mr06a60	0.770	0.069	0.095	0.008	0.498	0.053	0.002	580	40	584	50	318	71	581	75	0.92	0.444
mr06a46	0.844	0.069	0.096	0.007	0.424	0.063	0.001	621	38	591	39	698	42	606	66	0.46	0.722
mr05a08	0.802	0.025	0.097	0.002	0.307	0.061	0.001	598	14	597	11	626	18	597	20	0.96	1.087
mr05a42	0.824	0.028	0.097	0.003	0.395	0.061	0.001	610	15	599	15	650	18	604	26	0.51	0.644
se13a78	0.875	0.034	0.097	0.001	0.196	0.060	0.001	638	18	600	9	591	30	604	17	0.04	0.735
mr06a69	0.925	0.041	0.099	0.003	0.317	0.066	0.001	665	22	606	16	822	30	622	30	0.01	0.652
mr06a15	0.806	0.029	0.099	0.002	0.326	0.058	0.001	600	16	606	14	534	32	604	24	0.72	0.300
mr06a148	0.733	0.064	0.099	0.005	0.290	0.054	0.002	559	38	607	29	366	66	590	52	0.23	0.509
mr06a88	0.940	0.089	0.100	0.010	0.519	0.065	0.001	673	47	613	57	788	44	654	89	0.25	0.769
mr05a49	0.902	0.060	0.100	0.004	0.326	0.069	0.001	653	32	615	26	901	44	627	46	0.27	0.343
mr05a37	0.758	0.036	0.100	0.003	0.267	0.059	0.001	573	21	616	15	551	34	603	27	0.05	0.391
mr05a50	0.910	0.055	0.101	0.004	0.302	0.067	0.002	657	29	619	21	841	47	629	39	0.21	0.682
mr06a151	0.887	0.069	0.101	0.004	0.286	0.065	0.001	645	37	620	26	787	39	626	48	0.52	0.894
mr06a136	0.857	0.073	0.101	0.006	0.323	0.061	0.002	628	40	621	33	640	66	624	58	0.86	0.880
mr06a95	0.868	0.035	0.101	0.003	0.327	0.061	0.001	635	19	622	16	637	30	626	28	0.53	0.851
mr05a38	0.863	0.086	0.103	0.009	0.454	0.060	0.001	632	47	633	54	600	48	632	85	0.99	0.472
mr06a57	0.800	0.051	0.104	0.004	0.269	0.058	0.001	597	29	639	21	538	41	626	37	0.16	0.560
mr06a147	0.900	0.034	0.105	0.003	0.425	0.060	0.001	652	18	641	19	596	23	647	32	0.59	0.470
mr05a58	0.839	0.034	0.105	0.003	0.294	0.060	0.001	619	19	645	15	604	26	636	26	0.20	0.789
mr06a145	0.906	0.050	0.107	0.004	0.316	0.061	0.001	655	27	653	22	647	41	654	39	0.96	0.797
mr06a127	0.898	0.042	0.107	0.003	0.308	0.062	0.001	651	23	654	18	664	34	653	32	0.90	0.134
mr06a146	0.933	0.111	0.107	0.005	0.207	0.069	0.002	669	58	656	31	892	52	658	58	0.82	0.162
mr06a86	0.988	0.049	0.108	0.004	0.332	0.061	0.001	698	25	663	21	650	45	675	37	0.19	0.710
mr06a110	0.981	0.080	0.109	0.011	0.614	0.061	0.001	694	41	669	64	630	28	693	82	0.62	0.278
mr05a07	0.888	0.039	0.110	0.003	0.307	0.061	0.001	645	21	670	17	623	31	661	30	0.26	0.847
mr06a157	0.980	0.054	0.110	0.003	0.278	0.064	0.001	694	28	672	20	732	38	678	36	0.46	0.074
mr05a52	0.904	0.055	0.113	0.004	0.273	0.064	0.001	654	29	689	22	737	48	678	39	0.26	0.636

Shawsheen Gneiss	Measured Isotopic Ratios 207Pb /235U	1s error	206Pb /238U	1s error	Rho	207Pb/ 206Pb	1s error	Calculated Ages 207Pb /235U	1s error	206Pb /238U	1s error	207Pb/ 206Pb	1s error	Concordia age	2s error	Probability Of Concordance	Th/ U
mr05a47	1.236	0.214	0.114	0.015	0.373	0.085	0.001	817	97	693	85	1311	26	735	153	0.24	0.203
mr06a58	1.720	0.119	0.124	0.007	0.390	0.098	0.001	1016	44	751	38	1590	21	817	72	0.00	0.212
mr06a79	1.238	0.092	0.126	0.006	0.346	0.072	0.002	818	42	764	37	985	54	785	65	0.24	0.205
mr06a129	1.238	0.056	0.129	0.004	0.350	0.066	0.001	818	25	782	23	800	31	797	40	0.20	0.215
mr05a20	1.713	0.095	0.145	0.004	0.270	0.083	0.001	1013	35	872	24	1274	27	901	46	0.00	0.066
mr05a40	1.369	0.160	0.149	0.008	0.224	0.073	0.002	876	68	897	44	1005	45	892	80	0.77	0.601
mr06a68	1.664	0.136	0.153	0.010	0.395	0.076	0.001	995	52	918	55	1084	32	958	91	0.19	0.144
se13a76	1.904	0.160	0.154	0.007	0.287	0.090	0.002	1083	56	922	42	1424	34	960	77	0.01	0.445
mr06a106	1.808	0.102	0.167	0.008	0.432	0.077	0.001	1048	37	994	45	1111	27	1029	68	0.21	0.160
se13a81	2.107	0.108	0.174	0.008	0.432	0.080	0.001	1151	35	1033	42	1187	21	1105	66	0.00	0.207
se13a62	2.458	0.120	0.175	0.007	0.409	0.099	0.001	1260	35	1042	38	1613	16	1147	65	0.00	0.348
mr06a108	2.737	0.252	0.179	0.010	0.299	0.117	0.001	1339	68	1064	54	1913	19	1126	101	0.00	0.163
mr06a49	1.956	0.099	0.180	0.007	0.413	0.078	0.001	1101	34	1067	41	1138	16	1089	62	0.42	0.307
mr06a80	2.212	0.178	0.189	0.012	0.408	0.085	0.001	1185	56	1118	67	1315	34	1160	103	0.33	0.542
mr06a45	2.360	0.193	0.192	0.012	0.368	0.086	0.001	1231	58	1132	62	1347	33	1183	102	0.15	0.260
mr06a116	2.147	0.050	0.194	0.004	0.421	0.077	0.001	1164	16	1145	21	1126	14	1158	30	0.36	0.331
mr06a55	2.788	0.255	0.195	0.014	0.389	0.100	0.001	1352	68	1148	75	1621	20	1249	124	0.01	0.328
mr05a12	3.239	0.121	0.202	0.008	0.536	0.109	0.001	1467	29	1188	43	1787	20	1417	59	0.00	0.379
mr06a105	3.077	0.089	0.214	0.005	0.431	0.100	0.001	1427	22	1248	28	1631	19	1364	43	0.00	0.418
mr05a41	2.742	0.139	0.215	0.008	0.384	0.095	0.001	1340	38	1253	44	1536	25	1305	69	0.06	0.204
mr06a70	3.389	0.297	0.230	0.017	0.410	0.104	0.001	1502	69	1336	87	1702	25	1442	131	0.05	0.298
mr06a109	3.791	0.304	0.237	0.015	0.396	0.114	0.002	1591	64	1371	78	1859	25	1499	123	0.01	0.555
mr05a33	3.274	0.188	0.240	0.016	0.569	0.093	0.001	1475	45	1387	82	1486	28	1476	89	0.18	0.495
se13a59	2.973	0.178	0.252	0.013	0.433	0.098	0.002	1401	46	1448	67	1581	40	1409	88	0.45	0.198
mr05a28	3.269	0.093	0.256	0.007	0.452	0.090	0.001	1474	22	1471	34	1426	22	1473	43	0.94	1.670
mr05a17	3.287	0.071	0.257	0.005	0.407	0.093	0.001	1478	17	1476	23	1490	14	1477	32	0.92	0.295
mr05a59	3.078	0.251	0.259	0.013	0.318	0.092	0.001	1427	62	1487	69	1464	27	1452	105	0.44	0.217
se13a68	4.713	0.135	0.264	0.006	0.402	0.120	0.001	1770	24	1509	31	1952	13	1672	47	0.00	0.333
mr06a61	3.920	0.158	0.272	0.010	0.441	0.101	0.001	1618	33	1550	49	1648	22	1605	64	0.14	0.480
mr05a57	3.760	0.142	0.278	0.007	0.342	0.100	0.001	1584	30	1584	36	1618	22	1584	54	0.99	0.539
mr06a78	3.718	0.121	0.280	0.006	0.357	0.096	0.001	1575	26	1590	33	1544	26	1580	47	0.66	0.639

Shawsheen Gneiss	Measured Isotopic Ratios 207Pb /235U	1s error	206Pb /238U	1s error	Rho	207Pb/ 206Pb	1s error	Calculated Ages 207Pb /235U	1s error	206Pb /238U	1s error	207Pb/ 206Pb	1s error	Concordia age	2s error	Probability Of Concordance	Th/ U
mr06a87	4.121	0.178	0.283	0.010	0.419	0.103	0.001	1658	35	1608	52	1681	13	1648	68	0.31	0.416
mr06a98	4.118	0.177	0.284	0.010	0.418	0.104	0.001	1658	35	1614	51	1693	17	1649	68	0.37	0.950
mr06a67	4.670	0.204	0.289	0.010	0.399	0.113	0.001	1762	37	1637	50	1856	19	1727	70	0.01	0.764
mr06a101	4.418	0.135	0.299	0.008	0.444	0.104	0.001	1716	25	1687	40	1694	14	1712	50	0.44	0.920
mr05a23	4.399	0.113	0.303	0.006	0.387	0.105	0.001	1712	21	1708	30	1721	15	1711	40	0.89	0.341
mr05a22	4.311	0.151	0.307	0.008	0.389	0.105	0.002	1696	29	1726	41	1720	31	1702	54	0.45	0.317
mr06a115	5.410	0.427	0.316	0.020	0.409	0.125	0.001	1886	68	1772	100	2029	16	1861	132	0.23	0.112
se13a61	5.491	0.090	0.350	0.005	0.444	0.110	0.001	1899	14	1934	24	1800	14	1902	28	0.12	0.053
mr06a138	6.420	0.301	0.350	0.017	0.506	0.124	0.002	2035	41	1937	79	2013	25	2033	82	0.15	1.131
mr04a88	6.377	0.347	0.365	0.015	0.380	0.128	0.001	2029	48	2007	71	2073	14	2025	92	0.75	1.028
mr05a09	7.283	0.186	0.402	0.009	0.451	0.129	0.001	2147	23	2176	43	2082	15	2148	45	0.44	0.836
se13a77	12.45	0.290	0.439	0.010	0.490	0.187	0.001	2639	22	2345	45	2720	7	2635	44	0.00	0.331
mr06a107	9.912	0.292	0.444	0.012	0.440	0.154	0.001	2427	27	2367	51	2392	12	2423	54	0.20	0.289

Nashoba Formation Gneiss	Measured Isotopic Ratios 207Pb /235U	1s error	206Pb /238U	1s error	Rho	207Pb/ 206Pb	1s error	Calculated Ages 207Pb /235U	1s error	206Pb /238U	1s error	207Pb/ 206Pb	1s error	Concordia age	2s error	Probability Of Concordance	Th/U
mr02a22	0.422	0.021	0.056	0.002	0.281	0.054	0.001	358	15	353	10	383	36	354	18	0.78	0.014
mr02a14	0.449	0.036	0.057	0.002	0.252	0.058	0.001	376	25	360	14	523	46	363	27	0.52	0.024
mr02a19	0.422	0.033	0.058	0.003	0.298	0.053	0.001	357	23	366	16	312	41	364	30	0.72	0.021
mr02a15	0.491	0.031	0.060	0.003	0.385	0.056	0.001	405	21	375	18	463	34	385	32	0.17	0.019
mr04a43	0.459	0.015	0.061	0.001	0.358	0.054	0.001	384	10	384	9	372	28	384	15	0.99	0.008
mr06a09	0.507	0.023	0.062	0.003	0.488	0.055	0.001	416	15	386	16	415	28	403	28	0.06	0.037
mr02a44	0.506	0.035	0.063	0.003	0.343	0.057	0.001	416	23	392	18	507	38	399	33	0.33	0.157
mr02a23	0.519	0.032	0.063	0.002	0.251	0.058	0.001	424	21	393	12	511	44	398	23	0.15	0.013
mr04a50	0.477	0.016	0.063	0.002	0.384	0.054	0.001	396	11	397	10	390	25	397	17	0.95	0.007
mr04a46	0.505	0.027	0.064	0.003	0.447	0.056	0.001	415	18	402	19	454	31	409	31	0.50	0.029
mr06a08	0.472	0.032	0.065	0.003	0.346	0.052	0.001	393	22	404	19	277	47	400	33	0.64	0.016
mr06a29	0.486	0.021	0.065	0.002	0.271	0.056	0.001	402	15	408	9	470	34	406	18	0.71	0.034
mr04a64	0.496	0.022	0.067	0.003	0.420	0.055	0.001	409	15	415	15	425	23	412	26	0.68	0.030
mr02a07	0.485	0.019	0.067	0.001	0.282	0.054	0.001	401	13	419	9	385	29	414	16	0.19	0.008
mr02a37	0.498	0.023	0.067	0.002	0.375	0.053	0.001	410	16	420	14	343	22	416	25	0.55	0.005
mr06a28	0.518	0.015	0.068	0.001	0.326	0.055	0.001	424	10	425	8	396	23	425	14	0.88	0.184
mr02a40	0.491	0.031	0.069	0.002	0.233	0.058	0.001	406	21	429	12	534	39	425	23	0.28	0.089
mr06a34	0.550	0.028	0.070	0.003	0.352	0.055	0.001	445	19	437	15	428	32	440	27	0.69	0.022
mr02a17	0.581	0.028	0.071	0.002	0.296	0.057	0.001	465	18	444	12	489	41	449	22	0.26	0.408
mr02a67	0.575	0.037	0.072	0.002	0.214	0.063	0.001	461	24	445	12	718	41	447	23	0.51	0.032
mr02a08	0.538	0.034	0.073	0.002	0.268	0.057	0.001	437	22	451	15	492	43	448	27	0.54	0.027
mr02a79	0.679	0.115	0.073	0.002	0.088	0.113	0.004	526	69	454	13	1846	57	455	26	0.31	0.037
mr06a25	0.556	0.030	0.074	0.002	0.307	0.055	0.001	449	20	458	15	405	38	455	27	0.67	0.175
mr06a10	0.685	0.044	0.074	0.003	0.267	0.073	0.001	530	26	460	15	1021	33	471	29	0.01	0.191
mr06a39	0.607	0.025	0.074	0.002	0.396	0.058	0.001	482	16	463	15	513	31	471	26	0.26	0.439
mr04a87	0.532	0.056	0.075	0.004	0.283	0.058	0.001	433	37	468	27	524	47	457	49	0.37	0.624
mr06a17	0.582	0.025	0.076	0.002	0.325	0.053	0.001	466	16	471	13	339	41	469	23	0.76	0.289
mr02a31	0.618	0.048	0.077	0.002	0.208	0.061	0.001	488	30	476	15	641	49	478	29	0.69	0.208
mr06a19	0.564	0.047	0.077	0.004	0.311	0.055	0.001	454	31	477	24	414	54	469	43	0.47	0.643
mr02a34	0.608	0.037	0.077	0.002	0.202	0.061	0.001	482	23	477	11	657	49	478	22	0.82	0.050
mr02a06	0.580	0.026	0.077	0.002	0.316	0.057	0.001	464	17	480	13	477	36	475	24	0.39	0.445

Nashoba Formation Gneiss	Measured Isotopic Ratios 207Pb /235U	1s error	206Pb /238U	1s error	Rho	207Pb/ 206Pb	1s error	Calculated Ages 207Pb /235U	1s error	206Pb /238U	1s error	207Pb/ 206Pb	1s error	Concordia age	2s error	Probability Of Concordance	Th/U
mr06a20	0.664	0.034	0.077	0.003	0.370	0.059	0.001	517	20	481	17	556	38	494	31	0.09	0.174
mr06a07	0.620	0.069	0.078	0.004	0.207	0.056	0.001	490	43	483	21	444	46	484	41	0.87	0.591
mr02a18	0.661	0.044	0.078	0.003	0.306	0.065	0.001	515	27	484	19	769	44	491	35	0.26	0.372
mr02a46	0.815	0.092	0.080	0.004	0.194	0.075	0.003	605	52	495	21	1066	89	502	41	0.04	0.119
mr05a68	0.668	0.036	0.080	0.003	0.361	0.059	0.001	519	22	495	19	578	26	504	33	0.30	0.180
mr02a10	0.691	0.051	0.080	0.004	0.325	0.062	0.001	534	31	497	23	661	26	508	42	0.26	0.081
mr04a52	0.607	0.026	0.080	0.003	0.416	0.055	0.001	482	16	499	17	428	25	490	28	0.34	1.101
mr05a82	0.669	0.034	0.081	0.004	0.439	0.061	0.001	520	21	501	22	622	30	511	36	0.40	0.097
mr02a49	0.644	0.050	0.081	0.004	0.357	0.057	0.002	505	31	503	27	494	65	504	47	0.96	0.028
mr02a35	0.693	0.063	0.081	0.005	0.305	0.060	0.001	535	38	504	27	586	46	512	50	0.43	0.027
mr06a14	0.671	0.024	0.081	0.002	0.300	0.059	0.001	521	15	504	11	584	25	509	19	0.27	1.068
mr05a87	0.725	0.051	0.082	0.004	0.349	0.061	0.001	554	30	509	24	647	44	523	44	0.16	0.245
mr02a45	0.734	0.153	0.082	0.014	0.409	0.063	0.002	559	89	510	84	720	60	531	146	0.61	0.049
mr05a89	0.662	0.031	0.082	0.003	0.361	0.058	0.001	516	19	511	17	526	26	513	30	0.80	1.366
mr04a62	0.658	0.045	0.083	0.004	0.343	0.060	0.001	513	28	512	23	614	34	513	41	0.97	0.724
mr04a44	0.625	0.023	0.083	0.002	0.367	0.056	0.001	493	14	513	13	464	24	504	23	0.21	0.869
mr02a58	0.626	0.030	0.083	0.002	0.298	0.056	0.001	494	19	514	14	452	46	508	26	0.30	0.090
mr05a79	0.633	0.039	0.083	0.003	0.248	0.057	0.002	498	25	515	15	494	59	511	28	0.50	0.608
mr06a04	0.805	0.057	0.083	0.004	0.326	0.073	0.002	599	32	516	23	1001	46	535	43	0.01	1.503
mr05a91	0.665	0.041	0.083	0.004	0.359	0.058	0.001	518	25	516	22	514	30	517	39	0.95	0.763
mr02a85	0.664	0.047	0.083	0.003	0.266	0.057	0.002	517	29	516	19	497	61	516	35	0.97	0.220
mr06a26	0.697	0.027	0.083	0.003	0.406	0.057	0.001	537	16	517	16	487	29	526	27	0.25	0.365
mr04a45	0.720	0.025	0.084	0.002	0.344	0.059	0.001	551	15	518	12	583	33	528	21	0.03	0.575
mr05a81	0.585	0.073	0.084	0.005	0.224	0.057	0.002	468	47	519	28	508	68	508	52	0.29	1.054
mr02a32	0.689	0.029	0.085	0.002	0.336	0.056	0.001	532	17	524	14	462	32	527	25	0.65	1.074
mr02a80	0.753	0.055	0.085	0.003	0.277	0.071	0.001	570	32	527	20	952	35	536	38	0.20	0.321
mr02a59	0.783	0.045	0.086	0.004	0.367	0.065	0.001	587	26	531	21	788	43	550	39	0.04	0.108
mr02a78	0.708	0.023	0.086	0.002	0.406	0.058	0.001	544	13	531	13	537	22	537	22	0.36	2.266
mr04a71	0.635	0.044	0.086	0.004	0.363	0.057	0.001	499	27	531	26	508	30	516	43	0.29	1.120
mr04a68	0.679	0.041	0.086	0.004	0.368	0.060	0.001	526	25	532	23	600	19	529	39	0.85	0.784
mr02a13	0.718	0.069	0.086	0.005	0.319	0.061	0.001	550	41	532	31	627	30	537	57	0.68	0.929

Appendix C

Nashoba Formation Gneiss	**Measured Isotopic Ratios** 207Pb/235U	1s error	206Pb/238U	1s error	Rho	207Pb/206Pb	1s error	**Calculated Ages** 207Pb/235U	1s error	206Pb/238U	1s error	207Pb/206Pb	1s error	Concordia age	2s error	Probability Of Concordance	Th/U
mr06a35	0.671	0.045	0.086	0.003	0.301	0.057	0.001	522	27	534	21	494	34	530	37	0.67	1.175
mr02a42	0.636	0.064	0.086	0.004	0.250	0.059	0.001	500	40	535	26	577	49	526	47	0.40	1.040
mr06a36	0.689	0.041	0.087	0.004	0.370	0.057	0.001	532	24	535	22	503	22	534	39	0.90	0.695
mr06a30	0.693	0.031	0.087	0.002	0.262	0.061	0.001	535	19	538	12	650	37	537	23	0.86	0.084
mr02a77	0.849	0.040	0.087	0.002	0.251	0.069	0.001	624	22	538	12	908	35	550	24	0.00	0.183
mr02a24	0.716	0.047	0.087	0.003	0.272	0.058	0.002	548	28	539	18	522	65	541	34	0.74	0.806
mr05a70	0.652	0.059	0.087	0.004	0.255	0.058	0.001	510	36	539	24	536	30	531	44	0.44	0.806
mr05a69	0.650	0.086	0.087	0.006	0.262	0.057	0.001	509	53	540	36	505	57	532	65	0.57	0.786
mr04a61	0.760	0.036	0.087	0.003	0.419	0.064	0.001	574	21	541	21	736	17	557	35	0.13	0.040
mr04a54	0.697	0.026	0.088	0.003	0.424	0.059	0.000	537	16	543	16	567	16	540	27	0.70	1.869
mr04a77	0.706	0.026	0.088	0.002	0.301	0.060	0.001	542	15	544	11	601	26	543	21	0.92	0.674
mr05a92	0.762	0.029	0.088	0.002	0.324	0.059	0.001	575	17	546	13	572	36	555	24	0.10	1.006
mr04a86	0.960	0.403	0.089	0.020	0.271	0.108	0.002	683	209	550	120	1768	31	568	232	0.55	0.179
mr05a78	0.701	0.038	0.089	0.003	0.283	0.057	0.001	539	23	551	16	503	40	548	29	0.64	0.880
mr06a24	0.738	0.045	0.089	0.003	0.288	0.057	0.002	561	26	551	18	509	64	554	34	0.72	0.631
mr02a60	1.097	0.064	0.089	0.003	0.322	0.082	0.002	752	31	551	20	1257	42	578	39	0.00	0.973
mr05a71	0.672	0.054	0.089	0.004	0.249	0.060	0.001	522	33	552	21	591	38	545	39	0.37	0.882
mr05a90	0.739	0.031	0.090	0.003	0.347	0.060	0.001	562	18	553	15	591	34	556	27	0.65	1.129
mr02a63	1.554	0.106	0.090	0.002	0.203	0.118	0.003	952	42	556	15	1923	47	560	29	0.00	1.006
mr02a76	0.763	0.037	0.090	0.003	0.369	0.066	0.002	576	21	556	19	798	48	564	33	0.39	0.654
mr02a68	0.840	0.048	0.090	0.003	0.278	0.062	0.001	619	26	557	17	687	41	570	32	0.03	0.014
mr04a58	0.722	0.025	0.090	0.002	0.325	0.057	0.001	552	15	558	12	501	36	556	22	0.69	2.240
mr04a80	0.778	0.036	0.091	0.002	0.209	0.068	0.001	585	21	559	10	866	35	562	20	0.22	0.515
mr06a06	0.698	0.046	0.091	0.003	0.258	0.060	0.001	538	27	559	18	590	43	553	33	0.46	0.433
mr04a90	0.827	0.116	0.091	0.005	0.185	0.080	0.003	612	65	559	28	1196	65	564	54	0.43	0.839
mr02a36	0.683	0.054	0.091	0.004	0.283	0.056	0.001	529	33	562	24	471	55	552	43	0.33	1.760
mr04a72	0.598	0.053	0.091	0.003	0.213	0.054	0.001	476	34	563	20	385	51	542	37	0.01	0.625
mr04a55	1.702	0.197	0.091	0.003	0.138	0.161	0.004	1009	74	563	17	2467	42	564	35	0.00	1.836
mr04a89	0.724	0.072	0.091	0.005	0.271	0.061	0.002	553	43	564	29	623	57	561	54	0.81	0.618
mr02a33	0.732	0.042	0.091	0.003	0.237	0.059	0.001	558	25	564	15	559	47	563	28	0.80	0.319
mr06a05	0.956	0.127	0.092	0.006	0.231	0.081	0.002	681	66	566	33	1226	42	578	65	0.10	0.371

Nashoba Formation Gneiss	Measured Isotopic Ratios 207Pb /235U	1s error	206Pb /238U	1s error	Rho	207Pb/ 206Pb	1s error	Calculated Ages 207Pb /235U	1s error	206Pb /238U	1s error	207Pb/ 206Pb	1s error	Concordia age	2s error	Probability Of Concordance	Th/U
mr02a61	2.347	0.270	0.092	0.003	0.138	0.237	0.004	1227	82	569	17	3098	30	566	35	0.00	0.278
mr02a25	0.726	0.029	0.093	0.002	0.255	0.057	0.001	554	17	572	11	509	38	567	20	0.33	0.781
mr04a78	0.674	0.101	0.093	0.005	0.180	0.066	0.002	523	61	572	29	813	71	565	56	0.43	0.796
mr04a70	0.646	0.051	0.093	0.003	0.223	0.062	0.001	506	31	576	19	674	40	559	35	0.03	0.569
mr02a86	0.740	0.041	0.094	0.003	0.271	0.058	0.001	562	24	577	17	526	45	573	30	0.55	1.024
mr04a63	0.848	0.200	0.095	0.007	0.166	0.074	0.002	624	110	586	44	1043	55	589	86	0.74	1.003
mr04a41	0.757	0.026	0.096	0.003	0.382	0.059	0.001	572	15	588	15	557	21	581	25	0.34	0.640
mr02a69	0.931	0.041	0.096	0.003	0.395	0.067	0.001	668	21	593	20	836	32	622	35	0.00	1.314
mr05a67	0.800	0.033	0.097	0.004	0.463	0.060	0.001	597	19	595	22	616	29	596	34	0.96	1.085
mr05a88	0.801	0.050	0.097	0.003	0.220	0.065	0.001	598	28	598	16	762	47	598	29	0.99	0.761
mr04a81	0.996	0.142	0.100	0.009	0.305	0.086	0.002	702	72	616	51	1347	35	636	95	0.26	0.229
mr06a37	0.815	0.107	0.101	0.008	0.310	0.066	0.001	605	60	623	48	808	28	616	85	0.79	0.268
mr05a77	0.755	0.106	0.102	0.007	0.247	0.059	0.001	571	61	624	41	570	38	610	75	0.41	0.396
mr04a40	1.000	0.057	0.103	0.006	0.467	0.069	0.001	704	29	634	32	910	31	674	53	0.03	0.291
mr06a38	1.840	0.377	0.106	0.014	0.325	0.128	0.003	1060	135	652	83	2070	35	673	164	0.01	0.089
mr04a51	0.973	0.101	0.110	0.006	0.283	0.069	0.002	690	52	671	37	897	50	676	68	0.72	0.650
mr02a26	0.914	0.149	0.115	0.014	0.377	0.063	0.003	659	79	703	82	711	101	679	133	0.62	0.450
mr02a43	1.616	0.087	0.119	0.005	0.359	0.092	0.001	976	34	727	27	1460	23	779	51	0.00	0.178
mr02a05	1.435	0.178	0.121	0.010	0.346	0.082	0.002	904	74	739	60	1239	37	783	111	0.04	0.203
mr02a54	1.225	0.107	0.141	0.014	0.566	0.081	0.004	812	49	853	79	1214	88	814	98	0.54	0.273
mr06a18	1.581	0.119	0.145	0.006	0.294	0.081	0.001	963	47	874	36	1226	27	900	66	0.08	0.139
mr02a72	2.026	0.162	0.155	0.009	0.357	0.087	0.001	1124	54	928	49	1363	28	995	88	0.00	0.528
mr02a50	1.134	0.126	0.163	0.018	0.499	0.085	0.005	769	60	972	100	1325	109	781	118	0.02	0.391
mr02a55	1.595	0.084	0.167	0.005	0.308	0.068	0.002	968	33	993	30	877	53	982	50	0.51	0.590
mr06a40	3.041	0.263	0.172	0.012	0.407	0.130	0.001	1418	66	1021	67	2098	12	1141	122	0.00	0.222
mr06a16	3.134	0.239	0.201	0.012	0.402	0.115	0.001	1441	59	1179	66	1875	19	1307	110	0.00	0.150
mr04a67	1.983	0.134	0.205	0.009	0.341	0.077	0.001	1110	46	1201	50	1119	19	1146	77	0.10	0.366
mr02a62	3.684	0.307	0.208	0.014	0.406	0.103	0.002	1568	67	1219	75	1680	31	1376	128	0.00	0.239
mr05a80	2.574	0.093	0.222	0.006	0.350	0.084	0.001	1293	26	1291	29	1295	21	1292	46	0.94	0.371
mr02a87	2.693	0.197	0.228	0.013	0.403	0.082	0.002	1326	54	1322	71	1243	40	1325	101	0.95	0.201
mr02a16	2.986	0.105	0.235	0.006	0.342	0.089	0.001	1404	27	1360	30	1396	27	1385	46	0.18	0.315

Nashoba Formation Gneiss	Measured Isotopic Ratios 207Pb /235U	1s error	206Pb /238U	1s error	Rho	207Pb/ 206Pb	1s error	Calculated Ages 207Pb /235U	1s error	206Pb /238U	1s error	207Pb/ 206Pb	1s error	Concordia age	2s error	Probability Of Concordance	Th/U
mr04a42	3.279	0.215	0.250	0.012	0.372	0.100	0.001	1476	51	1439	63	1629	17	1463	93	0.57	0.272
mr04a76	5.491	0.445	0.299	0.018	0.377	0.141	0.002	1899	70	1684	90	2244	20	1822	134	0.02	0.379
mr02a82	5.549	0.195	0.307	0.010	0.468	0.127	0.001	1908	30	1727	50	2054	15	1885	61	0.00	0.462
mr04a60	5.371	0.179	0.316	0.009	0.425	0.124	0.001	1880	28	1768	44	2012	13	1859	56	0.01	0.873
mr02a09	3.704	0.214	0.321	0.015	0.409	0.095	0.003	1572	46	1793	74	1531	56	1600	88	0.00	0.400
mr04a69	6.427	0.311	0.339	0.012	0.381	0.145	0.001	2036	43	1880	60	2292	15	1993	82	0.01	0.402
mr04a88	6.377	0.347	0.365	0.015	0.380	0.128	0.001	2029	48	2007	71	2073	14	2025	92	0.75	1.028
mr04a82	6.915	0.166	0.379	0.009	0.491	0.130	0.001	2101	21	2073	42	2105	13	2100	43	0.45	0.950
mr02a52	8.364	0.784	0.451	0.044	0.522	0.151	0.007	2271	85	2402	196	2361	76	2264	170	0.44	0.176
mr02a41	12.92	0.336	0.507	0.011	0.434	0.180	0.002	2674	25	2644	49	2656	15	2673	49	0.50	0.846
mr04a49	13.55	0.895	0.534	0.020	0.284	0.192	0.002	2718	62	2757	84	2759	15	2730	112	0.66	0.898

Nashoba Formation Schist	Measured Isotopic Ratios							Calculated Ages									
	207Pb /235U	1s error	206Pb /238U	1s error	Rho	207Pb/ 206Pb	1s error	207Pb /235U	1s error	206Pb /238U	1s error	207Pb/ 206Pb	1s error	Concordia age	2s error	Probability Of Concordance	Th/U
se10a253	0.467	0.069	0.052	0.006	0.422	0.060	0.001	389	48	327	40	605	35	346	73	0.20	0.013
se10a258	0.387	0.039	0.052	0.003	0.266	0.058	0.002	332	29	328	17	511	75	329	32	0.89	0.015
se10a219	0.486	0.078	0.053	0.006	0.358	0.064	0.002	402	53	331	37	740	51	345	70	0.18	0.018
se14a50	0.377	0.031	0.053	0.002	0.244	0.053	0.001	324	23	331	13	338	48	330	24	0.77	0.005
se14a15	0.405	0.021	0.053	0.002	0.402	0.053	0.001	345	15	332	14	349	33	337	24	0.41	0.113
se14a34	0.424	0.031	0.053	0.002	0.296	0.055	0.001	359	22	334	14	402	37	339	27	0.27	0.008
se10a218	0.494	0.088	0.053	0.008	0.400	0.064	0.001	407	60	335	47	727	44	354	87	0.23	0.017
se10a263	0.469	0.034	0.054	0.003	0.405	0.058	0.001	390	23	336	19	548	37	353	35	0.02	0.012
se10a264	0.496	0.044	0.054	0.005	0.564	0.057	0.001	409	30	339	33	500	40	379	56	0.02	0.011
se10a255	0.413	0.048	0.054	0.004	0.328	0.055	0.001	351	34	340	25	425	40	343	46	0.74	0.014
se10a224	0.468	0.066	0.054	0.007	0.455	0.058	0.001	390	46	340	42	511	38	361	76	0.29	0.010
se10a177	0.477	0.076	0.054	0.004	0.216	0.066	0.002	396	52	341	23	807	48	346	45	0.30	0.012
se10a203	0.396	0.047	0.054	0.004	0.312	0.051	0.001	339	34	342	25	257	50	341	45	0.93	0.017
se14a46	0.458	0.029	0.055	0.003	0.419	0.055	0.001	383	21	343	18	428	38	358	32	0.06	0.014
se14a77	0.437	0.041	0.055	0.004	0.338	0.055	0.001	368	29	344	22	403	39	350	40	0.42	0.012
se10a175	0.492	0.070	0.055	0.005	0.335	0.059	0.001	406	48	344	32	553	51	357	61	0.21	0.019
se10a178	0.378	0.064	0.055	0.004	0.190	0.056	0.001	326	47	345	22	459	45	343	42	0.68	0.011
se10a246	0.587	0.036	0.055	0.004	0.622	0.063	0.001	469	23	346	26	715	43	416	45	0.00	0.010
se10a213	0.412	0.037	0.055	0.002	0.212	0.058	0.001	351	26	346	13	515	46	347	25	0.87	0.027
se10a198	0.403	0.035	0.055	0.002	0.252	0.055	0.001	344	25	348	15	419	38	347	28	0.88	0.016
se10a207	0.443	0.068	0.056	0.007	0.393	0.054	0.001	372	48	349	41	374	41	357	74	0.63	0.013
se14a07	0.429	0.040	0.056	0.003	0.326	0.055	0.001	362	28	349	21	392	28	353	38	0.65	0.028
se10a237	0.468	0.042	0.056	0.005	0.523	0.054	0.001	390	29	349	32	375	38	373	53	0.17	0.016
se14a17	0.401	0.045	0.056	0.003	0.256	0.058	0.001	342	33	349	20	513	43	348	37	0.83	0.015
se14a48	0.422	0.032	0.056	0.003	0.306	0.052	0.001	358	23	351	16	304	52	353	30	0.79	0.007
se10a223	0.421	0.028	0.056	0.002	0.304	0.052	0.001	357	20	352	14	295	40	353	26	0.83	0.012
se14a75	0.450	0.068	0.056	0.007	0.420	0.054	0.001	378	47	353	43	352	40	363	76	0.61	0.011
se10a239	0.543	0.021	0.056	0.002	0.366	0.061	0.001	440	14	353	10	633	32	371	19	0.00	0.019
se14a25	0.408	0.047	0.056	0.003	0.201	0.058	0.001	348	34	353	16	537	47	352	31	0.87	0.017
se14a69	0.399	0.060	0.056	0.004	0.256	0.055	0.001	341	43	353	26	405	45	351	49	0.78	0.016
se10a265	0.431	0.043	0.057	0.004	0.365	0.053	0.001	364	30	354	25	314	33	358	45	0.76	0.012
se14a67	0.450	0.036	0.057	0.003	0.334	0.056	0.001	377	26	355	19	453	36	361	35	0.39	0.012
se14a68	0.456	0.036	0.057	0.003	0.362	0.056	0.001	381	25	355	20	442	32	363	36	0.32	0.010
se10a235	0.485	0.030	0.057	0.004	0.535	0.055	0.001	402	20	356	23	406	28	383	38	0.03	0.017

Nashoba Formation Schist	Measured Isotopic Ratios							Calculated Ages									
	207Pb /235U	1s error	206Pb /238U	1s error	Rho	207Pb/ 206Pb	1s error	207Pb /235U	1s error	206Pb /238U	1s error	207Pb /206Pb	1s error	Concordia age	2s error	Probability Of Concordance	Th/U
se14a44	0.469	0.040	0.057	0.003	0.359	0.055	0.001	391	27	356	21	403	35	366	39	0.22	0.016
se14a16	0.434	0.053	0.057	0.005	0.330	0.055	0.001	366	38	356	28	425	27	359	52	0.80	0.013
se10a243	0.550	0.034	0.057	0.005	0.703	0.059	0.001	445	22	357	30	572	39	439	45	0.00	0.009
se10a257	0.470	0.033	0.057	0.003	0.401	0.056	0.001	391	23	357	20	444	37	369	36	0.15	0.010
se10a174	0.497	0.057	0.057	0.005	0.346	0.059	0.001	410	39	357	27	566	40	369	52	0.18	0.015
se13a20	0.484	0.054	0.057	0.006	0.490	0.054	0.001	401	37	358	38	372	50	380	66	0.26	0.013
se10a183	0.428	0.048	0.057	0.004	0.275	0.056	0.001	362	34	358	21	434	45	359	40	0.92	0.029
se10a206	0.399	0.040	0.057	0.003	0.245	0.054	0.001	341	29	358	17	355	43	355	32	0.56	0.011
se10a226	0.467	0.030	0.057	0.002	0.294	0.058	0.001	389	21	359	13	518	43	365	25	0.16	0.009
se10a208	0.456	0.052	0.057	0.005	0.364	0.056	0.001	382	37	359	29	463	37	366	53	0.55	0.029
se10a248	0.428	0.058	0.057	0.004	0.271	0.057	0.001	362	41	359	26	485	45	360	48	0.96	0.009
se10a214	0.438	0.049	0.057	0.002	0.186	0.066	0.001	369	34	360	14	793	40	361	28	0.80	0.015
se14a45	0.486	0.023	0.057	0.002	0.446	0.054	0.001	402	16	360	15	381	22	378	27	0.01	0.011
se10a254	0.473	0.038	0.058	0.003	0.332	0.057	0.001	393	26	361	19	494	41	369	35	0.23	0.010
se14a18	0.426	0.054	0.058	0.003	0.187	0.067	0.002	360	38	362	17	837	60	362	32	0.98	0.022
se10a238	0.436	0.065	0.058	0.005	0.266	0.056	0.001	368	46	362	28	462	44	363	53	0.91	0.012
se14a59	0.442	0.040	0.058	0.004	0.340	0.053	0.001	372	28	364	22	311	38	366	40	0.79	0.014
se14a51	0.476	0.063	0.058	0.006	0.358	0.056	0.001	395	43	364	34	446	26	373	62	0.49	0.005
se10a236	0.430	0.033	0.058	0.003	0.291	0.055	0.001	363	23	365	16	429	47	364	29	0.96	0.012
se10a184	0.442	0.054	0.058	0.004	0.302	0.055	0.001	371	38	366	26	413	44	367	49	0.89	0.012
se10a165	0.434	0.075	0.058	0.003	0.144	0.061	0.002	366	53	366	18	630	57	366	35	1.00	0.015
se14a30	0.467	0.031	0.058	0.003	0.339	0.055	0.001	389	21	366	16	411	35	372	29	0.29	0.009
se10a227	0.436	0.044	0.058	0.003	0.248	0.061	0.001	367	31	366	18	624	39	366	33	0.97	0.031
se14a70	0.456	0.038	0.058	0.003	0.343	0.054	0.001	381	26	366	20	382	28	371	37	0.59	0.010
se14a74	0.458	0.038	0.059	0.003	0.269	0.057	0.001	383	26	367	16	479	46	370	30	0.55	0.014
se10a244	0.477	0.033	0.059	0.002	0.280	0.058	0.001	396	22	367	14	541	41	372	26	0.20	0.006
se13a08	0.474	0.022	0.059	0.002	0.344	0.055	0.001	394	15	370	11	398	26	377	21	0.12	0.007
se14a20	0.467	0.034	0.059	0.003	0.395	0.055	0.001	389	24	371	21	407	26	378	37	0.48	0.009
se10a196	0.452	0.041	0.059	0.003	0.311	0.055	0.001	378	29	371	21	417	32	373	38	0.81	0.016
se14a57	0.460	0.079	0.059	0.006	0.291	0.056	0.001	384	55	372	36	448	34	374	67	0.83	0.005
se14a26	0.434	0.039	0.059	0.002	0.235	0.058	0.001	366	27	372	15	547	33	371	29	0.85	0.020
se10a228	0.448	0.207	0.059	0.016	0.292	0.056	0.001	376	145	372	97	441	41	373	181	0.98	0.011
se10a176	0.642	0.024	0.059	0.003	0.677	0.064	0.001	503	15	372	18	750	21	470	29	0.00	0.050

Nashoba Formation Schist	Measured Isotopic Ratios 207Pb /235U	1s error	206Pb /238U	1s error	Rho	207Pb/ 206Pb	1s error	Calculated Ages 207Pb /235U	1s error	206Pb /238U	1s error	207Pb/ 206Pb	1s error	Concordia age	2s error	Probability Of Concordance	Th/U
se14a47	0.461	0.034	0.059	0.002	0.270	0.055	0.001	385	24	372	15	429	41	375	27	0.60	0.011
se14a21	0.481	0.034	0.060	0.004	0.449	0.054	0.001	399	23	373	23	388	25	385	39	0.28	0.008
se14a40	0.466	0.027	0.060	0.002	0.344	0.054	0.001	388	19	373	15	374	26	378	27	0.44	0.008
se13a10	0.497	0.023	0.060	0.003	0.475	0.055	0.001	410	15	373	16	392	22	392	27	0.02	0.006
se14a27	0.446	0.044	0.060	0.003	0.266	0.056	0.001	375	31	374	19	448	36	374	36	0.97	0.009
se14a11	0.439	0.034	0.060	0.002	0.202	0.060	0.002	369	24	375	11	596	77	374	22	0.83	0.010
se10a217	0.456	0.099	0.060	0.005	0.190	0.067	0.001	382	69	375	30	832	46	375	58	0.92	0.021
se10a204	0.523	0.076	0.060	0.008	0.441	0.058	0.001	427	51	375	47	547	42	396	83	0.32	0.011
se14a56	0.457	0.040	0.060	0.003	0.286	0.054	0.001	382	28	375	18	373	33	377	34	0.81	0.005
se10a205	0.433	0.031	0.060	0.002	0.213	0.056	0.001	366	22	376	11	451	44	374	21	0.65	0.007
se10a182	0.458	0.071	0.060	0.003	0.153	0.066	0.002	383	49	376	17	794	66	376	34	0.89	0.015
se10a185	0.436	0.050	0.060	0.002	0.178	0.059	0.001	368	35	376	15	579	49	375	29	0.82	0.021
se10a267	0.479	0.069	0.060	0.005	0.287	0.057	0.001	397	47	377	30	495	43	381	57	0.67	0.014
se14a09	0.396	0.062	0.060	0.003	0.160	0.058	0.001	338	45	377	18	525	47	373	35	0.39	0.019
se10a225	0.462	0.060	0.060	0.005	0.297	0.056	0.001	385	42	378	28	435	38	380	53	0.86	0.018
se14a10	0.408	0.039	0.060	0.002	0.214	0.055	0.001	348	28	378	15	432	42	373	29	0.29	0.016
se14a37	0.474	0.051	0.061	0.004	0.313	0.054	0.001	394	35	379	25	389	39	383	46	0.67	0.014
se13a11	0.495	0.019	0.061	0.002	0.386	0.055	0.001	408	13	379	11	403	24	389	19	0.03	0.011
se10a195	0.490	0.045	0.061	0.003	0.266	0.058	0.001	405	31	380	18	540	43	384	34	0.42	0.011
se10a215	0.466	0.087	0.061	0.008	0.361	0.054	0.001	389	60	380	50	391	49	383	89	0.89	0.022
se13a09	0.494	0.020	0.061	0.002	0.345	0.054	0.001	408	13	382	10	381	30	389	19	0.06	0.015
se10a163	0.591	0.087	0.061	0.011	0.589	0.059	0.002	471	56	383	65	583	76	439	108	0.11	0.011
se13a28	0.482	0.056	0.061	0.005	0.377	0.054	0.001	400	39	383	33	389	33	389	58	0.67	0.008
se13a23	0.463	0.033	0.061	0.004	0.430	0.050	0.001	386	23	383	23	214	31	385	39	0.89	0.006
se10a167	0.505	0.029	0.061	0.002	0.236	0.056	0.001	415	19	383	10	448	38	387	19	0.11	0.009
se14a28	0.453	0.037	0.061	0.003	0.276	0.055	0.001	379	26	383	17	416	38	382	32	0.88	0.014
se14a66	0.494	0.037	0.061	0.003	0.324	0.055	0.001	408	25	384	18	405	39	390	33	0.35	0.012
se14a29	0.449	0.062	0.061	0.005	0.287	0.054	0.001	377	43	385	29	380	46	383	54	0.86	0.013
se14a35	0.532	0.029	0.062	0.002	0.350	0.058	0.001	433	19	385	14	540	35	398	27	0.02	0.021
se13a21	0.461	0.059	0.062	0.004	0.238	0.057	0.001	385	41	385	23	506	51	385	43	0.99	0.021
se10a172	0.645	0.045	0.062	0.003	0.311	0.070	0.001	505	28	386	16	938	39	401	32	0.00	0.023
se10a256	0.547	0.033	0.062	0.003	0.425	0.059	0.001	443	22	388	19	584	32	408	35	0.01	0.020
se14a61	0.433	0.045	0.062	0.003	0.209	0.054	0.001	365	32	388	16	361	45	384	31	0.48	0.009

Nashoba Formation Schist	Measured Isotopic Ratios 207Pb /235U	1s error	206Pb /238U	1s error	Rho	207Pb/ 206Pb	1s error	Calculated Ages 207Pb /235U	1s error	206Pb /238U	1s error	207Pb/ 206Pb	1s error	Concordia age	2s error	Probability Of Concordance	Th/U
se13a17	0.485	0.042	0.062	0.004	0.333	0.055	0.001	401	28	388	22	424	30	392	39	0.66	0.007
se13a18	0.465	0.026	0.062	0.002	0.334	0.054	0.001	388	18	389	14	355	30	389	25	0.97	0.176
se10a192	0.475	0.046	0.062	0.004	0.304	0.056	0.001	394	31	389	22	463	37	391	41	0.87	0.008
se14a38	0.515	0.029	0.063	0.002	0.351	0.055	0.001	422	19	392	15	419	31	401	28	0.13	0.038
se14a58	0.572	0.072	0.063	0.005	0.323	0.061	0.001	459	47	392	31	655	43	405	59	0.16	0.011
se10a229	0.475	0.043	0.063	0.003	0.227	0.057	0.001	395	29	393	16	501	53	393	30	0.95	0.016
se10a233	0.526	0.137	0.063	0.014	0.442	0.057	0.001	429	91	393	88	486	34	410	153	0.70	0.128
se14a12	0.474	0.045	0.063	0.003	0.231	0.056	0.001	394	31	394	17	454	56	394	32	0.99	0.010
se10a216	0.566	0.039	0.063	0.003	0.384	0.060	0.001	455	25	394	20	594	40	412	37	0.02	0.047
se14a49	0.462	0.040	0.063	0.002	0.207	0.056	0.001	386	28	394	14	433	41	393	26	0.76	0.012
se13a12	0.491	0.027	0.063	0.002	0.272	0.054	0.001	405	19	395	12	377	37	397	22	0.59	0.010
se10a247	0.481	0.043	0.063	0.003	0.268	0.056	0.001	399	29	396	18	440	41	396	34	0.91	0.021
se13a27	0.487	0.040	0.063	0.003	0.277	0.056	0.001	403	28	396	18	453	36	398	33	0.82	0.006
se10a173	0.482	0.043	0.064	0.002	0.166	0.056	0.001	399	29	397	11	469	48	397	22	0.94	0.030
se10a249	0.484	0.096	0.064	0.005	0.189	0.056	0.001	401	66	398	29	462	56	399	56	0.97	0.009
se10a162	0.550	0.039	0.064	0.002	0.200	0.061	0.001	445	25	399	11	645	49	403	21	0.08	0.013
se14a65	0.481	0.901	0.064	0.037	0.154	0.062	0.002	399	618	399	223	663	84	399	437	1.00	0.010
se10a168	0.643	0.040	0.064	0.003	0.415	0.064	0.002	504	25	399	20	742	52	428	38	0.00	0.010
se14a08	0.472	0.042	0.064	0.002	0.184	0.061	0.002	393	29	401	13	647	61	400	24	0.79	0.009
se10a188	0.464	0.064	0.064	0.004	0.208	0.060	0.001	387	45	402	22	617	52	400	43	0.74	0.207
se14a19	0.752	0.034	0.064	0.003	0.482	0.072	0.002	570	20	403	17	986	46	447	33	0.00	0.302
se14a13	0.509	0.060	0.065	0.003	0.181	0.058	0.001	418	40	404	17	513	57	405	33	0.74	0.012
se14a39	0.508	0.040	0.065	0.003	0.295	0.055	0.001	417	27	404	18	401	35	407	34	0.64	0.029
se10a194	0.465	0.066	0.065	0.003	0.177	0.060	0.001	388	46	405	20	612	51	403	38	0.70	0.022
se10a186	0.498	0.047	0.065	0.003	0.278	0.057	0.001	411	32	406	21	475	44	407	38	0.89	0.009
se14a36	0.496	0.040	0.065	0.003	0.278	0.054	0.001	409	27	407	18	372	42	407	33	0.94	0.017
se14a60	0.509	0.048	0.066	0.003	0.244	0.056	0.001	418	32	410	18	444	49	411	34	0.81	0.006
se13a29	0.547	0.040	0.066	0.003	0.284	0.060	0.001	443	26	412	16	595	44	418	31	0.24	0.078
se10a193	0.510	0.045	0.066	0.003	0.281	0.056	0.001	418	30	413	20	453	43	414	37	0.85	0.037
se10a245	0.511	0.100	0.067	0.005	0.199	0.058	0.001	419	67	416	31	526	54	416	61	0.96	0.018
se10a268	0.508	0.110	0.067	0.003	0.092	0.071	0.002	417	74	417	16	944	55	417	32	1.00	0.037
se10a166	0.548	0.027	0.067	0.002	0.226	0.056	0.001	444	18	418	9	465	37	422	18	0.17	0.028
se10a187	0.515	0.073	0.067	0.003	0.169	0.060	0.002	422	49	419	19	591	62	419	38	0.94	0.010

Nashoba Formation Schist	Measured Isotopic Ratios 207Pb /235U	1s error	206Pb /238U	1s error	Rho	207Pb/ 206Pb	1s error	Calculated Ages 207Pb /235U	1s error	206Pb /238U	1s error	207Pb/ 206Pb	1s error	Concordia age	2s error	Probability Of Concordance	Th/U
se10a209	3.014	0.522	0.209	0.026	0.363	0.104	0.001	1411	132	1223	140	1692	20	1312	234	0.23	0.546
se10a234	0.515	0.044	0.067	0.002	0.173	0.063	0.002	422	29	420	12	709	65	420	23	0.95	0.012
se13a19	0.596	0.027	0.069	0.002	0.389	0.059	0.001	475	17	430	15	565	29	446	26	0.01	0.470
se14a76	0.543	0.033	0.069	0.002	0.230	0.056	0.001	440	22	433	12	469	43	434	22	0.75	0.022
se10a199	0.646	0.046	0.070	0.003	0.279	0.063	0.001	506	28	439	17	703	45	450	32	0.02	0.061
se13a22	0.620	0.062	0.077	0.005	0.350	0.056	0.001	490	39	477	32	448	38	481	57	0.75	0.286
se10a164	0.752	0.058	0.087	0.003	0.249	0.064	0.001	569	34	538	20	739	38	544	38	0.37	1.161
se13a13	0.834	0.283	0.099	0.016	0.236	0.070	0.002	616	157	611	94	942	58	612	176	0.98	0.273

	Measured Isotopic Ratios							Calculated Ages									1/3
Nashoba Formation Calc-Silicate	207Pb /235U	1s error	206Pb /238U	1s error	Rho	207Pb/ 206Pb	1s error	207Pb /235U	1s error	206Pb /238U	1s error	207Pb/ 206Pb	1s error	Concordia age	2s error	Probability Of Concordance	Th/U
se10a153	0.396	0.054	0.049	0.006	0.428	0.053	0.001	339	39	310	35	344	34	321	63	0.47	0.18
se13a45	0.393	0.022	0.051	0.002	0.394	0.054	0.001	336	16	320	14	387	24	326	25	0.34	0.15
se10a143	0.411	0.038	0.052	0.003	0.351	0.056	0.001	349	27	327	21	464	35	333	38	0.42	0.16
se10a130	0.393	0.052	0.052	0.004	0.283	0.056	0.001	337	38	329	24	455	36	331	45	0.85	0.18
se10a120	0.389	0.040	0.053	0.003	0.258	0.056	0.001	334	29	331	17	436	47	332	32	0.93	0.29
se13a98	0.384	0.029	0.053	0.002	0.293	0.053	0.001	330	21	332	14	322	38	332	26	0.93	0.18
se13a43	0.411	0.012	0.053	0.001	0.354	0.054	0.001	349	8	334	7	361	26	339	12	0.08	0.16
se10a133	0.429	0.034	0.053	0.003	0.387	0.055	0.001	362	24	334	20	406	31	344	37	0.27	0.19
se13a97	0.433	0.058	0.053	0.005	0.366	0.056	0.001	365	41	334	32	437	49	344	58	0.46	0.20
se10a111	0.414	0.038	0.054	0.003	0.316	0.055	0.001	352	28	336	19	427	32	340	36	0.59	0.15
se13a96	0.413	0.033	0.054	0.003	0.303	0.055	0.001	351	24	337	16	431	34	340	30	0.55	0.13
se13a46	0.407	0.017	0.054	0.001	0.253	0.055	0.001	347	12	337	7	425	30	338	13	0.42	0.23
se10a142	0.426	0.036	0.054	0.004	0.394	0.054	0.001	361	26	337	22	388	27	346	40	0.38	0.22
se10a131	0.404	0.029	0.054	0.002	0.304	0.054	0.001	345	21	339	15	382	34	341	27	0.80	0.14
se10a102	0.413	0.046	0.054	0.004	0.355	0.054	0.001	351	33	340	26	371	33	343	47	0.74	0.15
se13a91	0.430	0.049	0.054	0.005	0.396	0.055	0.001	363	35	341	30	401	36	349	53	0.54	0.14
se13a41	0.427	0.016	0.054	0.002	0.497	0.053	0.000	361	11	341	12	348	19	353	20	0.09	0.11
se13a39	0.416	0.015	0.054	0.001	0.330	0.055	0.001	353	11	342	8	400	23	345	15	0.33	0.15
se10a152	0.437	0.022	0.055	0.002	0.338	0.054	0.001	368	16	342	12	379	30	349	21	0.11	0.14
se13c101	0.413	0.080	0.055	0.007	0.338	0.054	0.001	351	58	344	44	392	29	346	80	0.91	0.12
se10a100	0.401	0.092	0.055	0.005	0.215	0.059	0.002	342	67	345	33	559	56	345	64	0.96	0.17
se13a40	0.427	0.016	0.055	0.002	0.373	0.056	0.001	361	12	346	10	436	21	351	17	0.20	0.15
se10a119	0.404	0.031	0.055	0.002	0.288	0.055	0.001	345	23	346	15	425	41	346	28	0.94	0.19
se10a104	0.391	0.053	0.055	0.003	0.174	0.057	0.001	335	39	347	16	505	53	346	31	0.77	0.22
se10a151	0.428	0.049	0.055	0.004	0.346	0.054	0.001	362	35	347	27	385	31	352	49	0.69	0.14
se13c113	0.431	0.024	0.055	0.003	0.414	0.053	0.001	364	17	347	16	338	24	354	28	0.36	0.17
se10a129	0.421	0.039	0.055	0.004	0.375	0.053	0.001	357	28	348	23	338	23	351	42	0.76	0.13
se10a124	0.430	0.050	0.056	0.005	0.358	0.055	0.001	363	36	349	28	416	31	354	52	0.71	0.17
se13a42	0.409	0.020	0.056	0.002	0.309	0.053	0.001	348	15	349	10	327	24	349	19	0.93	0.19
se10a112	0.476	0.030	0.056	0.004	0.633	0.054	0.001	396	21	350	27	366	25	388	41	0.03	0.14
se13c112	0.423	0.078	0.056	0.007	0.337	0.054	0.001	359	56	351	42	384	39	353	77	0.89	0.14
se13a44	0.449	0.027	0.056	0.002	0.266	0.060	0.001	376	19	352	11	619	22	356	21	0.20	0.15
se13a94	0.426	0.029	0.057	0.002	0.320	0.055	0.001	361	21	355	15	407	30	357	28	0.81	0.09

Nashoba Formation Calc-Silicate	Measured Isotopic Ratios 207Pb /235U	1s error	206Pb /238U	1s error	Rho	207Pb/ 206Pb	1s error	Calculated Ages 207Pb /235U	1s error	206Pb /238U	1s error	207Pb/ 206Pb	1s error	Concordia age	2s error	Probability Of Concordance	Th/U
se13c115	0.443	0.043	0.057	0.004	0.334	0.055	0.001	373	30	358	22	426	34	362	41	0.63	0.13
se13c107	0.474	0.027	0.057	0.003	0.542	0.053	0.001	394	18	358	21	346	26	381	35	0.06	0.10
se10a149	0.453	0.054	0.057	0.005	0.355	0.055	0.001	379	38	358	30	402	42	365	54	0.59	0.20
se13c116	0.447	0.037	0.057	0.004	0.380	0.054	0.001	375	26	359	22	358	37	365	39	0.54	0.14
se10a144	0.473	0.026	0.057	0.003	0.396	0.056	0.001	393	18	359	15	440	30	371	28	0.07	0.14
se10a134	0.452	0.047	0.058	0.004	0.327	0.056	0.001	379	33	361	24	466	26	365	44	0.60	0.20
se10a138	0.489	0.035	0.058	0.004	0.460	0.057	0.001	404	24	361	23	482	21	380	40	0.07	0.17
se10a103	0.483	0.048	0.058	0.005	0.419	0.057	0.001	400	33	361	29	504	43	376	52	0.24	0.14
se10a118	0.437	0.031	0.058	0.003	0.313	0.054	0.001	368	22	361	16	385	32	363	29	0.74	0.14
se10a110	0.456	0.076	0.058	0.007	0.345	0.055	0.001	382	53	362	40	421	27	368	74	0.72	0.15
se10a132	0.443	0.055	0.058	0.004	0.289	0.055	0.001	372	39	362	25	411	34	365	47	0.80	0.15
se10a98	0.444	0.033	0.058	0.003	0.348	0.053	0.001	373	23	364	18	338	31	367	33	0.69	0.12
se10a108	0.458	0.024	0.058	0.002	0.319	0.054	0.001	383	17	364	12	389	27	368	22	0.28	0.15
se13c102	0.454	0.025	0.058	0.002	0.352	0.054	0.001	380	18	364	14	389	36	369	25	0.39	0.16
se10a139	0.494	0.024	0.058	0.002	0.405	0.057	0.001	408	17	365	14	475	30	380	26	0.01	0.31
se13c117	0.463	0.028	0.058	0.003	0.432	0.053	0.001	387	20	366	19	328	28	375	32	0.30	0.12
se13c105	0.468	0.027	0.059	0.003	0.419	0.053	0.001	390	19	368	17	320	36	377	30	0.27	0.13
se10a99	0.444	0.023	0.059	0.002	0.309	0.056	0.001	373	16	370	12	451	30	371	22	0.84	0.16
se10a123	0.464	0.073	0.060	0.006	0.335	0.056	0.001	387	51	376	39	436	31	379	71	0.83	0.12
se10a141	0.482	0.020	0.060	0.002	0.407	0.055	0.001	399	14	377	13	397	29	386	22	0.13	0.19
se10a113	0.505	0.030	0.061	0.003	0.386	0.057	0.001	415	20	379	17	502	25	391	31	0.09	0.37
se13a92	0.461	0.053	0.061	0.005	0.344	0.054	0.001	385	37	379	29	383	40	381	53	0.88	0.15
se10a128	0.480	0.037	0.061	0.004	0.389	0.055	0.001	398	25	381	22	404	28	388	39	0.51	0.13
se10a150	0.483	0.021	0.062	0.002	0.353	0.054	0.001	400	14	386	12	385	24	391	21	0.36	0.12
se13a93	0.475	0.047	0.062	0.004	0.299	0.056	0.001	395	33	387	22	468	33	389	41	0.82	0.10
se10a114	0.486	0.026	0.062	0.002	0.308	0.057	0.002	402	18	389	12	500	82	392	23	0.48	0.12
se10a101	0.527	0.026	0.065	0.002	0.308	0.056	0.001	430	17	404	12	451	30	410	22	0.15	0.11
se10a140	0.557	0.032	0.067	0.003	0.347	0.057	0.001	450	21	418	16	483	25	428	29	0.14	0.15
se13c111	0.629	0.023	0.067	0.002	0.362	0.060	0.001	496	14	420	11	589	29	440	20	0.00	0.14
se10a122	0.575	0.036	0.067	0.003	0.380	0.058	0.001	461	23	421	19	513	30	434	35	0.09	0.13
se13c103	0.591	0.037	0.070	0.003	0.379	0.056	0.001	472	24	434	20	455	40	447	36	0.13	0.16
se10a109	0.682	0.030	0.077	0.002	0.353	0.062	0.001	528	18	478	14	662	26	493	26	0.01	0.24
se10a121	0.657	0.034	0.081	0.004	0.430	0.056	0.001	513	21	500	21	453	26	506	36	0.56	0.20

Nashoba Formation Calc-Silicate	Measured Isotopic Ratios							Calculated Ages									
	207Pb /235U	**1s error**	**206Pb /238U**	**1s error**	**Rho**	**207Pb/ 206Pb**	**1s error**	**207Pb /235U**	**1s error**	**206Pb /238U**	**1s error**	**207Pb/ 206Pb**	**1s error**	**Concordia age**	**2s error**	**Probability Of Concordance**	**Th/U**
se13c114	1.086	0.057	0.105	0.004	0.397	0.069	0.001	747	28	641	25	894	23	681	45	0.00	0.10

Tadmuck Brook Schist	Measured Isotopic Ratios							Calculated Ages								Probability Of Concordance	Th/U
	207Pb /235U	1s error	206Pb /238U	1s error	Rho	207Pb/ 206Pb	1s error	207Pb /235U	1s error	206Pb /238U	1s error	207Pb/ 206Pb	1s error	Concordia age	2s error		
se10a52	0.775	0.169	0.057	0.012	0.487	0.078	0.001	583	96	359	74	1156	23	387	145	0.02	1.50
se10a71	0.648	0.121	0.068	0.007	0.287	0.061	0.001	507	74	424	44	657	36	437	85	0.28	0.79
se10a62	0.577	0.081	0.069	0.004	0.191	0.055	0.001	463	52	432	22	406	48	435	43	0.56	0.05
se10a49	0.627	0.162	0.070	0.007	0.198	0.061	0.001	494	101	436	43	624	51	441	84	0.57	0.07
se10a29	0.636	0.115	0.071	0.008	0.300	0.057	0.001	500	72	443	47	496	37	455	88	0.45	0.04
se10a41	0.741	0.114	0.073	0.007	0.317	0.063	0.001	563	67	451	43	701	47	470	82	0.11	0.16
se10a81	0.685	0.042	0.073	0.003	0.302	0.060	0.001	530	25	455	16	610	25	469	31	0.00	0.25
se10a31	0.798	0.080	0.073	0.005	0.351	0.067	0.001	596	45	456	31	841	37	480	59	0.00	1.11
se09b20	0.663	0.089	0.075	0.006	0.286	0.059	0.001	516	55	466	35	555	38	476	66	0.37	0.24
se10a72	0.695	0.333	0.075	0.009	0.125	0.071	0.002	536	199	466	54	966	63	469	107	0.73	0.52
se10a28	0.708	0.075	0.075	0.006	0.381	0.063	0.002	544	44	469	36	702	57	492	67	0.10	0.08
se10a27	0.645	0.117	0.075	0.008	0.302	0.057	0.001	505	72	469	49	495	51	477	92	0.62	0.20
se09b09	0.762	0.048	0.078	0.003	0.305	0.060	0.001	575	28	482	18	615	38	499	34	0.00	0.55
se10a42	0.742	0.130	0.078	0.010	0.367	0.056	0.001	563	76	486	60	471	37	508	111	0.33	0.41
se10a67	0.702	0.107	0.079	0.005	0.195	0.059	0.001	540	64	492	28	566	37	497	55	0.47	0.08
se10a38	0.656	0.169	0.080	0.009	0.220	0.062	0.001	512	104	497	54	673	42	499	104	0.89	0.17
se10a11	0.733	0.081	0.081	0.005	0.289	0.061	0.001	558	48	500	31	626	43	511	58	0.23	0.37
se10a18	0.754	0.086	0.082	0.007	0.388	0.060	0.001	571	49	506	43	608	26	529	77	0.22	0.12
se10a22	0.699	0.068	0.085	0.004	0.262	0.059	0.001	538	40	524	26	564	28	527	48	0.73	0.37
se09b29	0.774	0.050	0.087	0.003	0.248	0.061	0.001	582	29	536	17	625	44	544	32	0.12	1.30
se09b08	0.796	0.103	0.087	0.006	0.267	0.062	0.001	594	58	540	36	687	49	550	68	0.37	0.63
se10a58	0.896	0.122	0.088	0.009	0.371	0.060	0.001	650	65	542	52	616	31	572	97	0.11	0.76
se10a40	0.807	0.693	0.088	0.015	0.102	0.094	0.003	601	389	543	91	1499	65	545	181	0.89	0.09
se09b19	0.903	0.124	0.091	0.009	0.363	0.063	0.001	654	66	564	54	694	28	591	98	0.20	0.19
se10a70	0.818	0.205	0.093	0.009	0.197	0.062	0.002	607	114	574	54	684	58	578	104	0.78	1.04
se09b12	0.955	0.052	0.094	0.004	0.353	0.064	0.001	681	27	577	21	730	22	605	39	0.00	0.82
se10a17	0.900	0.061	0.095	0.005	0.355	0.064	0.001	652	33	588	27	745	25	609	49	0.07	0.19
se10a26	0.911	0.104	0.096	0.010	0.444	0.062	0.000	658	55	588	57	675	15	623	96	0.24	0.36
se10a39	0.853	0.272	0.096	0.010	0.156	0.080	0.002	626	149	593	56	1187	55	596	110	0.83	0.36
se10a56	1.013	0.081	0.098	0.005	0.345	0.064	0.001	711	41	605	32	732	28	634	59	0.01	0.21
se09b18	1.033	0.070	0.099	0.005	0.383	0.061	0.001	720	35	609	30	645	47	646	55	0.00	0.72

Tadmuck Brook Schist	Measured Isotopic Ratios 207Pb /235U	1s error	206Pb /238U	1s error	Rho	207Pb/ 206Pb	1s error	Calculated Ages 207Pb /235U	1s error	206Pb /238U	1s error	207Pb/ 206Pb	1s error	Concordia age	2s error	Probability Of Concordance	Th/U
se10a22	0.699	0.068	0.085	0.004	0.262	0.059	0.001	538	40	524	26	564	28	527	48	0.73	0.37
se09b29	0.774	0.050	0.087	0.003	0.248	0.061	0.001	582	29	536	17	625	44	544	32	0.12	1.30
se09b08	0.796	0.103	0.087	0.006	0.267	0.062	0.001	594	58	540	36	687	49	550	68	0.37	0.63
se10a58	0.896	0.122	0.088	0.009	0.371	0.060	0.001	650	65	542	52	616	31	572	97	0.11	0.76
se10a40	0.807	0.693	0.088	0.015	0.102	0.094	0.003	601	389	543	91	1499	65	545	181	0.89	0.09
se09b19	0.903	0.124	0.091	0.009	0.363	0.063	0.001	654	66	564	54	694	28	591	98	0.20	0.19
se10a70	0.818	0.205	0.093	0.009	0.197	0.062	0.002	607	114	574	54	684	58	578	104	0.78	1.04
se09b12	0.955	0.052	0.094	0.004	0.353	0.064	0.001	681	27	577	21	730	22	605	39	0.00	0.82
se10a17	0.900	0.061	0.095	0.005	0.355	0.064	0.001	652	33	588	27	745	25	609	49	0.07	0.19
se10a26	0.911	0.104	0.096	0.010	0.444	0.062	0.000	658	55	588	57	675	15	623	96	0.24	0.36
se10a39	0.853	0.272	0.096	0.010	0.156	0.080	0.002	626	149	593	56	1187	55	596	110	0.83	0.36
se10a56	1.013	0.081	0.098	0.005	0.345	0.064	0.001	711	41	605	32	732	28	634	59	0.01	0.21
se09b18	1.033	0.070	0.099	0.005	0.383	0.061	0.001	720	35	609	30	645	47	646	55	0.00	0.72
se09b21	0.947	0.109	0.101	0.006	0.245	0.065	0.001	677	57	617	33	769	45	627	63	0.32	0.43
se10a30	0.837	0.242	0.103	0.008	0.138	0.061	0.001	617	134	630	48	639	49	629	93	0.92	0.33
se09b11	1.113	0.062	0.103	0.004	0.323	0.063	0.001	760	30	634	22	709	45	663	41	0.00	0.08
se10a78	1.061	0.098	0.104	0.007	0.384	0.062	0.001	734	48	637	43	688	27	672	77	0.06	0.50
se10a36	1.021	0.175	0.104	0.008	0.234	0.062	0.001	714	88	641	49	669	36	652	93	0.42	0.15
se09b28	1.339	0.653	0.112	0.031	0.280	0.066	0.007	863	284	685	178	806	220	711	342	0.56	0.54
se10a10	1.013	0.114	0.114	0.006	0.226	0.062	0.001	710	57	699	34	682	30	701	63	0.84	0.41
se10a66	1.385	0.452	0.124	0.025	0.304	0.073	0.001	883	192	755	141	1023	32	786	263	0.54	0.61
se10a13	1.360	0.101	0.128	0.008	0.403	0.067	0.001	872	43	776	44	851	42	821	74	0.05	0.34
se10a68	1.519	0.095	0.137	0.004	0.208	0.072	0.001	938	38	830	20	990	42	845	39	0.01	0.81
se09b07	1.792	0.084	0.140	0.005	0.349	0.077	0.001	1043	31	844	26	1134	35	902	48	0.00	0.05
se10a09	2.120	0.276	0.142	0.017	0.452	0.098	0.001	1155	90	856	94	1595	22	973	168	0.00	0.60
se10a32	1.904	0.139	0.152	0.011	0.478	0.073	0.001	1083	49	914	60	1002	30	1019	94	0.00	0.16
se09b10	1.818	0.152	0.156	0.007	0.272	0.086	0.003	1052	55	937	40	1347	68	966	73	0.06	0.41
se10a12	1.686	0.101	0.158	0.005	0.240	0.093	0.010	1003	38	944	25	1498	209	958	47	0.15	0.35
se10a80	1.982	0.113	0.166	0.006	0.339	0.074	0.001	1109	39	992	36	1048	24	1038	62	0.01	0.82
se09b23	2.307	0.154	0.172	0.009	0.381	0.090	0.007	1214	47	1025	48	1434	157	1108	83	0.00	0.39
se10a07	1.756	0.643	0.173	0.029	0.230	0.072	0.001	1029	237	1030	161	992	26	1030	292	1.00	0.14

Tadmuck Brook Schist	Measured Isotopic Ratios 207Pb /235U	1s error	206Pb /238U	1s error	Rho	207Pb/ 206Pb	1s error	Calculated Ages 207Pb /235U	1s error	206Pb /238U	1s error	207Pb/ 206Pb	1s error	Concordia age	2s error	Probability Of Concordance	Th/U
se10a60	2.399	0.249	0.181	0.012	0.312	0.084	0.001	1242	74	1073	64	1293	25	1128	115	0.05	0.22
se10a21	2.247	0.175	0.196	0.009	0.289	0.077	0.001	1196	55	1155	48	1131	24	1171	82	0.51	0.10
se10a37	4.014	0.322	0.204	0.013	0.409	0.117	0.001	1637	65	1198	72	1911	13	1360	128	0.00	0.59
se10a51	2.942	0.494	0.218	0.017	0.237	0.089	0.001	1393	127	1271	92	1399	30	1302	168	0.39	0.51
se10a69	3.240	0.905	0.222	0.034	0.277	0.098	0.001	1467	217	1294	182	1581	27	1348	325	0.49	0.07
se09b27	3.682	0.244	0.239	0.010	0.323	0.093	0.004	1568	53	1383	53	1489	80	1463	90	0.00	0.22
se14a84	4.463	0.149	0.286	0.009	0.455	0.102	0.001	1724	28	1622	44	1658	24	1708	55	0.01	0.09
se09b22	6.523	0.415	0.291	0.012	0.315	0.124	0.002	2049	56	1646	58	2018	24	1792	102	0.00	0.97
se10a76	5.235	0.452	0.295	0.023	0.460	0.103	0.001	1858	74	1667	116	1682	14	1827	148	0.07	0.65
se09b13	6.011	0.235	0.296	0.012	0.512	0.119	0.001	1977	34	1673	59	1943	16	1951	69	0.00	0.03
se10a59	7.097	0.608	0.354	0.022	0.360	0.121	0.001	2124	76	1955	104	1970	15	2071	146	0.11	0.02
se10a19	8.135	0.471	0.359	0.016	0.396	0.147	0.009	2246	52	1979	78	2315	110	2178	105	0.00	0.12
se10a57	9.348	0.514	0.423	0.027	0.578	0.127	0.001	2373	50	2273	122	2060	11	2382	98	0.32	0.57
se09b17	8.606	0.318	0.424	0.015	0.464	0.134	0.003	2297	34	2279	66	2152	37	2297	67	0.75	0.18
se10a77	17.83	4.278	0.543	0.107	0.412	0.195	0.001	2981	231	2796	449	2787	11	2967	464	0.65	0.34

Newbury Volcanic Complex	Measured Isotopic Ratios							Calculated Ages								Probability Of Concordance	Th/U
	207Pb /235U	1s error	206Pb /238U	1s error	Rho	207Pb/ 206Pb	1s error	207Pb /235U	1s error	206Pb /238U	1s error	207Pb/ 206Pb	1s error	Concordia age	2s error		
se08a09	0.471	0.008	0.054	0.001	0.458	0.055	0.000	392	5	337	5	413	12	359	9	0.00	10.39
se08a21	0.491	0.015	0.054	0.002	0.473	0.056	0.000	406	10	342	10	469	15	368	17	0.00	14.94
se08a22	0.496	0.005	0.055	0.001	0.558	0.057	0.000	409	3	345	4	474	9	383	6	0.00	33.65
se08a28	0.503	0.009	0.055	0.001	0.307	0.058	0.000	414	6	347	4	522	13	358	7	0.00	11.66
se08a17	0.497	0.008	0.057	0.001	0.428	0.056	0.000	410	5	356	4	458	11	376	8	0.00	13.14
se08a30	0.503	0.012	0.057	0.001	0.405	0.056	0.000	414	8	359	7	465	15	377	12	0.00	0.14
se08b09	0.548	0.057	0.058	0.005	0.377	0.060	0.001	444	37	365	28	598	41	384	52	0.04	1.17
se08a07	0.510	0.007	0.058	0.001	0.500	0.055	0.000	418	5	365	5	418	14	392	8	0.00	9.91
se08a36	0.484	0.006	0.059	0.001	0.396	0.056	0.000	401	4	367	3	434	8	379	6	0.00	11.96
se08a47	0.524	0.021	0.059	0.002	0.446	0.060	0.000	428	14	369	13	614	14	392	23	0.00	18.66
se08a39	0.499	0.006	0.059	0.001	0.511	0.057	0.000	411	4	369	5	484	10	393	8	0.00	31.25
se08a37	0.482	0.011	0.059	0.001	0.428	0.055	0.000	399	8	370	7	420	13	382	13	0.00	7.51
se08a57	0.503	0.008	0.059	0.001	0.472	0.057	0.000	414	5	371	5	475	13	392	9	0.00	14.10
se08b23	0.718	0.065	0.060	0.004	0.340	0.076	0.002	550	38	373	22	1102	46	389	44	0.00	0.63
se08a32	0.514	0.019	0.061	0.003	0.583	0.056	0.000	421	13	380	16	449	18	410	25	0.00	29.09
se08a58	0.541	0.009	0.061	0.001	0.346	0.059	0.000	439	6	382	5	567	11	395	8	0.00	17.79
se08a56	0.498	0.017	0.061	0.001	0.333	0.056	0.000	410	11	384	8	464	13	391	16	0.03	25.18
se08a16	0.526	0.037	0.062	0.003	0.352	0.057	0.001	429	25	385	19	478	24	397	35	0.09	0.42
se09a43	0.522	0.179	0.063	0.009	0.206	0.065	0.002	427	119	396	54	764	72	399	105	0.80	0.64
se09a23	0.599	0.246	0.066	0.007	0.124	0.085	0.004	477	156	411	41	1319	85	413	81	0.68	0.81
se09a30	0.415	0.055	0.066	0.002	0.135	0.055	0.002	353	39	411	14	401	66	406	28	0.13	0.96
se08b25	0.935	0.112	0.066	0.003	0.184	0.113	0.003	670	59	412	18	1846	53	415	35	0.00	1.37
se08b29	0.691	0.315	0.066	0.011	0.176	0.086	0.002	533	189	415	65	1349	46	420	128	0.55	0.91
se09a72	0.469	0.215	0.067	0.015	0.243	0.057	0.002	390	149	417	90	481	73	411	168	0.86	0.61
se09a83	0.533	0.132	0.067	0.010	0.308	0.058	0.002	434	87	417	62	535	63	422	114	0.85	1.18
se08b27	0.683	0.122	0.067	0.005	0.194	0.069	0.003	529	73	418	28	909	99	424	55	0.15	0.92
se09a78	0.633	0.209	0.067	0.008	0.191	0.082	0.003	498	130	420	51	1250	71	425	101	0.56	0.74
se08a50	0.499	0.042	0.068	0.002	0.208	0.059	0.001	411	29	425	14	561	34	423	28	0.63	1.21
se08a05	0.720	0.088	0.076	0.003	0.141	0.065	0.001	551	52	473	16	764	32	477	31	0.16	0.31
se08a27	0.664	0.044	0.078	0.005	0.508	0.056	0.000	517	27	482	32	446	12	505	50	0.23	14.22
se08b24	2.314	0.330	0.079	0.009	0.412	0.182	0.006	1217	101	488	55	2671	52	436	109	0.00	0.40

Newbury Volcanic Complex	Measured Isotopic Ratios 207Pb /235U	1s error	206Pb /238U	1s error	Rho	207Pb/ 206Pb	1s error	Calculated Ages 207Pb /235U	1s error	206Pb /238U	1s error	207Pb/ 206Pb	1s error	Concordia age	2s error	Probability Of Concordance	Th/U
se09a73	1.497	1.871	0.082	0.019	0.093	0.275	0.009	929	761	507	113	3334	51	508	227	0.65	1.59
se09a18	0.793	0.101	0.083	0.008	0.392	0.063	0.002	593	57	512	49	697	58	539	89	0.18	1.16
se09a63	3.297	0.340	0.088	0.004	0.194	0.193	0.007	1480	80	542	21	2770	60	527	42	0.00	1.13
se09a37	0.881	0.073	0.090	0.008	0.567	0.062	0.001	641	40	553	50	661	31	617	77	0.04	0.51
se09a67	0.962	0.436	0.090	0.009	0.112	0.102	0.003	684	225	558	54	1653	51	561	107	0.60	1.06
se08b16	0.814	0.100	0.098	0.006	0.260	0.059	0.001	605	56	600	37	567	54	601	68	0.94	1.46
se09a52	1.366	0.440	0.107	0.018	0.261	0.095	0.002	875	189	655	105	1537	37	677	204	0.29	0.25
se09a20	3.804	0.645	0.142	0.035	0.721	0.159	0.002	1594	136	854	195	2446	20	615	396	0.00	0.28
se09a40	1.596	0.128	0.152	0.007	0.276	0.074	0.001	969	50	911	38	1029	30	928	68	0.29	0.13
se08a10	1.643	0.106	0.156	0.006	0.312	0.071	0.001	987	41	937	35	952	25	955	62	0.27	0.26
se08b26	3.604	2.071	0.170	0.019	0.097	0.261	0.009	1550	457	1013	104	3250	57	1016	208	0.36	0.35
se09a79	2.084	0.172	0.177	0.016	0.555	0.081	0.001	1143	57	1048	89	1230	34	1135	114	0.20	0.55
se09a71	2.147	0.145	0.203	0.008	0.287	0.081	0.001	1164	47	1191	42	1214	29	1179	71	0.62	0.32
se09a62	9.652	2.986	0.223	0.015	0.105	0.208	0.012	2402	285	1296	77	2892	92	1294	153	0.02	0.33
se09a70	3.639	0.307	0.253	0.013	0.304	0.107	0.001	1558	67	1452	67	1752	24	1501	110	0.18	0.58
se09a61	3.431	0.309	0.255	0.011	0.243	0.098	0.002	1512	71	1464	57	1590	38	1481	100	0.56	0.51
se08a41	3.492	0.100	0.257	0.005	0.337	0.095	0.001	1525	23	1473	25	1523	10	1503	39	0.06	0.73
se09a22	6.142	0.247	0.259	0.016	0.787	0.141	0.002	1996	35	1484	84	2236	20	2150	51	0.00	0.51
se09a58	9.069	2.624	0.282	0.034	0.207	0.276	0.005	2345	265	1601	170	3340	30	1640	336	0.04	0.38
se09a32	5.329	3.071	0.305	0.032	0.092	0.139	0.003	1873	493	1716	159	2212	35	1725	313	0.77	0.20
se09a47	8.508	0.397	0.332	0.013	0.419	0.160	0.002	2287	42	1850	63	2457	26	2156	89	0.00	0.72
se09a53	15.31	1.456	0.340	0.088	0.900	0.275	0.005	2835	91	1888	422	3335	29	3243	0	0.00	0.52
se09a59	9.664	1.805	0.342	0.051	0.399	0.190	0.003	2403	172	1897	245	2740	28	2214	366	0.03	0.29
se09a31	21.14	2.951	0.417	0.024	0.206	0.359	0.009	3145	135	2246	109	3744	40	2318	213	0.00	0.55
se09a10	21.74	3.363	0.521	0.041	0.255	0.280	0.004	3172	150	2703	174	3365	24	2910	285	0.02	0.78